

University of Louisville

ThinkIR: The University of Louisville's Institutional Repository

Electronic Theses and Dissertations

12-2023

Investigation of heterocyclic amines and N-acetyltransferase 2 genetic polymorphism in the dysregulation of hepatic energy homeostasis: A gene-environment approach.

Kennedy M Walls
University of Louisville

Follow this and additional works at: <https://ir.library.louisville.edu/etd>



Part of the [Biochemical Phenomena, Metabolism, and Nutrition Commons](#), [Medical Genetics Commons](#), and the [Medical Toxicology Commons](#)

Recommended Citation

Walls, Kennedy M, "Investigation of heterocyclic amines and N-acetyltransferase 2 genetic polymorphism in the dysregulation of hepatic energy homeostasis: A gene-environment approach." (2023). *Electronic Theses and Dissertations*. Paper 4224.
<https://doi.org/10.18297/etd/4224>

This Doctoral Dissertation is brought to you for free and open access by ThinkIR: The University of Louisville's Institutional Repository. It has been accepted for inclusion in Electronic Theses and Dissertations by an authorized administrator of ThinkIR: The University of Louisville's Institutional Repository. This title appears here courtesy of the author, who has retained all other copyrights. For more information, please contact thinkir@louisville.edu.

INVESTIGATION OF HETEROCYCLIC AMINES AND *N*-
ACETYLTRANSFERASE 2 GENETIC POLYMORPHISM IN THE
DYSREGULATION OF HEPATIC ENERGY HOMEOSTASIS: A GENE-
ENVIRONMENT APPROACH

By

Kennedy M. Walls

B.S. Chemistry, track in biochemistry, University of Louisville, 2019

M.S. Pharmacology and Toxicology, University of Louisville, 2021

A Dissertation submitted to the Faculty of the School of Medicine of the
University of Louisville in partial fulfillment of the requirements for the degree of

Doctor of Philosophy in Pharmacology and Toxicology

Department of Pharmacology and Toxicology

University of Louisville

Louisville, Kentucky

December 2023

Copyright 2023 by Kennedy M. Walls

All rights reserved

INVESTIGATION OF HETEROCYCLIC AMINES AND N-
ACETYLTRANSFERASE 2 GENETIC POLYMORPHISM IN THE
DYSREGULATION OF HEPATIC ENERGY HOMEOSTASIS: A GENE-
ENVIRONMENT APPROACH

By

Kennedy M. Walls

B.S. Chemistry, track in Biochemistry, University of Louisville, 2019

M.S. Pharmacology and Toxicology, University of Louisville, 2021

A Dissertation approved on

November 16, 2023

By the following Dissertation committee:

David Hein, Ph.D.

Kyung Hong, Ph.D.

Daniel Conklin, Ph.D.

Bradford Hill, Ph.D.

Joshua Hood, Ph.D.

DEDICATION

I dedicate this dissertation to the educators who inspired me to pursue science, and to my friends and family that supported and motivated me.

ACKNOWLEDGEMENTS

I'd like to thank my current and former lab members, Mariam Habil, Madeline Martinez, Jonathan Joh, Dr. Raul Salazar-Gonzalez, Dr. James Wise, and Mark Doll for their help and guidance with my work. I'd also like to thank my mentors, Drs. Kyung Hong and David Hein, for their continued support. I offer special thanks to my committee members, Dr. Joshua Hood, Dr. Bradford Hill, and Dr. Daniel Conklin, for their insight and assistance with my project. Lastly, I'd like to express gratitude to my family and friends who have supported me throughout my academic career and aided in my success.

ABSTRACT

INVESTIGATION OF HETEROCYCLIC AMINES AND *N*- *ACETYLTRANSFERASE 2* GENETIC POLYMORPHISM IN THE DYSREGULATION OF HEPATIC ENERGY HOMEOSTASIS: A GENE- ENVIRONMENT APPROACH

Kennedy M. Walls

November 16, 2023

Heterocyclic amines (HCAs) are mutagens generated when cooking meat for prolonged periods of time or until well-done. Recent epidemiological studies reported significant associations between dietary HCA exposure and insulin resistance and type II diabetes. However, no previous studies have examined if HCAs, independent of meat consumption, contributes to pathogenesis of insulin resistance or metabolic disease. It is well known that HCAs require hepatic bioactivation by cytochrome P450 1A2 (CYP1A2) and *N*-acetyltransferase 2 (NAT2). *NAT2* expresses a well-defined genetic polymorphism in humans that, depending on the combination of *NAT2* alleles, correlate to rapid, intermediate, or slow acetylator phenotypes that exhibit differential metabolism of aromatic amines and HCAs. We hypothesize that HCAs will induce insulin resistance and disrupt energy homeostasis in human hepatocytes, and that the effect will be dependent on *NAT2* genetic polymorphism. HCA treatment on human hepatocytes induced insulin resistance, glucose production, and expression of several key genes involved in gluconeogenesis, and these effects were more

apparent in rapid NAT2 acetylator hepatocytes than in slow. Additionally, HCAs lead to neutral lipid accumulation and increased levels of triglycerides, cholesterol, and free fatty acids, in addition to dysregulated expression of genes involved in lipid homeostasis. Potential mechanisms of HCA-induced insulin resistance and disrupted energy homeostasis were also explored. HCAs increased JNK activity, a well-known mechanism of hepatic insulin resistance, and blocking JNK activity restored insulin signaling in HCA-treated hepatocytes. Additionally, HCAs led to increased reactive oxygen species and induction of *TNF*, indicating oxidative stress and inflammation as potential mechanisms of insulin resistance. An RNA-sequencing study also indicated endoplasmic reticulum stress as a potential mechanism. Taken together, the findings presented here indicate that HCAs lead to insulin resistance and dysregulation of energy homeostasis in human hepatocytes, and that these outcomes are differentially affected by *NAT2* genetic polymorphism. These studies provide insight into the novel role of HCAs in the development of conditions associated with metabolic syndrome and fatty liver, and elucidate the crucial need to consider the gene-environmental interactions when investigating these conditions.

TABLE OF CONTENTS

DEDICATION	iii
ACKNOWLEDGMENTS.....	iv
ABSTRACT	v
LIST OF FIGURES.....	viii
CHAPTER 1: INTRODUCTION.....	1
CHAPTER 2: HETEROCYCLIC AMINES REDUCE INSULIN-INDUCED AKT PHOSPHORYLATION AND INDUCE GLUCONEOGENIC GENE EXPRESSION IN HUMAN HEPATOCYTES.....	19
CHAPTER 3: INDUCTION OF GLUCOSE PRODUCTION BY HETEROCYCLIC AMINES IS DEPENDENT ON <i>N</i> -ACETYLTRANSFERASE 2 GENETIC POLYMORPHISM IN HUMAN HEPATOCYTES.....	50
CHAPTER 4: METABOLIC EFFECTS OF HETEROCYCLIC AMINES IS DEPENDENT ON <i>N</i> -ACETYLTRANSFERASE 2 GENETIC POLYMORPHISM IN HUMAN HEPATOCYTES.....	61
CHAPTER 5: ACTIVATION OF C-JUN N-TERMINAL KINASE PROMOTES HETEROCYCLIC AMINE-INDUCED INSULIN RESISTANCE IN HUMAN HEPATOCYTES.....	81
CHAPTER 6: HETEROCYCLIC AMINES DISRUPT LIPID HOMEOSTASIS IN HUMAN HEPATOCYTES.....	107
CHAPTER 7: SUMMARY AND CONCLUSIONS.....	134
REFERENCES.....	143
APPENDIX.....	175
CURRICULUM VITAE.....	186

LIST OF FIGURES

Figure 1.1. PI3K/AKT signaling in hepatocytes.....	4
Figure 1.2. Structures of common HCAs.....	8
Figure 1.3. Bioactivation of PhIP.....	12
Figure 2.1. Chemical structures of HCAs and relative cell viability of HepG2 and cryopreserved human hepatocytes following HCA treatment.....	28
Figure 2.2. Insulin-induced AKT phosphorylation following HCA treatment in HepG2 cells.....	31
Figure 2.3. Insulin-induced AKT phosphorylation following HCA treatment in cryopreserved human hepatocytes.....	33
Figure 2.4. Increases in insulin receptor-target genes involved in gluconeogenesis following HCA treatment.....	36
Figure 2.5. Changes in expression of genes and protein that regulate gluconeogenesis following HCA treatment in cryopreserved human hepatocytes.....	40
Figure 2.6. Increases in glucose production following HCA treatment in cryopreserved human hepatocytes.....	43
Figure 3.1. Glucose production in slow, intermediate, and rapid NAT2 acetylator cryopreserved human hepatocytes following MeIQ treatment.....	56
Figure 3.2. Glucose production in slow, intermediate, and rapid NAT2 acetylator cryopreserved human hepatocytes following MeIQx treatment.....	57
Figure 3.3. Glucose production in slow, intermediate, and rapid NAT2 acetylator cryopreserved human hepatocytes following PhIP treatment.....	58

Figure 4.1. Insulin-induced AKT phosphorylation following HCA treatment in slow and rapid NAT2 acetylator cryopreserved human hepatocytes.....	70
Figure 4.2. Changes in expression of insulin receptor-target genes involved in gluconeogenesis following HCA treatment in slow and rapid NAT2 acetylator cryopreserved human hepatocytes.....	73
Figure 4.3. Changes in expression of the insulin receptor-target gene <i>FOXO1</i> , which regulates gluconeogenesis, following HCA treatment in slow and rapid NAT2 acetylator cryopreserved human hepatocytes.....	75
Figure 4.4. Changes in expression of additional genes that regulate gluconeogenesis following HCA treatment in slow and rapid NAT2 acetylator cryopreserved human hepatocytes.....	77
Figure 5.1. HCA treatment induces phosphorylation of JNK in cryopreserved human hepatocytes.....	91
Figure 5.2. HCA treatment interferes with insulin signaling at IRS1 and AKT, but inhibiting JNK with SP600125 restores insulin signaling at both IRS1 and AKT in cryopreserved human hepatocytes.....	94
Figure 5.3. HCA treatment leads to increased levels of ROS and increased expression of TNF in cryopreserved human hepatocytes.....	97
Figure 5.4. HCA treatment leads to neutral lipid accumulation in cryopreserved human hepatocytes.....	99
Figure 5.5. Gene Ontology (GO) biological processes, molecular functions, and cellular components significantly enriched among genes upregulated by PhIP treatment in cryopreserved human hepatocytes include indicators of endoplasmic reticulum stress.....	102
Figure 5.6. Reactome pathways significantly enriched among genes upregulated by PhIP treatment in cryopreserved human hepatocytes.....	103
Figure 6.1. Neutral lipid accumulation following HCA treatment in cryopreserved human hepatocytes.....	116
Figure 6.2. Increases in expression of lipid droplet genes following HCA treatment in cryopreserved human hepatocytes.....	119

Figure 6.3. Increased cholesterol and decreased expression of <i>PON1</i> following HCA treatment in cryopreserved human hepatocytes.....	122
Figure 6.4. Increased triglycerides and increased expression of genes involved in triglyceride synthesis following HCA treatment in cryopreserved human hepatocytes.....	125
Figure 6.5. Increased free fatty acids and dysregulated expression of genes involved in free fatty acid uptake and metabolism following HCA treatment in cryopreserved human hepatocytes.....	129
Figure 7.1. Summary of dissertation findings.....	134
Figure 7.2. Summary of Chapter 2.....	135
Figure 7.3. Summary of Chapters 3 and 4.....	136
Figure 7.4. Summary of Chapter 5.....	137
Figure 7.5. Summary of Chapter 6.....	138

CHAPTER 1: INTRODUCTION

1.1. Metabolic Syndrome and Insulin Resistance

Metabolic syndrome is characterized by a cluster of adverse health conditions including insulin resistance and hyperglycemia, in addition to hypertension, central obesity, and abnormal cholesterol or triglyceride levels [1]. In the United States, the prevalence of obesity, hypertension, and type II diabetes has steadily increased over the past three decades, and it is estimated that more than one third of the U.S. adult population has metabolic syndrome [2], [3]. These individuals are at an increased risk of health complications including type II diabetes mellitus, heart attack, fatty liver, and stroke [4]. Some have argued that insulin resistance may be the underlying etiology of metabolic syndrome [5].

Insulin is an endocrine peptide hormone that elicits an anabolic response to nutrient availability. It instructs its target organs to uptake glucose and store excess nutrients in the form of glycogen and lipids [6]. The liver plays a crucial role in systemic regulation of glucose and lipid metabolism, and aberrant hepatic insulin action is considered a potential primary factor in insulin resistance [7]. Under a normal physiologic fasting state, high glucagon-to-insulin ratio decreases glucose consumption and shifts the liver into glucose production by consuming stored glycogen (i.e., glycogenolysis) and from glucogenic precursors

(i.e., gluconeogenesis) [8]. In pathological insulin resistance, insulin fails to regulate hepatic metabolism, leading to altered glucose metabolism and excess glucose production, while increased lipid synthesis continues. This condition is known as selective hepatic insulin resistance [9] and leads to hyperglycemia and fatty liver.

Hepatic Insulin Signaling and Lipid Metabolism

Evidence has indicated that the phosphoinositide 3-phosphate kinase (PI3K)/Akt pathway is the primary signaling pathway that mediates insulin's effects on anabolic metabolism [10]. Figure 1.1 models the primary insulin signaling pathway in hepatocytes. Following a meal, secreted insulin binds to the insulin receptor on the surface of the liver. The receptor recruits and activates insulin receptor substrate (IRS), which then activates phosphoinositide 3-kinase (PI3K) [11]. PI3K phosphorylates phosphatidylinositol 4,5-bisphosphate (PIP₂) into phosphatidylinositol (3,4,5)-trisphosphate (PIP₃) in a process that is opposed by phosphatase and tensin homolog (PTEN). PIP₃ activates 3-phosphoinositide-dependent protein kinase 1 (PDK1), which phosphorylates protein kinase B (AKT) at Thr308. mTOR complex 2 (mTORC2) also phosphorylates AKT at Ser473 to fully activate AKT.

Various pathways for controlling glucose and lipid homeostasis branch out from AKT. Glycogen synthesis is induced through AKT inhibition of glycogen synthase kinase 3 (GSK3). AKT can also promote glycogen synthesis independent of GSK3 via activation of glycogen synthase 2 (GYS2) by glucose-6-phosphate (G6PC). AKT inhibition of tuberous sclerosis protein (TSC) activates

mTORC1, which then activates sterol regulatory element-binding transcription factor 1 (SREBP1c) and glucokinase (GCK), resulting in phosphorylation of glucose to G6PC. G6PC feeds into glycolysis and glycogen synthesis. Additionally, G6PC activates carbohydrate-responsive element-binding protein (ChREBP), which activates lipogenesis along with SREBP1c. AKT also inhibits forkhead box protein O1 (FOXO1), causing inhibition of gluconeogenesis by suppressing expression of *G6PC* and *PCK1*. Free fatty acids (FFAs) can also promote gluconeogenesis and be taken up by the liver and converted to acetyl-CoA, which activates pyruvate carboxylase and contributes to insulin resistance [7].

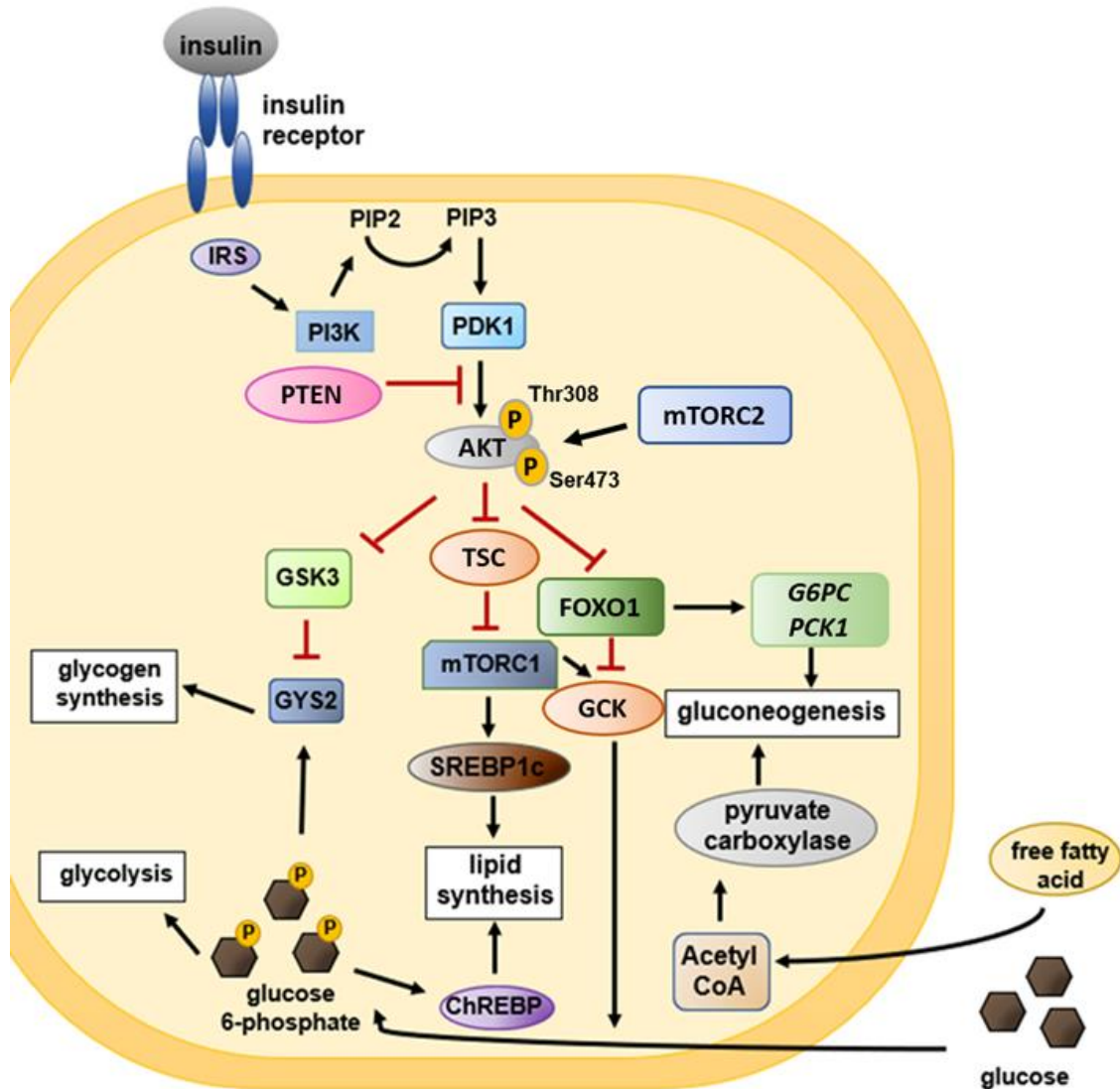


Figure 1.1. PI3K/AKT signaling in hepatocytes. Adapted from [7].

Underlying molecular mechanisms of insulin resistance

A variety of mechanisms, acting individually or synergistically, have been known to cause insulin resistance [6], [10], [12]. First, insulin signaling may be altered by decreased expression (or increased degradation) of any one of the components of the insulin signaling cascade. Additionally, increased protein expression can also act as negative feedback signals. Second, insulin signaling

proteins may undergo post-translational modifications, changing their activity. Specifically, inhibitory serine phosphorylation of IRS1/2 alters the ability of the protein to engage in insulin-receptor signaling [11]. Among the IRS-modifying enzymes, activation of stress-activated protein kinase JNK, inhibitory kappa B kinase beta (IKK β), and protein kinase C (PKC) is central to mediating insulin resistance in response to stress factors like lipid metabolites, pro-inflammatory cytokines, oxidative stress, and stress of the endoplasmic reticulum (ER stress) [13]. In fact, pathological features that are commonly associated with cellular insulin resistance include inflammation [14], mitochondrial dysfunction [15], ER stress [16], and lipotoxicity [17]. One of the common underlying attributes of these features is increased reactive oxygen species (ROS) [6] and ROS have been shown to play a causal role in different forms of insulin resistance [18].

Oxidative Stress

Oxidative stress is associated with hepatic steatosis, a condition closely linked with insulin resistance. The precise origin of this oxidative stress is debated, but it is theorized that increased activity of CYP2E1 or CYP4As may contribute to the production of reactive oxygen species, leading to the induction of a stress response via JNK and NF- κ B [19], [20]. In fact, over-expression of *CYP2E1* in hepatic cell lines induces insulin resistance by decreasing tyrosine phosphorylation and increasing serine phosphorylation of IRS1/2 in response to insulin [21]. Additional studies are required to understand the precise link between oxidative stress and insulin resistance.

Fatty acids

The role of fatty acids and their metabolites in inducing hepatic insulin resistance has been explored. Recent experiments have proposed mechanistic links between intrahepatic lipids and insulin resistance. Mice in which liver-lipoprotein lipase (LPL) was over-expressed primarily in the liver resulted in severe alterations in hepatic insulin signaling, including absence of tyrosine phosphorylation of IRS2 and downstream activation of PKB/Akt [22]. Similarly, rats subjected to a 3-day high fat diet to stimulate hepatic fat accumulation failed to inhibit hepatic glucose output following insulin infusion, demonstrating hepatic insulin resistance [23]. Thus, hepatic fat accumulation serves a novel role in development of hepatic insulin resistance and requires additional investigation to understand the link between fat accumulation and other conditions resulting from and leading to insulin resistant states.

1.2. Heterocyclic Amines (HCAs)

Heterocyclic amines (HCAs) are known mutagens and carcinogens [24]. The main source of human exposure to HCAs is through cooked meat [25], [26]. They are primarily formed in muscle foods including meats and fish, which provide precursors, such as creatinine, amino acids, and aldehydes, required for the formation reaction [27]–[29]. Cooking meat at high temperatures or for long periods of time favors HCA formation, and certain cooking methods, such as frying, grilling, and roasting, substantially enhance their formation [28].

HCA Structures and Classifications

Thus far, more than 25 different HCAs have been isolated from food samples [30]. All HCAs contain at least one aromatic structure and one heterocyclic structure, and most of them contain an exocyclic amino group. The amino-carboline HCAs contain a five-membered heterocyclic aromatic ring wedged between two six-membered aromatic rings. In contrast, the aminoimidazo-azaarene (AIA) HCAs have an *N*-attached methyl group at the imidazole ring. Amino-carbolines, instead, either lack a methyl group entirely, or the methyl group is attached to a six-membered ring.

Classification of mutagens from proteinaceous foods is determined by the critical heating temperature of 300 degrees Celsius. Protein pyrolysates, including amino-carbolines, form above 300 degrees Celsius. Those formed below 300 degrees Celsius are considered 2-amino-imidazole-type mutagens, also known as aminoimidazo-azaarenes (AIAs) [31], [32]. The most abundant HCAs found in cooked meat include PhIP (2-amino-1-methyl-6-phenylimidazo[4,5-b]pyridine), MeIQx (2-amino-3,8-dimethylimidazo[4,5-f]quinoxaline) and MeIQ (2-amino-3,4-dimethylimidazo[4,5-f]quinoline) (Fig. 1.2). Each these HCAs share a common imidazole-ring structure with an exocyclic amino group and, therefore, are classified as AIAs. These HCAs have been detected in different types of cooked meat at levels ranging up to 150 ng/g [33].

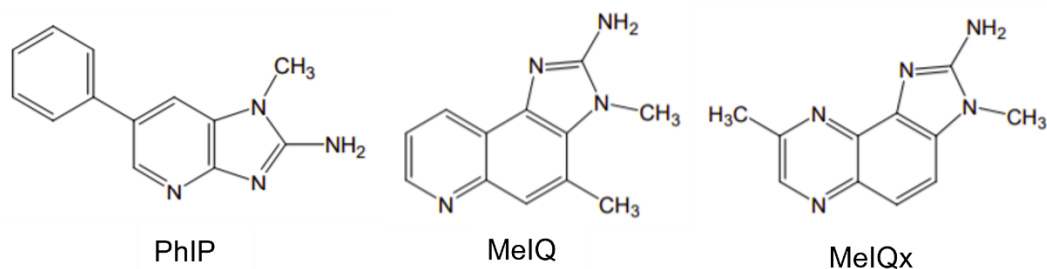


Figure 1.2. Structures of common HCAs.

HCA formation

Formation of HCAs is a series of complex chemical reactions. The browning reaction was proposed by Maillard to account for the brown pigments and polymers produced from the reaction of the amino group of an amino acid and the carbonyl group of a sugar. The Maillard reaction encompasses a network of reactions, including the formation of pyrazines, quinoxalines, and pyrido[3,4-d]imidazoles, which are involved in the formation of HCAs [34], [35].

Amino acids or proteins are the precursors of amino-carbolines, and creatinine is not required for their formation. However, creatinine may function as an additional source of structural fragments. Free radical reactions occurring at high temperatures is the suggested pathway for producing reactive fragments in amino-carbolines [32]. However, this hypothesis has yet to be fully investigated due to difficult manipulation of high temperatures required for experimental setups.

AIAs are responsible for most of the mutagenic activity in cooked foods, especially in Western diets [36]. IQ- and IQx-type HCAs (Fig. 1.2) and their methylated forms are likely formed from creatinine, sugars, free amino acids, and dipeptides through Maillard reaction and Strecker degradation upon heating [34], [35]. Creatinine was determined to be important for AIA-type HCA formation because HCA yield was increased with the addition of creatinine to the surface of meat prior to frying it [32]. It was demonstrated that cyclization and water elimination of creatinine formed the amino-imidazo structure of IQ and IQx, and the Maillard reaction between amino acids and hexose formed the Strecker degradation products like pyridines or pyrazines, which formed the remainder of the molecule, likely by aldol condensation [37]. While the reaction is favored at temperature above 100 °C, pyrazine and pyridine yield from Maillard reaction and Strecker degradation is still low. This phenomenon was considered a factor for low HCA yield in foods and common model systems, making it difficult to investigate AIAs [38].

HCA mutagenesis and carcinogenesis

Meat consumption has been associated with increased risk of many common cancers, including prostate, lung, breast, and colon cancer [39]–[41]. Genetic variations in the *NAT2* gene have been suggested to modify the association of meat intake with some cancers through its influence on metabolism of HCAs. Thus, epidemiological studies have reported inconsistent associations between dietary HCA intake via meat consumption and increased cancer risk, as *NAT2* allelic variations occur naturally in the sampled human

population [42], which will be discussed further in section 1.3. Despite inconsistent epidemiological reports, HCAs are highly mutagenic *in vitro* and *in vivo*. However, bioactivation by CYP1A2 and NAT2 are required to generate the metabolite responsible for mutagenic effects, and so consideration of HCA metabolism is crucial when evaluating their proposed hazards to human health.

HCAs and insulin resistance/fatty liver epidemiology

Recent epidemiological studies have suggested a novel link between HCAs and insulin resistance and fatty liver. Zelber-Sagi and colleagues reported that consumption of meat cooked via “unhealthy” methods (e.g., grilling or broiling to well-done level or frying) is related to insulin resistance and found that there is a significant association between estimated HCA consumption via cooked meat and insulin resistance, among both general population and patients with non-alcoholic fatty liver disease (odds ratio [OR] = 1.92; 95% confidence interval [CI] = 1.12-3.30) [43]. Importantly, after multivariate adjustment, the association was independent of cholesterol and saturated fat intake. A higher frequency of unhealthy cooking methods, such as broiling, barbequing, and roasting, was each independently associated with a higher risk of type II diabetes. In contrast, the frequency of stewing or boiling red meats was not associated with type II diabetes risk [44]. These studies imply that unhealthy cooking methods, which favor production of HCAs, significantly increase the risk of developing insulin resistance or type II diabetes. Accordingly, the authors suggested exposure to polycyclic aromatic hydrocarbons and HCAs commonly present in cooked meat as a potential underlying, biological mechanism for this

phenomenon [45]. In the follow-up study of three prospective cohorts, the authors reported that open-flame and/or high-temperature cooking >15 times/month, compared with <4 times/month, the hazard ratio and 95% CI of type II diabetes was 1.28 and 1.18-1.39, respectively [44]. In addition, estimated intake of HCAs was also associated with an increased type II diabetes risk, and this was the first study linking higher estimated dietary HCA intake with an increased risk of type II diabetes [44]. These epidemiological studies provide the basis for investigating a potential link between HCA exposure and insulin resistance.

1.3. Arylamine *N*-acetyltransferase 2 (*NAT2*)

Arylamine *N*-acetyltransferases (*NATs*) are phase II metabolic enzymes that detoxify or bioactivate xenobiotics and drugs [46]. Two *NAT* genes (*NAT1* and *NAT2*) have been identified and characterized in humans. *NAT1* and *NAT2* are similar in structure, but they differ in substrate selectivity and physiological function [47]. *NAT1* is expressed ubiquitously, while *NAT2* expression is restricted to the liver and gastrointestinal tract [48]. The importance of substrate selectivity and organ-specific expression of *NAT2* will be discussed in later sections.

NAT2 functions as catalysts for either *N*-acetylation or *O*-acetylation of drugs and aromatic amines. *NAT2* catalyzes *N*-acetylation of drugs like sulfamethazine, hydralazine and dapson, and this is primarily a detoxification pathway [49]. In contrast, many HCAs, including PhIP, MeIQx, and MeIQ are bioactivated by *NAT2*-mediated *O*-acetylation following hydroxylation by cytochrome P450 (CYP450), mainly isozyme 1A2 [50], [51] (Fig. 1.3). Some

compounds like aminobiphenyl can either be detoxified or bioactivated by NATs depending on substrate availability and enzymatic activity.

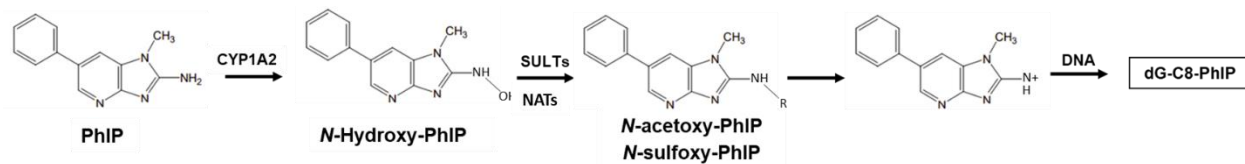


Figure 1.3. Bioactivation of PhIP.

NAT2 genetic polymorphism

NAT2 expresses a well-defined genetic polymorphism in humans [52]. Single nucleotide polymorphisms (SNPs) occur when a DNA sequence variation occurs due to a single nucleotide substitution, producing varying alleles within a locus. For any given SNP, the SNP can (1) occur in a coding region but not result in a change in amino acid; (2) occur in a coding region and result in an amino acid change; (3) occur in a regulatory region resulting in a change in gene expression; or (4) occur in a region between genes [53]. *NAT2* SNPs occur in the coding region of the gene, resulting in amino acid changes and thus generating different alleles that produce slow, intermediate, or rapid acetylator phenotypes. These different acetylator phenotypes exhibit differential metabolism of drugs

and aromatic amines, including HCAs, and thus modify risk of toxicity after an exposure [52].

There are 108 *NAT2* alleles generated by SNPs, and allelic frequencies differ among different populations [54]. As mentioned, these allelic variants are associated with varying enzymatic activity and stability. *NAT2*4*, commonly considered the reference allele, is associated with the rapid acetylator phenotype [55]. *NAT2*4* allele frequency is highest among Asian populations (50% in Chinese and 70% in Japanese) [56]–[58], although *NAT2*4* makes up 20 to 25% of alleles in Caucasians and 36 to 41% in African Americans [59]. The remaining common alleles, *NAT2*5*, *NAT2*6*, *NAT2*7*, and their subtypes, are typically associated with the slow acetylator phenotype [59]. The prevalence of the slow acetylator phenotype is highly variable among different ethnic groups. It is estimated that 50 to 70% of Caucasians, 35 to 55% of African Americans, and 10 to 30% of Asians exhibit the slow acetylator phenotype. *NAT2*5* allele is most common among Caucasians (44%), and among the individuals of African descent (25%). However, it is less prevalent among Asians (1.9 to 5.5%) [60]. *NAT2*6* is evenly distributed across the different ethnic groups with frequency of about 30%. *NAT2*7* is the most common slow acetylator-associated allele among Asians (10 to 12%), while *NAT2*7* is less prevalent among Caucasians (less than 2%) and Africans (3 to 6%) [61] (see Table 1.1).

NAT2 alleles	Africans	Asians	Caucasians
NAT2*4	36-41%	44-79%	20-25%
NAT2*5	25-27%	1.9-5.5%	44%
NAT2*6	30%	30%	30%
NAT2*7	3-6%	10-12%	<2%

Table 1.1. NAT2 allelic frequencies among ethnic populations.

NAT2 and drug toxicity or cancer risk

Increased risk for drug toxicity and cancer are associated with different NAT2 genotypes and phenotypes [46]. For example, people with the slow NAT2 phenotype have an increased risk of isoniazid-induced liver injury relative to those with the rapid NAT2 phenotype [62]. Isoniazid is a drug used for the treatment and prevention of tuberculosis, but treatment had frequently been compromised by isoniazid-induced hepatotoxicity and liver failure [63]. A previous study found that the incidence of isoniazid-induced hepatotoxicity differed among rapid (2.9%), intermediate (9.8%), and slow (22%) NAT2 acetylators [63]. Slow acetylators are significantly more likely to experience hepatotoxicity from isoniazid treatment for tuberculosis than rapid acetylators because slow acetylators retain a higher plasma concentration of the drug for an extended time [64].

Additionally, carriers of the slow acetylator genotype are correlated with greater adverse health responses after hydralazine treatment relative to rapid acetylators. Hydralazine is indicated in treatment of chronic hypertension, short-term therapy of pregnancy-induced hypertension and eclampsia, and in therapy

of hypertensive crisis [44]. A rare side effect of hydralazine, a systemic lupus erythematosus-like syndrome, has been observed and can have serious adverse health consequences. Hydralazine treatment for hypertension is modified by acetylator phenotype following oral administration [65], and there is substantial evidence supporting a correlation between NAT2 acetylator phenotype or genotype and urine and plasma hydralazine concentrations. Like the previously discussed drug isoniazid, slow acetylators are more likely to experience adverse effects of hydralazine because they maintain higher plasma concentrations of the drug for a longer period, and thus *NAT2* genotype should be considered when dosing hydralazine.

In addition to alterations in drug toxicity, both rapid and slow NAT2 acetylator phenotypes have been associated with increased risk of cancer in different target organs following arylamine exposure [66]. Rapid acetylators detoxify aromatic amines to a greater extent than slow acetylators via *N*-acetylation so they may be excreted from the body more quickly. However, following *N*-hydroxylation, the metabolites can undergo bioactivation via the *O*-acetylation pathway. The *O*-acetylation pathway often leads to formation of aryl-nitrenium ions and DNA adducts, then carcinogenesis if DNA cannot be repaired. For this reason, slow NAT2 acetylation has been associated with higher risk of developing urinary bladder cancer due to decreased ability to detoxify aromatic amines by *N*-acetylation [67], [68].

In contrast to urinary bladder cancer, the risk of colorectal cancer from well-done cooked meat was higher among rapid NAT2 acetylators compared to

slow acetylators resulting from increased rate of metabolism of HCAS [69]–[71]. Additionally, rapid acetylators are more prone to liver cancers following exposure to carcinogenic aromatic amines [72]–[74]. To elaborate on this paradoxical phenomenon, as mentioned previously, CYP450 mediates *N*-hydroxylation followed by NAT2 *O*-acetylation of aromatic amines, resulting in a carcinogenic metabolite. Since this metabolic bioactivation process occurs in the liver, rapid acetylators are at greater risk of developing liver cancers [75]. However, in the case of urinary bladder cancer, aromatic amines exit the liver, unaltered by slow NAT2 acetylation, and reach the bladder, where DNA adducts are formed following an acid-catalyzed reaction with urothelial DNA [76]. Therefore, rapid NAT2 acetylation increases risk of liver cancer, while slow NAT2 acetylation increases risk of urinary bladder cancer. These data indicate the association of cancer risk with NAT2 phenotype may be exposure and organ specific.

NAT2 and insulin resistance

Recently, certain genetic variants/polymorphisms of NAT2 have been linked to insulin resistance, high serum triglyceride, and coronary artery disease as well as high fasting plasma glucose levels [77]–[80]. Analysis of Nat1-knockout (homolog of human NAT2) mice revealed that Nat1 deficiency leads to development of insulin resistance and metabolic defects at the systemic level, supporting the previously unrecognized role of NAT2 in regulating metabolism and insulin sensitivity [81], [82]. However, it is currently unknown how NAT2 influences cellular metabolism and insulin sensitivity.

Application to Toxicogenomics

The study of genetics has been broadly applied in precision medicine, and one of the emerging applications is pharmacogenomics-informed pharmacotherapy, tailoring drug selection and dosing to the patient's genetic features [83]. A similar approach can be applied to toxicants when evaluating risk of toxicity after an exposure, specifically if the toxicant is known to be metabolized by a gene exhibiting variations among the human population. A primary example of this includes metabolism of HCAs by NAT2. In the present studies we will show that HCAs induce insulin resistance and metabolic dysregulation in human hepatocytes, and that this effect is dependent on metabolism by NAT2. Thus, our studies indicate a crucial need for considering both genetic and environmental factors when evaluating risk of developing type II diabetes or metabolic syndrome following consumption of cooked meat and exposure to HCAs.

OVERALL GOALS AND SPECIFIC AIMS

This dissertation project encompasses two specific aims. Listed are the specific aims and the hypotheses. The following chapters describe the experiments performed to test these hypotheses, the analyses of the results, and major conclusions.

Aim 1. Determine the effects of HCA exposure on insulin sensitivity and energy homeostasis in human hepatocytes.

We hypothesize that HCA treatment on human hepatocytes will lead to insulin resistance and increased and sustained glucose and lipids.

Aim 2. Investigate the role of *NAT2*-mediated metabolism of HCAs on dysregulation of energy homeostasis and potential mechanisms of HCA-induced insulin resistance in human hepatocytes.

We hypothesize that metabolism by *NAT2* will enhance HCA-mediated metabolic dysregulation in human hepatocytes, and that lipotoxicity and ER stress are potential mechanisms of HCA-induced insulin resistance.

Please note that several of the following chapters are published or will be submitted for publication as separate papers, and so there will be repetition of content in the introductions and methods sections.

CHAPTER 2
HETEROCYCLIC AMINES REDUCE INSULIN-INDUCED AKT
PHOSPHORYLATION AND INDUCE GLUCONEOGENIC GENE EXPRESSION
IN HUMAN HEPATOCYTES

INTRODUCTION

Heterocyclic amines (HCAs) are known mutagens and carcinogens [24], [84]. The main source of human exposure to HCAs is through cooked meat, although they are also found in other products including cigarette smoke [25], [26]. They are primarily formed in muscle foods including meats and fish, which provide precursors, such as creatinine, amino acids, and aldehydes, required for the formation reaction [27]–[29]. Cooking meat at high temperatures or for long periods of time favors HCA formation, and certain cooking methods, such as frying, grilling, and roasting, substantially enhance their formation [28]. Thus far, more than 25 different HCAs have been isolated from food samples [30]. The most abundant HCAs found in cooked meat include PhIP (2-amino-1-methyl-6-phenylimidazo[4,5-b]pyridine), MeIQx (2-amino-3,8-dimethylimidazo[4,5-f]quinoxaline) and MeIQ (2-amino-3,4-dimethylimidazo[4,5-f]quinoline) (Fig. 1A). These HCAs have been detected in different types of cooked meat at levels ranging up to 150 ng/g [33]. Many HCAs require hepatic

bioactivation to yield mutagenic and carcinogenic effects [72], [73]. The initial step of HCA metabolism is the generation of *N*-hydroxy-HCA derivatives, which is catalyzed by cytochrome P450, mainly isoenzyme CYP1A2 [72]. Further metabolism and activation are carried out by arylamine *N*-acetyltransferase 2 (NAT2) and sulfotransferases, which result in esterification and formation of nitrenium ions. These products are highly genotoxic and capable of direct interaction with DNA by adduct formation. The resulting HCA-DNA adducts can cause errors in DNA replication and result in mutations, which contribute to carcinogenesis [72], [85].

Existing studies of HCAs have examined primarily their mutagenicity and carcinogenicity. However, a recent epidemiological study has linked HCA exposure via cooked meat to development of insulin resistance [43]. This was a cross-sectional study evaluating non-alcoholic fatty liver disease and insulin resistance. Dietary HCA intake was estimated based on by questionnaires on meat type and cooking methods. The authors observed a significant association between HCA consumption and insulin resistance (odds ratio [OR] = 1.92; 95% confidence interval [CI] = 1.12-3.30) even after multivariate analyses adjusted for 1) age, gender, energy intake per day and BMI and 2) weekly hours of physical activity, smoking status, weekly alcohol portions, saturated fat and cholesterol intake. This study suggests that exposure to HCAs via consumption of cooked meat may contribute to development of insulin resistance.

Insulin is an endocrine peptide hormone that elicits an anabolic response to nutrient availability. It instructs its target organs to uptake glucose and store

excess nutrients in the form of glycogen and lipids [6]. The liver plays a crucial role in systemic regulation of glucose and lipid metabolism, and aberrant hepatic insulin action is considered a potential primary factor in insulin resistance [7]. Under a normal physiologic fasting state, high glucagon-to-insulin ratio decreases glucose consumption and shifts the liver into glucose production by consuming stored glycogen (i.e., glycogenolysis) and from glucogenic precursors (i.e., gluconeogenesis) [8]. In pathological insulin resistance, insulin fails to regulate hepatic metabolism, leading to altered glucose metabolism and excess glucose production, while increased lipid synthesis continues. This condition is known as selective hepatic insulin resistance [9] and leads to hyperglycemia and fatty liver. Importantly, risk factors represented by metabolic syndrome include insulin resistance and hyperglycemia, in addition to hypertension, central obesity, and abnormal cholesterol or triglyceride levels [1]. An individual with metabolic syndrome is at an increased risk of serious health complications, including atherosclerosis, type II diabetes mellitus, heart attack, kidney disease, fatty liver, vascular disease, and stroke [1]. Some have argued that insulin resistance may be the underlying etiology of metabolic syndrome [5]. Nearly one-third of adults in the United States have metabolic syndrome, and 30.2 million adults (12.2% of US adults) have type II diabetes, and these numbers are growing [1]. Thus, understanding environmental factors that contribute to pathogenesis of insulin resistance and metabolic syndrome is necessary to combat this problem.

The aforementioned epidemiological study [43] suggested a causal link between HCA consumption and insulin resistance. However, no studies have

examined the effect of HCA exposure on insulin sensitivity or glucose homeostasis. In the present study, we investigated the effects of MeIQ, MeIQx, and PhIP, three common HCAs generated when cooking meat, on insulin signaling and glucose production in a hepatocellular carcinoma cell line, HepG2, and cryopreserved human hepatocytes.

MATERIALS AND METHODS

Heterocyclic amines (HCAs)

PhIP, MeIQx, and MeIQ were purchased from Toronto Research Chemicals. They were prepared into a solution with dimethyl sulfoxide (DMSO) at a stock concentration of 10 mM. The media containing the indicated concentrations of HCAs used for experiments was prepared freshly using the stock solution at the time of experiment.

Cell culture

Cryopreserved human hepatocytes were purchased from BioIVT and stored in liquid nitrogen until use. Hepatocyte samples were collected from consenting donors under IRB approved protocols at the FDA licensed donor center at BioIVT (<http://www.bioivt.com/>). Hepatocytes were prepared from fresh human tissue and were isolated and frozen within 24 hours of organ removal by BioIVT. The hepatocytes are from human transplant rejected livers and tested negative for hepatitis B and C and HIV1 and 2. Hepatocytes were thawed according to the manufacturer's instructions by warming a vial of the hepatocytes at 37 °C for 90 seconds and suspending them in InVitroGRO HT medium (BioIVT) containing 1

mL TORPEDO™ Antibiotic Mix (BioIVT) per 45 mL media. Hepatocytes were then plated on Biocoat® collagen-coated plates (Corning) and remained in an incubator with a humidified air (95%) and carbon dioxide (CO₂, 5%) condition at 37 °C. HepG2 hepatocellular carcinoma cells were purchased from American Type Culture Collection (ATCC, HB-8065™). The HepG2 cells were cultured in Dulbecco's modified Eagle's medium (DMEM, Gibco) containing 10% fetal bovine serum (FBS, Gibco BRL), 5.5 mM D-glucose, 1 mM pyruvate, 4 mM L-glutamine, and penicillin-streptomycin were kept in an incubator with a humidified air (95%) and carbon dioxide (CO₂, 5%) condition at 37 °C.

Western blot

HepG2 cells or cryopreserved human hepatocytes were plated the day before the treatment on 24-well plates. Cells were incubated for 2 days with complete DMEM containing indicated HCAs (PhIP, MeIQ, or MeIQx) at varying concentrations (0, 10, 25, and 50 µM), then incubated overnight with serum-free DMEM containing indicated HCA treatment conditions. Prior to lysis, cells were treated with insulin (Sigma-Aldrich) at 100 nM (freshly prepared in PBS) for 10 minutes. The cells were lysed immediately in Laemmli buffer (50 mM Tris-Cl [pH 6.8], 2% sodium dodecyl sulfate [SDS; w/v], 0.1% bromophenol blue, 10% [v/v] glycerol) and boiled for 10 minutes. Protein concentrations were determined using Pierce BCA Assay kit (Thermo Scientific) per manufacturer's instructions. One to two µL of 2-mercaptoethanol was added to each sample and boiled again for 5 minutes. Twenty-five to fifty µg of protein per sample was loaded and separated on 4–12% gradient Bis-Tris Plus polyacrylamide gels (Invitrogen). The

gel was transferred to a PVDF membrane and blocked in 5% (w/v) skim milk in tris-buffered saline containing 0.1% Tween 20 (TBST) for 30 minutes. Membranes were incubated with primary antibodies (1:3,000) overnight at 4°C. Membranes were washed 3 times for 5 minutes each with TBST. Membranes were incubated for 1 hour at room temperature with an HRP-conjugated secondary antibody (1:5,000). Membranes were washed with TBST 3 times and then protein-antibody complex was detected with chemiluminescent substrate (Thermo Scientific). Densitometry was performed using Image J analysis software (NIH). Insulin-stimulated phospho-AKT (p-AKT) (Ser473) protein band was quantified and normalized to total AKT. Values presented represent the p-AKT/total-AKT ratio in response to insulin following treatment with indicated HCAs, relative to the vehicle-treated control group. Phospho-FOXO1/FOXO3a/FOXO4 protein band was quantified relative to total FOXO1 protein and normalized to GAPDH. The following antibodies were purchased from Cell Signaling Technology: phosphorylated protein kinase B (p-AKT Ser473; Cat. No. 4060); and protein kinase B (AKT) (Cat. No. 4091); and anti-rabbit IgG, HRP-linked (Cat. No. 7074); and phosphorylated FOXO1 (T24)/FOXO3a (T32)/FOXO4 (T28) (Cat. No. 42022); and FOXO1 (Cat. No. 2880); and GAPDH (Cat. No. 2118). Each experiment was conducted three times with three biological replicates per experiment. For experiments using cryopreserved human hepatocytes, three different donor batches were used with three biological replicates from each batch.

Gene expression analysis by RT-qPCR

HepG2 cells or cryopreserved human hepatocytes were plated the day before the treatment on 12-well plates. Cells were incubated for 3 days with complete media containing indicated HCAs (PhIP, MeIQ, or MeIQx) at varying concentrations (0, 10, 25, and 50 μ M). RNA was isolated from the treated cells using E.Z.N.A. Total RNA Kit 1 (OmegaBiotek) per manufacturer's protocol. cDNA was synthesized using High Capacity cDNA Reverse Transcriptase PCR (Thermo Scientific) per manufacturer's instructions. Gene-specific cDNA was amplified and detected using iTaq Universal SYBR Green Supermix (Bio-Rad) and gene-specific primers and StepOne real-time PCR system (Applied Biosystems). The following primers were used: G6PC, forward 5'-ACGAATCTACCTTGCTGCTCA-3'; reverse 5'-AAAATCCGATGGCGAAGCTG3'. PCK1 or PEPCK, forward 5'-TGATGAGCCGCTAGCTTCAG-3'; reverse 5'-GCCTTTATGTTCTGCAGCCG-3'. FOXO1, forward 5'-AGTGGATGGTCAAGAGCGTG-3', reverse 5'-TTTGAGCTAGTTCGAGGGCG-3'. PPAR α , forward 5'-GATTCGCAATCCATCGGCG-3', reverse 5'-AAACGAATCGCGTTGTGTGAC-3'. PGC1 α , forward 5'-CACGGACAGAACTGAGGGAC-3', reverse 5'-TTCGTTTGACCTGCGCAAAG-3'. 18S rRNA, forward 5'-GGAAGGGCACCACCAGGAGT-3'; reverse 5'-TGCAGCCCCGGACATCTAAG-3'. GAPDH, forward 5'-GGTGAAGCAGGCGTCGGAGG-3'; reverse 5'-GAGGGCAATGCCAGCCCCAG-3'. Results in HepG2 cells were normalized to 18S rRNA, and results in cryopreserved human hepatocytes were normalized to GAPDH. The relative fold change was calculated using the delta-delta Ct ($2^{-\Delta\Delta Ct}$) method with StepOne

software (Applied Biosystems). Each experiment was conducted three times with three biological replicates per experiment. For experiments using cryopreserved human hepatocytes, three different donor batches were used with three biological replicates from each batch.

Extracellular glucose measurements

Twenty-four hours after plating, hepatocytes were incubated for 2 days with media containing the indicated HCA at varying concentrations. Then, hepatocytes were incubated for 6 hours with serum-free, glucose-free DMEM containing varying concentrations of indicated HCAs. Hepatocytes were then incubated for 24 hours with serum-free, glucose-free DMEM containing gluconeogenic substrates (2 mM pyruvate, 20 mM lactate, 0.5 mM L-lysine, and 5 mM glycerol) in addition to the indicated HCAs. Media was collected from individual wells following HCA treatment for extracellular measurement of glucose. Glucose levels from the collected media were measured using a colorimetric glucose oxidase assay kit (Sigma-Aldrich, GAGO-20). Three different donor batches of hepatocytes were used with three biological replicates from each batch. At the end of treatment, cells were washed twice with PBS, fixed with 3.7% formaldehyde (in PBS) for 10 minutes at room temperature, permeabilized with 0.25% Triton X-100 in PBS for 10 minutes at room temperature, and stained with 1 µg/mL DAPI (4',6-diamidino-2-phenylindole) solution for 5 minutes at room temperature. Cells were observed under a fluorescence microscope (BioTek Cytation 5) using the DAPI channel to measure the total number of cells per well. Glucose measurements were normalized to the total number of cells.

Statistical analysis

Differences in relative gene expression, glucose production, and p-AKT/total AKT ratio between the treatment groups vs. control groups were tested for significance by one-way ANOVA followed by Dunnett's Comparison Test. Dose-response linear trend was tested for significance by the post test for linear trend using a linear regression model. All statistical analyses were performed using GraphPad Prism v8.2.1 (GraphPad Software). The results are expressed as the mean \pm the standard error of the mean (SEM). Statistical significance was determined per the following p-values: * indicates $p < 0.05$, ** indicates $p < 0.01$, *** indicates $p < 0.001$, **** indicates $p < 0.0001$.

RESULTS

Measuring cytotoxicity and determining treatment concentrations of HCAs.

We first determined optimal concentrations for HCA treatment by treating HepG2 cells or cryopreserved human hepatocytes with varying concentrations (0 – 50 μ M) of MeIQ, MeIQx, or PhIP (Fig. 2.1A). We selected these concentrations initially, for we and others have previously used similar concentrations for in vitro experiments with HCAs [86]. Following 3 days of treatment, there was no significant cell death at any of the concentrations tested in both HepG2 and cryopreserved human hepatocytes (Fig. 2.1B and C). Thus, we proceeded with a dosing regimen of 0 – 50 μ M of HCAs for following experiments.

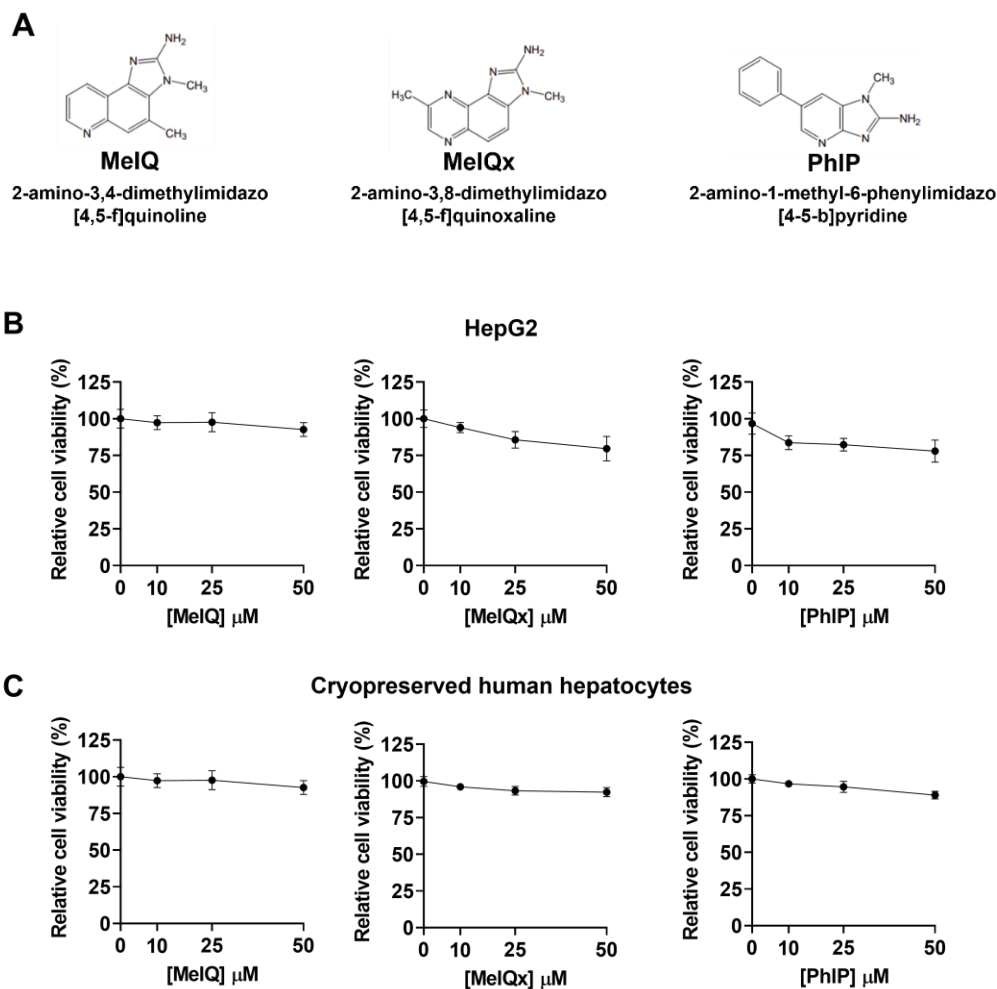


Figure 2.1. Chemical structures of HCAs and relative cell viability of HepG2 and cryopreserved human hepatocytes following HCA treatment. A, Chemical structures of the HCAs (MeIQ, MeIQx, and PhIP) used in the present study. B and C, Relative cell viability after 3-day treatment with HCAs. HepG2 cells (panel B) or cryopreserved human hepatocytes (panel C) were treated with varying concentrations of the indicated HCA for 3 days. Cells were fixed and stained with DAPI solution, and the total cell count was obtained using fluorescence imaging. Each cell count was presented as a percentage of the value in the vehicle-control group. Data points represent mean \pm SEM.

HCAs decrease insulin signaling in HepG2 cells. Decreased insulin signaling is one of the key features of insulin resistance and type II diabetes [6]. Insulin-insulin receptor interaction activates an intrinsic tyrosine protein kinase, which auto-phosphorylates the receptor and downstream substrates [6]. AKT (protein kinase B) is a major downstream effector of insulin signaling and regulates a variety of insulin-mediated responses downstream (e.g., suppression of gluconeogenesis and promotion of lipid synthesis) [6], [87]. For this reason, the level of insulin-induced AKT phosphorylation is often used as an index of insulin sensitivity [87]. Insulin signaling leads to AKT phosphorylation at Thr308 and Ser473. The Thr308 site is phosphorylated first by upstream kinases, and then the Ser473 site is phosphorylated to fully activate the AKT protein [88], [89].

To evaluate the effects of HCAs on insulin sensitivity, we assessed insulin-induced phosphorylation of AKT at Ser473 following HCA treatment in HepG2 cells. HepG2 cells have been used to study hepatic insulin signaling [90], [91], and so we conducted initial experiments using this model and later confirmed these findings in cryopreserved human hepatocytes. HepG2 cells were treated with varying concentrations with MeIQ, MeIQx, or PhIP for 3 days prior to the insulin treatment. Phosphorylated AKT (at Ser473) and total AKT levels were measured using Western blot. HepG2 cells treated with MeIQ and MeIQx showed a concentration-dependent decrease in phosphorylated AKT to total AKT ratio (p-AKT/AKT) in response to insulin, compared to vehicle-control group (Fig. 2.2). There was a 25.0% ($p < 0.01$), 32.0% ($p < 0.01$), and 56.5% ($p < 0.001$) significant reduction in insulin-stimulated p-AKT/AKT following treatment with

MelQ at 10 μ M, 25 μ M and 50 μ M, respectively (Fig. 2.2A). MelQx treatment caused a dose-dependent reduction (linear trend, $p = 0.0002$) in insulin-stimulated p-AKT/AKT, with a 27.7% ($p < 0.05$), 45% ($p < 0.01$), and 51.3% ($p < 0.001$) significant reduction at 10 μ M, 25 μ M, and 50 μ M, respectively (Fig. 2.2B). PhIP treatment at 10 μ M caused a 19% ($p < 0.05$) significant reduction in insulin-stimulated AKT activation, but this reduction was not observed at higher concentrations of PhIP (Fig. 2.2C).

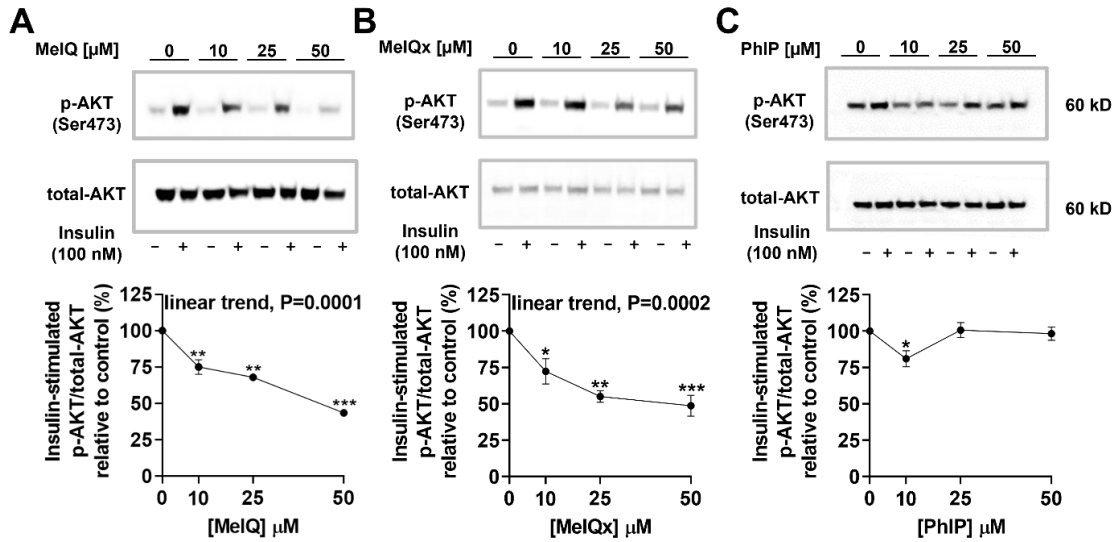


Figure 2.2. Insulin-induced AKT phosphorylation following HCA treatment in HepG2 cells. HepG2 cells were cultured with the indicated concentration of MelQ (panel A), MelQx (panel B), and PhIP (panel C) for 2 days, followed by a serum-starvation overnight. Prior to harvest, cells were treated with 100 nM insulin for 10 minutes. The relative levels of phospho-AKT (p-AKT) (Ser473) and total AKT (AKT) were measured using Western blot. The insulin-stimulated p-AKT/total-AKT ratio was expressed as a percentage of the vehicle-treated control cells. Data points represent mean \pm SEM. Significance of linear trend was determined using the post test for linear trend (linear regression model). *, $p < 0.05$; **, $p < 0.01$; ***, $p < 0.001$.

HCA decrease insulin signaling in cryopreserved human hepatocytes.

Next, we sought to confirm the findings in HepG2 cells using cryopreserved human hepatocytes. We repeated the study using pooled cryopreserved human hepatocytes which represented a mixture of hepatocytes from 10 or 20 donors. Cryopreserved human hepatocytes were treated with 25 μ M MeIQ, MeIQx, or PhIP for 3 days prior to the insulin treatment.

Phosphorylated AKT (at Ser473) and total AKT levels were measured using Western blot. Cryopreserved human hepatocytes treated with MeIQ and MeIQx showed a significant decrease in phosphorylated AKT to total AKT ratio (p-AKT/AKT) in response to insulin, compared to vehicle-control group (Fig. 2.3). There was a 53.5% ($p < 0.05$), 58.5% ($p < 0.01$), and 13.5% reduction in insulin-stimulated p-AKT/AKT following treatment with MeIQ, MeIQx, or PhIP respectively (Fig. 2.3), although the reduction in PhIP-treated cells was not statistically significant, likely because PhIP treatment alone induced p-AKT even in the absence of insulin. These findings are consistent with observations made in HCA-treated HepG2 cells.

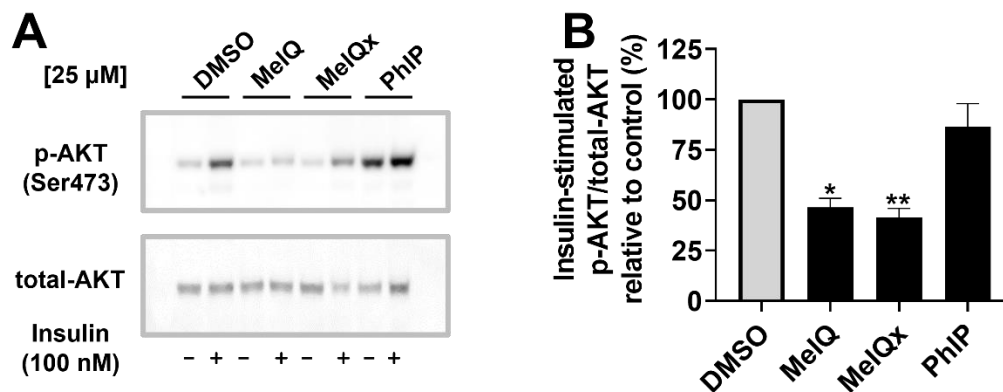


Figure 2.3. Insulin-induced AKT phosphorylation following HCA treatment in cryopreserved human hepatocytes. Cryopreserved human hepatocytes were cultured with 25 μ M of MeIQ, MeIQx, or PhIP for 2 days, followed by a serum-starvation overnight. Prior to harvest, cells were treated with 100 nM insulin for 10 minutes. The relative levels of phospho-AKT (p-AKT) at Ser473 and total AKT (AKT) were measured using Western blot. The insulin-stimulated p-AKT/total-AKT ratio was expressed as a percentage of the vehicle-treated control cells. Data points represent mean \pm SEM. *, $p < 0.05$; **, $p < 0.01$.

HCAs induce expression of gluconeogenic genes in HepG2 cells. The liver plays a key role in regulation of glucose homeostasis by controlling various pathways of glucose metabolism, including glycogenolysis, glycolysis and gluconeogenesis [92]. Regulation of enzymes involved in these pathways is required to maintain proper glucose homeostasis. The gluconeogenesis metabolic pathway generates glucose from non-carbohydrate carbon substrates. Key regulatory enzymes in this pathway are induced under fasting conditions [92] and include glucose 6-phosphatase (G6PC) and phosphoenolpyruvate carboxykinase (PCK1; PEPCK). In insulin resistance, insulin fails to properly phosphorylate AKT, which can lead to dysregulation of gluconeogenic enzymes like G6PC and PCK1, ultimately causing sustained glucose production, despite insulin secretion [7], [87].

To investigate the effects of HCAs on glucose homeostasis, we examined if HCA treatment altered expression of gluconeogenic, insulin receptor-target genes, *G6PC* and *PCK1*, in HepG2 cells. G6PC catalyzes the final step of gluconeogenesis, hydrolyzing glucose-6-phosphate to generate free glucose and inorganic phosphate [93]. PCK1 is the first rate-limiting enzyme of gluconeogenesis that converts oxaloacetate and GTP into phosphoenolpyruvate (PEP) and CO₂ [93]. Treatment of HepG2 cells with MelQ, MelQx, or PhIP resulted in an increase in *G6PC* gene transcripts (Fig. 2.4A-C). Each of the HCAs showed a statistically significant increase in *G6PC* gene transcript levels at the 50 μM concentration, compared to vehicle-control (MelQ, $p < 0.05$; MelQx, $p < 0.0001$; PhIP, $p < 0.0001$). In particular, MelQx treatment at 50 μM resulted in a

nearly 10-fold increase in *G6PC* mRNA compared to the vehicle-control (Fig. 2.4B) and exhibited a dose-response (linear trend, $p = 0.0003$). Similarly, PhIP exhibited a dose-dependent (linear trend, $p < 0.0001$) increase in *G6PC* mRNA (Fig. 2.4C). Additionally, treatment with MeIQ, MeIQx, or PhIP resulted in a significant increase ($p < 0.05$) in *PCK1* gene transcripts in HepG2 cells at the 50 μM concentration, and MeIQx and PhIP both exhibited significant concentration-dependent increases in *PCK1* mRNA (MeIQx, $p = 0.0022$; PhIP, $p = 0.0152$) (Fig. 2.4A-C).

HCAs induce expression of gluconeogenic genes in cryopreserved human hepatocytes. Next, we determined if HCAs altered expression of gluconeogenic, insulin receptor-target genes, *G6PC* and *PCK1*, in cryopreserved human hepatocytes as well. Similar to our findings in HepG2 cells, we observed significant increases in *G6PC* and *PCK1* mRNA levels following MeIQ, MeIQx or PhIP treatment in cryopreserved human hepatocytes (Fig. 2.4D-F). MeIQ, MeIQx, or PhIP treatment each exhibited statistically significant linear dose-response trend in *G6PC* gene transcript levels (MeIQ, $p = 0.0002$; MeIQx, $p < 0.0001$; PhIP, $p = 0.0066$), and MeIQ or MeIQx treatment each exhibited a statistically significant linear dose-response trend in *PCK1* gene transcript levels (MeIQ, $p = 0.0005$; MeIQx, $p = 0.0002$). These results agreed with the observations made in HepG2 cells.

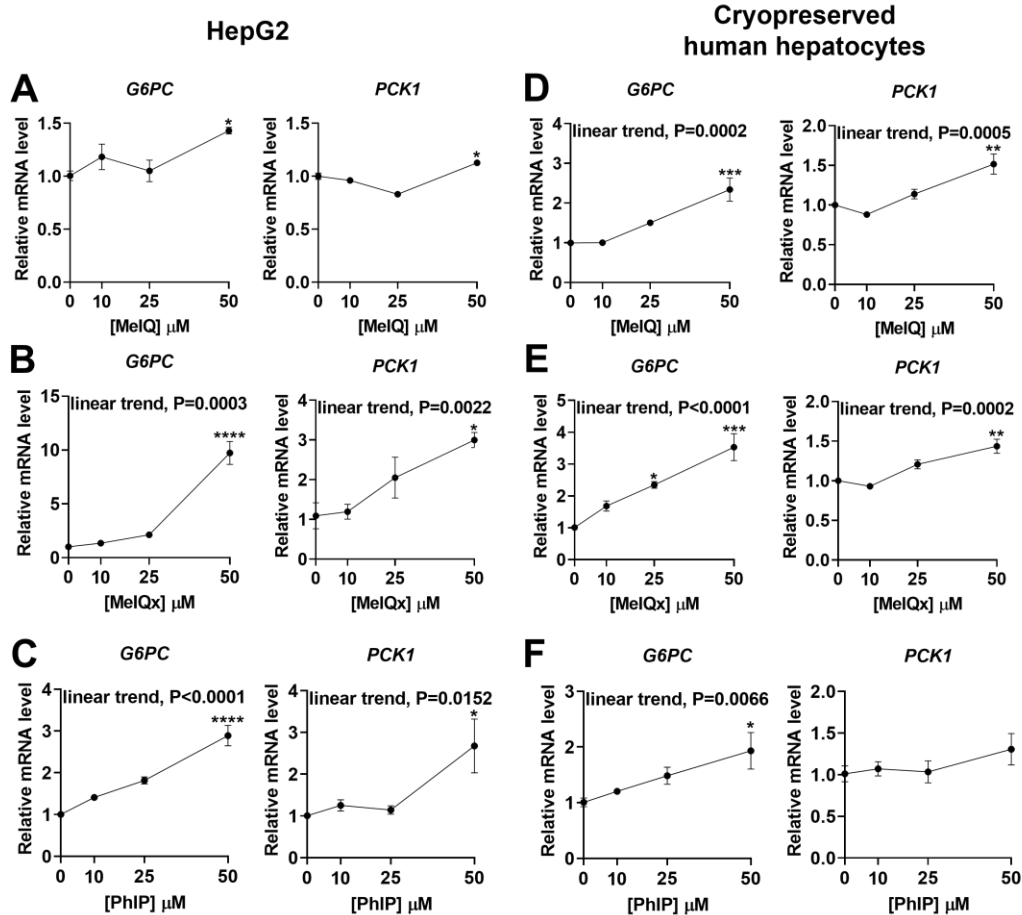


Figure 2.4. Increases in insulin receptor-target genes involved in gluconeogenesis following HCA treatment. HepG2 cells (panels A-C) and cryopreserved human hepatocytes (panels D-F) were cultured with varying concentrations of the indicated HCA (MelQ, MelQx, or PhIP) for 3 days. The relative mRNA level of *G6PC* or *PCK1* was measured by RT-qPCR using 18S ribosomal RNA as an internal control for HepG2 cells and using GAPDH as an internal control for hepatocytes. The mRNA levels were expressed as changes relative to that in the vehicle-control. Data points represent mean \pm SEM. Significance of linear trend was determined using the post test for linear trend (linear regression model). *, $p < 0.05$; **, $p < 0.01$; ***, $p < 0.001$; ****, $p < 0.0001$.

HCAs alter expression of genes that regulate gluconeogenesis in

cryopreserved human hepatocytes. Since HCA treatment induced expression of *G6PC* and *PCK1*, in cryopreserved human hepatocytes, we investigated if HCAs altered the expression of additional genes that regulate gluconeogenesis, including *FOXO1*, *PPAR α* and *PGC1 α* . Forkhead box O1 (*FOXO1*) gene encodes a transcription factor protein that regulates metabolic homeostasis and insulin signaling [94]. *FOXO1* regulates expression of gluconeogenic genes, *G6PC* and *PCK1*, and increased expression of *FOXO1* correlates with increased expression of *G6PC* and *PCK1* [95]. Our study also showed an increased *FOXO1* expression following treatment with HCAs in hepatocytes (Fig. 2.5 A-C). Cryopreserved human hepatocytes treated with MeIQx showed a statistically significant increase ($p < 0.05$) in *FOXO1* mRNA levels, and hepatocytes treated with MeIQ showed a slight increase in *FOXO1* mRNA, though not statistically significant, while PhIP-treated hepatocytes did not show a change in *FOXO1* levels.

Furthermore, peroxisome proliferator activated receptor alpha (*PPAR α*) regulates expression of genes involved in glucose and lipid metabolism and transport [96]. Although hepatocytes treated with MeIQ showed only a marginal increase in *PPAR α* mRNA levels that was not statistically significant, hepatocytes treated with MeIQx and PhIP showed a significant increase ($p < 0.01$, $p < 0.0001$, respectively) in *PPAR α* mRNA levels (Fig. 2.5 A-C). These results indicate that HCA treatment of hepatocytes lead to changes in gene expression of some of the key regulators of gluconeogenesis.

PPARG Coactivator 1 Alpha ($PGC1\alpha$) is a transcriptional co-activator that regulates expression of genes involved in glucose and fatty acid metabolism and is a known regulator of hepatic gluconeogenesis [97], [98]. Cryopreserved human hepatocytes treated with MeIQ, MeIQx, or PhIP expressed a significant decrease ($p < 0.001$) in $PGC1\alpha$ mRNA levels (Fig. 2.5 A-C). These results contradict what was expected since a reduction in gene expression of this co-activator of gluconeogenic genes does not correlate with increased expression of $G6PC$ and $PKC1$ genes observed after exposure to HCAs. However, $PGC1\alpha$ is not the sole regulator of these genes. Additionally, type 2 diabetic patient livers have been shown to have decreased $PGC1\alpha$ levels [99]–[101], and mice with low hepatic $PGC1\alpha$ accumulate excess lipids in their livers [102]–[104], which is a hallmark of insulin resistance. Thus, decreased $PGC1\alpha$ expression may be associated with the metabolic changes observed after HCA treatment, and this association and its mechanism need to be explored further.

To further investigate the mechanism by which HCAs lead to increased gluconeogenic gene expression in hepatocytes, we investigated changes in FOXO1, a transcription factor for gluconeogenic genes, at the protein level. FOXO1 is transcriptionally active only in its non-phosphorylated form [93]. FOXO1 protein is phosphorylated by AKT, which alters DNA binding activity and thus halts transcription of gluconeogenic genes [93]. Failure to phosphorylate FOXO1 renders the protein active and thus induces gluconeogenesis [105]. Cryopreserved human hepatocytes treated with MeIQ, MeIQx, or PhIP showed a statistically significant decrease in phospho-FOXO1 (Thr24) relative to total

FOXO1 protein when compared to the vehicle-treated control (MeIQ, $p < 0.001$; MeIQx, $p < 0.01$; PhIP, $p < 0.001$) (Fig. 2.5 D-E). This indicates that increased FOXO1 activity may be partially responsible for increased gluconeogenic gene expression in HCA-treated hepatocytes.

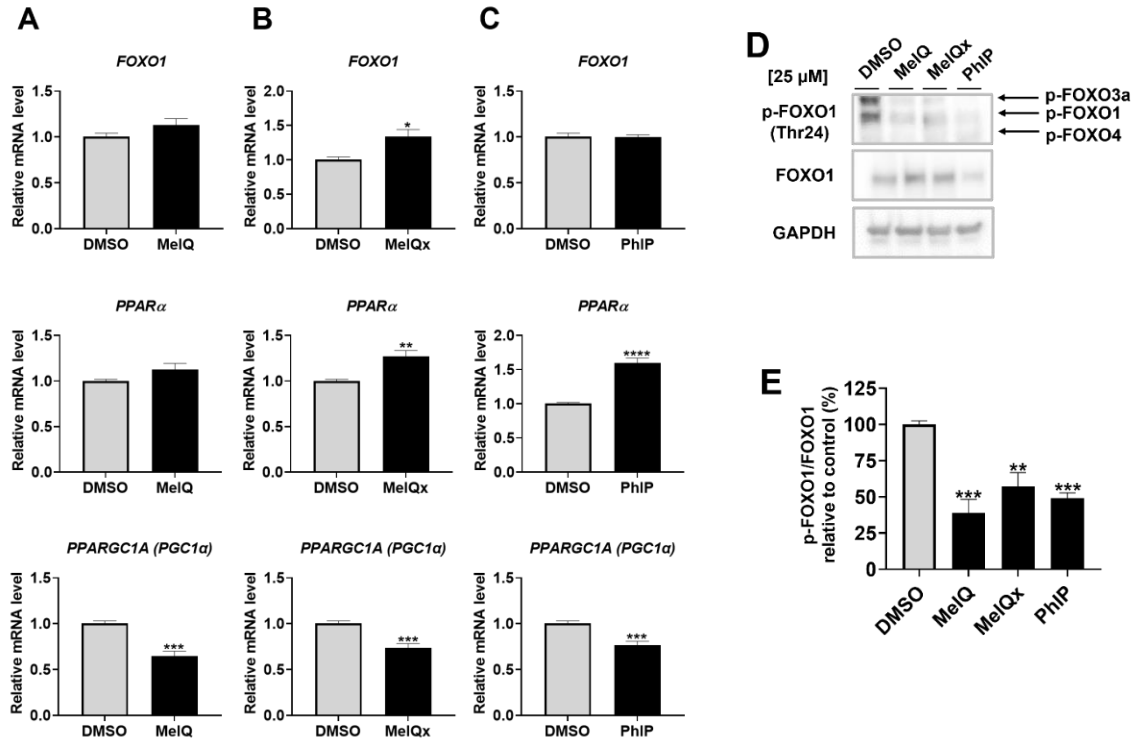


Figure 2.5. Changes in expression of genes and protein that regulate gluconeogenesis following HCA treatment in cryopreserved human hepatocytes. Cryopreserved human hepatocytes were cultured with 25 μ M of the indicated HCA (MelQ, MelQx, or PhIP) for 3 days. The relative mRNA level of the indicated gene was measured by RT-qPCR using GAPDH as an internal control (panels A-C). The mRNA levels were expressed as changes relative to that in the vehicle-control. Relative levels of phospho-FOXO1 (p-FOXO1) at Thr24, FOXO1, and GAPDH were measured using Western blot (panel D). The p-FOXO1 protein level was measured relative to total FOXO1 protein level and normalized to GAPDH protein level, then presented as relative change compared to the vehicle-control (panel E). Bars represent mean \pm SEM. *, $p < 0.05$; **, $p < 0.01$; ***, $p < 0.001$; ****, $p < 0.0001$.

HCAAs increase glucose production in cryopreserved human hepatocytes.

Development of insulin resistance leads to altered glucose homeostasis, and as a result, increased and sustained glucose production is a hallmark of insulin resistance and type II diabetes [6]. Since HCA treatment on HepG2 cells and hepatocytes lead to an increase in expression of gluconeogenic, insulin receptor-target genes, *G6PC* and *PCK1*, we tested if HCA treatment leads to increased glucose production in cryopreserved human hepatocytes. During the HCA treatment, hepatocytes were serum- and glucose-starved before being provided with gluconeogenic substrate media containing pyruvate, lactate, L-lysine, and glycerol. The level of extracellular glucose in the media was measured using a glucose oxidase-based assay and then normalized to total cell count. The HCA treatments resulted in an increase in extracellular glucose in cryopreserved human hepatocytes, suggestive of an increase in glucose production (Fig. 2.6). Although the differences in the extracellular glucose level between the control group and individual MeIQ treatment groups were not found statistically significant, there was a statistically significant linear trend (i.e., concentration-dependent increase, $p = 0.0032$) (Fig. 2.6A). There was a similar concentration-dependent effect ($p = 0.0228$) by MeIQx, and the highest concentration of MeIQx caused nearly a 2-fold increase in extracellular glucose, compared to the vehicle-control (Fig. 2.6B). PhIP treatment also caused an averaged 34% increase in extracellular glucose although there was no dose-response observed (Fig. 2.6C).

These results suggest that HCAs can induce glucose production in human hepatocytes at variable levels.

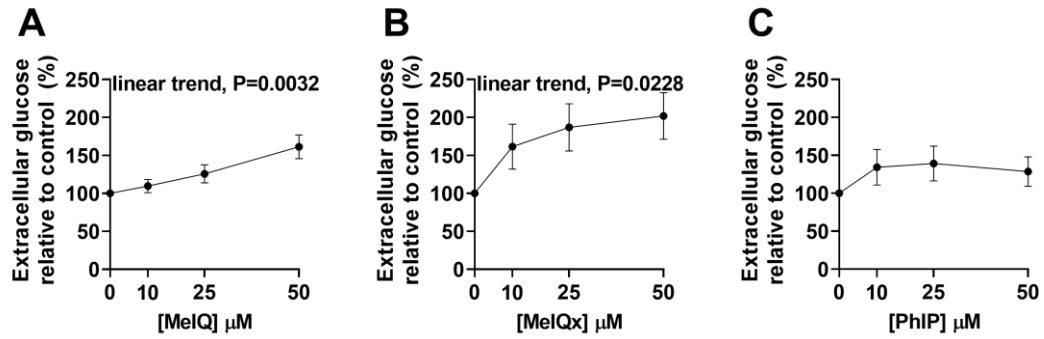


Figure 2.6. Increases in glucose production following HCA treatment in

cryopreserved human hepatocytes. Cryopreserved human hepatocytes were cultured with varying concentrations of the indicated HCA MeIQ (panel A), MeIQx (panel B), or PhIP (panel C) for 2 days, and glucose- and serum-starved overnight. The cells were then incubated in a gluconeogenic media containing 2 mM pyruvate, 0.5 mM lysine, 20 mM lactate, and 5 mM glycerol for 24 hours. Media was collected, and extracellular glucose was measured using a glucose oxidase-based assay. Glucose concentration was normalized to total cell count and expressed as a percentage of the value found in the vehicle-control cells. Data points represent mean \pm SEM. Significance of linear trend was determined using the post test for linear trend (linear regression model).

DISCUSSION

The current study demonstrated, for the first time, that common HCAs found in cooked meat can cause insulin resistance and increases in glucose production and gluconeogenic gene expression in human hepatocytes. Notably, three different HCAs commonly found in cooked meats (i.e., MeIQ, MeIQx, and PhIP) and two different cell model systems (i.e., HepG2 and cryopreserved human hepatocytes) were used to establish these findings, indicating that they are not unique to a particular HCA or exclusive to one type of cell population.

The present findings imply that exposure to HCAs via consumption of cooked meat could potentially lead or contribute to development of insulin resistance and hyperglycemia, which are key hallmarks of type II diabetes and metabolic syndrome. This is supported by several epidemiological studies. As previously mentioned, Zelber-Sagi and colleagues reported that consumption of meat cooked via “unhealthy” methods (e.g., grilling or broiling to well-done level or frying) is related to insulin resistance and found that there is a significant association between estimated HCA consumption via cooked meat and insulin resistance, among both general population and patients with non-alcoholic fatty liver disease (odds ratio [OR] = 1.92; 95% confidence interval [CI] = 1.12-3.30) [43]. Importantly, after multivariate adjustment, the association was independent of cholesterol and saturated fat intake. A higher frequency of unhealthy cooking methods, such as broiling, barbequing, and roasting, was each independently associated with a higher risk of type II diabetes. In contrast, the frequency of stewing or boiling red meats was not associated with type II diabetes risk [44].

These studies suggest that unhealthy cooking methods, which favor production of HCAs, significantly increase the risk of developing insulin resistance or type II diabetes. Accordingly, the authors suggested exposure to polycyclic aromatic hydrocarbons and HCAs commonly present in cooked meat as a potential underlying, biological mechanism for this phenomenon [45]. In the follow-up study of three prospective cohorts, the authors reported that open-flame and/or high-temperature cooking >15 times/month, compared with <4 times/month, the hazard ratio and 95% CI of type II diabetes was 1.28 and 1.18-1.39, respectively [44]. In addition, estimated intake of HCAs was also associated with an increased type II diabetes risk, and this was the first study linking higher estimated dietary HCA intake with an increased risk of type II diabetes [44]. Taken together, these previous and our present findings support the hypothesis that exposure to HCAs produced during unhealthy cooking of meat contributes to pathogenesis of insulin resistance and type II diabetes.

The mechanism by which HCAs induce insulin resistance in hepatocytes is unknown. Pathological features that are commonly associated with cellular insulin resistance include inflammation [14], mitochondrial dysfunction [15], ER stress [16], and lipotoxicity [17]. One of the common underlying attributes of these features is increased reactive oxygen species (ROS) [6] and ROS have been shown to play a causal role in different forms of insulin resistance [18]. Multiple mechanisms by which elevated ROS may induce or contribute to insulin resistance have been proposed. For example, ROS are known to activate JNK and IKK α [106], [107] which are considered key contributors to the development

of insulin resistance in obesity and diabetes [108]. JNK and IKK can inhibit insulin receptor signaling by phosphorylating insulin receptor substrate 1 (IRS1) at serines. Serine-phosphorylation of IRS1 inhibits its association with the insulin receptors, promotes its degradation and suppresses binding of PI3K [6], [108], thus, blunting the effects of downstream insulin signaling. Likewise, a mechanism by which HCAs induces insulin resistance in hepatocytes may be contributed by increased ROS. In fact, consumption of HCA from cooked meat has been associated with increased systemic level of oxidative stress. A study of 561 adults in Brazil found that estimated intake of HCAs from meat is associated with the level of oxidative stress, estimated by malondialdehyde concentration in the plasma (OR 1.17; 95% CI 1.01-1.38) [109]. In support, we have observed that HCAs, including PhIP and MeIQx, cause increases in DNA damage and ROS level in Chinese hamster ovary (CHO) cells that express human *CYP1A2* and *NAT2* [110], [111]. Moreover, the level of DNA damage and ROS production was higher in cells expressing a rapid allele of *NAT2* (*NAT2*4*), compared to a slow allele, *NAT2*5B* [110]. This data indicates that HCAs induce cellular ROS levels, and this effect is dependent on their metabolism by *CYP1A2* and *NAT2*. Based on this, we speculate that a potential mechanism for HCA-induced insulin resistance may be related to the formation of ROS during or following HCA metabolism. It is well-known that mutagenicity of HCAs requires metabolism. Metabolic activation of HCAs occurs primarily in the liver by *CYP1A2*-mediated *N*-oxidation of the exocyclic amine groups to form the *N*-hydroxy-HCA derivatives [50], [51]. The *N*-hydroxy-HCA metabolites can undergo phase II conjugation

reactions to form highly reactive esters. These esters may undergo heterolytic cleavage to generate reactive nitrenium ions, which are the ultimate carcinogenic metabolite [112]. NAT2 is one of the primary enzymes responsible for catalyzing this phase II metabolism. *NAT2* expresses a well-defined genetic polymorphism in humans [113]. Depending on the combination of *NAT2* alleles they carry, individuals can be categorized into rapid, intermediate, or slow acetylators who exhibit differential metabolism of aromatic amines, including HCAs [113]. However, it is currently unknown if metabolism of HCAs is also required for their effects on hepatic insulin resistance and glucose production. Additionally, our lab has reported that human *NAT2* is transcriptionally regulated by glucose and insulin in liver cancer cell lines, including HepG2 cells [114]. We speculate that *NAT2*-mediated metabolism of HCAs is an important determinant of their metabolic effects in hepatocytes. A further investigation is required to assess the contribution of HCA metabolism to their effects on insulin sensitivity and glucose production.

A notable observation from the current study is that MeIQ and MeIQx caused a dose-dependent reduction in insulin sensitivity and a dose-dependent increase in glucose production, while the effects of PhIP were either not dose-dependent or absent. Although PhIP did, however, lead to a significant decrease ($p < 0.05$) in insulin sensitivity at 10 μM in HepG2 cells, it failed to produce a similar response in cryopreserved hepatocytes and its ability to induce glucose production was marginal. The differences in structure of these HCAs (Fig. 2.1A) and their metabolism are potentially responsible for this observation. The

structure of PhIP is notably different from other compounds in its classification. Most HCAs, including MeIQ and MeIQx, have fully planar aromatic structures with no bulky out-of-plane functionalities [24]. PhIP, in contrast, possesses a phenyl moiety that is not necessarily co-planar with the main bicyclic imidazopyridine, and so the metabolism of PhIP is different from other HCAs. CYP1A2 primarily catalyzes the detoxification of MeIQx by oxidation of the 8-methyl group, whereas it catalyzes the bioactivation of PhIP by oxidation of the exocyclic amine group [115], [116], and so it is speculated that alternative enzymes may be involved in PhIP-induced toxicity. In the neonatal mouse model, higher incidences of lymphoma and hepatocellular adenoma occurred in female P4501A2-knockout mice than in wild-type mice exposed to high doses of PhIP (11 or 22 mg/kg), indicating that PhIP-induced carcinogenesis is independent of P450 1A2 expression [117]. It was also observed that PhIP-DNA adduct formation was independent of NAT2 acetylator activity in adult female congenic rapid and slow rats, while MeIQx-DNA adducts, particularly in the liver, were significantly lower in slow acetylators [118]. The structural and metabolic differences responsible for discrepancies in HCA-induced genotoxicity and carcinogenicity could also potentially be responsible for the discrepancies reported here (i.e., PhIP not exhibiting a linear dose-response in the results reported).

In summary, HCAs commonly found in cooked meat caused insulin resistance and increased glucose production in HepG2 and human hepatocytes. We have also shown that insulin receptor-target genes involved in

gluconeogenesis are upregulated in human hepatocytes following exposure to HCAs, indicating that upregulation in gluconeogenesis may, at least in part, contribute to HCA-induced increase in glucose production. Taken together, the current findings imply that, independent of meat consumption, dietary exposure to HCAs contribute to pathogenesis of insulin resistance and hyperglycemia. Additional studies are required to determine the precise mechanism by which HCAs elicit the responses reported here. Future studies should also explore the role of metabolism of HCAs as well as *NAT2* genetic polymorphisms on metabolic effects of HCAs.

CHAPTER 3

INDUCTION OF GLUCOSE PRODUCTION BY HETEROCYCLIC AMINES IS DEPENDENT ON *N*-ACETYLTRANSFERASE 2 GENETIC POLYMORPHISM IN HUMAN HEPATOCYTES

INTRODUCTION

Metabolic syndrome is characterized by a cluster of adverse health conditions, including insulin resistance and hyperglycemia, in addition to hypertension, central obesity, and abnormal cholesterol or triglyceride levels [1]. In the United States, it is estimated that more than one third of the U.S. adult population has metabolic syndrome [2], [3]. These individuals are at an increased risk of health complications including, heart attack, fatty liver, and stroke [4]. Poor diet, lack of exercise, exposure to environmental pollutants, and genetic variants involved in glucose and lipid metabolism have been identified as some of the risk factors for insulin resistance, type II diabetes, and metabolic syndrome [1], [119]–[122].

Heterocyclic amines (HCAs) are known mutagens and carcinogens [24], [84] primarily found in cooked meat. While most existing studies of HCAs have assessed their mutagenicity and carcinogenicity, a recent epidemiological study has linked dietary HCA exposure via cooked meat to the development of insulin resistance [43]. In support of this finding, we have recently reported that HCAs induce insulin resistance and promote glucose production in human hepatocytes [122], suggesting that exposure to HCAs may contribute to the development of metabolic syndrome or type II diabetes.

Many HCAs require hepatic bioactivation to yield mutagenic and carcinogenic effects [72], [73], and, for this reason, the extent of metabolism of HCAs is known to impact their mutagenicity and carcinogenicity [110], [123]–[125]. In general, following *N*-hydroxylation mediated by CYP1A2 [72], HCAs are often *O*-acetylated by arylamine *N*-acetyltransferase 2 (NAT2). *NAT2* expresses a well-defined genetic polymorphism in humans [113]. Depending on the combination of *NAT2* alleles they carry, individuals can be categorized into rapid, intermediate, or slow acetylators who exhibit differential metabolism of aromatic amines and HCAs [113]. However, it is currently unknown if metabolism of HCAs alters their effects on hepatic insulin sensitivity and glucose production. In the present study, we investigated the contribution of *NAT2* genetic polymorphism to increased glucose production in hepatocytes following exposure to HCAs.

MATERIALS AND METHODS

Heterocyclic amines (HCAs)

All HCAs were purchased from Toronto Research Chemicals. Stock concentrations of 10 mM were prepared into solution with dimethyl sulfoxide (DMSO). Stock solutions were used to freshly prepare media containing the indicated working concentrations (10, 25, or 50 μ M) of HCAs at the time of experiment.

Cell culture

Cryopreserved human hepatocytes were purchased from BioIVT and stored in liquid nitrogen until use. Hepatocyte samples were collected from consenting donors under IRB approved protocols at the FDA licensed donor center at BioIVT (<http://www.bioivt.com/>). Hepatocytes were prepared from fresh human tissue and were isolated and frozen within 24 hours of organ removal by BioIVT. The hepatocytes are from human transplant rejected livers and tested negative for hepatitis B and C and HIV1 and 2. Hepatocytes were thawed and plated according to the manufacturer's instructions as previously reported [122].

Determination of NAT2 genotype and phenotype

Genomic DNA was isolated from pelleted cells prepared from cryopreserved human hepatocyte samples using the QIAamp DNA Mini Kit (QIAGEN, Valencia, CA) per manufacturer's instructions, and NAT2 genotypes and deduced phenotypes were determined as previously described [126]. Individuals possessing two NAT2 alleles associated with rapid acetylation activity (*NAT2*4*)

were classified as rapid acetylators; individuals possessing one of these alleles and one allele associated with slow acetylation activity (*NAT2*5B*, *NAT2*6A*, and *NAT2*7B*) were classified as intermediate acetylators, and those individuals possessing two slow acetylation alleles were classified as slow acetylators.

Extracellular glucose measurements

To measure glucose production, twenty-four hours after plating, hepatocytes were incubated for 2 days with media containing the indicated HCA. Then, hepatocytes were incubated for 6 hours with serum-free, glucose-free DMEM containing indicated HCAs. Hepatocytes were then incubated for 24 hours with serum-free, glucose-free DMEM containing gluconeogenic substrates (2 mM pyruvate, 20 mM lactate, 0.5 mM L-lysine, and 5 mM glycerol) in addition to the indicated HCAs. Glucose levels from the media were measured using a colorimetric glucose oxidase assay kit (Sigma-Aldrich, GAGO-20), and data was normalized to total number of cells, as previously reported [122].

Statistical analysis

Changes in glucose production are presented relative to the control group and were tested for significance by one-way ANOVA followed by Dunnett's Comparison Test. Dose-response linear trend was tested for significance by the post test for linear trend using a linear regression model. The results are expressed as the mean \pm the standard error of the mean (SEM). Statistical significance was determined per the following p-values: * indicates $p < 0.05$, ** indicates $p < 0.01$, *** indicates $p < 0.001$, **** indicates $p < 0.0001$.

RESULTS

Changes in glucose production following HCA exposure in human

hepatocytes is dependent on NAT2 acetylator phenotype. To investigate if the rate of HCA metabolism by NAT2 affects HCA-induced alteration in glucose homeostasis in hepatocytes, we treated cryopreserved human hepatocytes categorized according to NAT2 acetylator phenotype (i.e., slow, intermediate, or rapid) with HCAs and measured extracellular glucose level using a glucose oxidase-based assay (see Materials and Methods). In slow NAT2 acetylator human hepatocytes, we found no difference in glucose production between the control group and HCA-treated groups for any HCA at any concentration (Fig. 3.1A, Fig. 3.2A, Fig. 3.3A). In intermediate NAT2 acetylator human hepatocytes, we found a statistically significant increase ($p < 0.01$) in glucose production among hepatocytes treated with 25 and 50 μM MeIQ (Fig. 3.1B). There was also a statistically significant, dose-dependent linear increase in glucose production among intermediate NAT2 acetylator hepatocytes treated with MeIQ or MeIQx (MeIQ, $p = 0.0007$; MeIQx, $p = 0.0245$) (Fig. 3.1B, Fig. 3.2B). No significant ($p > 0.05$) changes in glucose production were observed in PhIP-treated hepatocytes that were either slow or intermediate NAT2 acetylators (Fig. 3.3A and B), and the changes in glucose production with MeIQ and MeIQx treatment in slow and intermediate NAT2 acetylators were modest in comparison to rapid NAT2 acetylators. In contrast, rapid NAT2 acetylator human hepatocytes showed a significant increase in glucose production at nearly every concentration with all 3 HCAs tested (Fig. 3.1C, Fig. 3.2C, Fig. 3.3C). Additionally, rapid NAT2 acetylator

human hepatocytes showed a statistically significant, dose-dependent linear increase in glucose production after exposure to MeIQ ($p = 0.0023$), MeIQx ($p < 0.0001$), and PhIP ($p = 0.0049$).

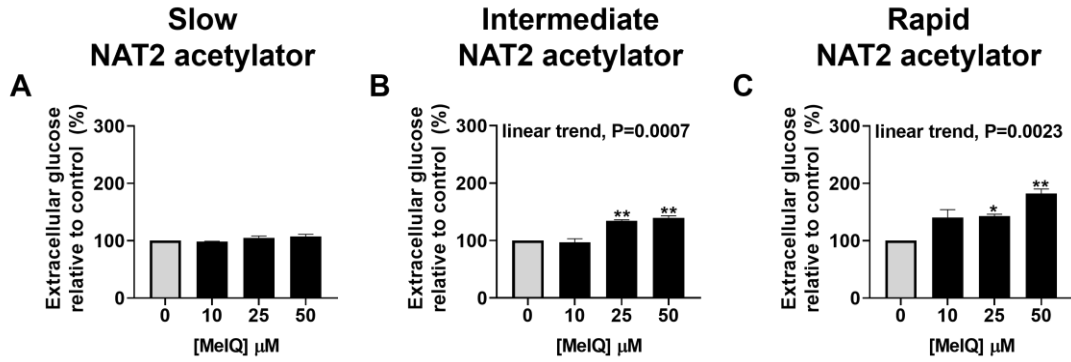


Figure 3.1. Glucose production in slow, intermediate, and rapid NAT2 acetylator cryopreserved human hepatocytes following MeIQ treatment.

Slow (panel A), intermediate (panel B), or rapid (panel C) cryopreserved human hepatocytes were cultured with varying concentrations of MeIQ for 2 days, and glucose- and serum-starved overnight. The cells were then incubated in a gluconeogenic media containing 2 mM pyruvate, 0.5 mM lysine, 20 mM lactate, and 5 mM glycerol for 24 hours. Media was collected, and extracellular glucose was measured using a glucose oxidase-based assay. Glucose concentration was normalized to total cell count and expressed as a percentage of the value found in the vehicle-control cells. Bars represent mean \pm SEM. Statistical significance was determined by one-way ANOVA followed by Dunnett's Comparison Test. Significance of linear trend was determined using the post test for linear trend (linear regression model). *, $p < 0.05$; **, $p < 0.01$.

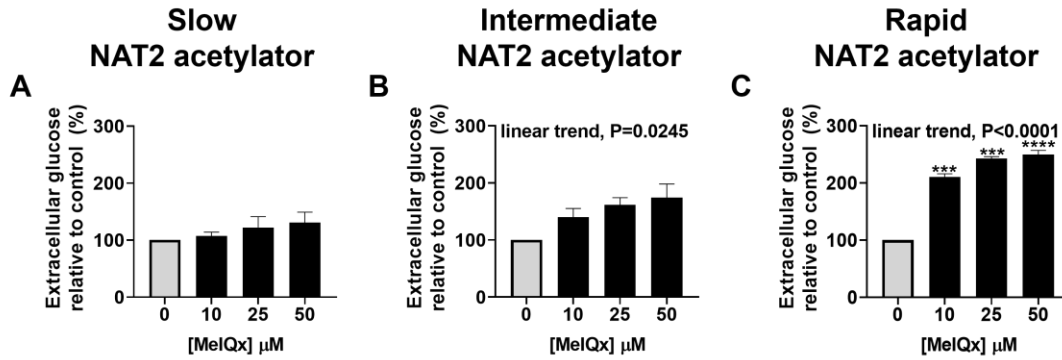


Figure 3.2. Glucose production in slow, intermediate, and rapid NAT2

acetylators cryopreserved human hepatocytes following MelQx treatment.

Slow (panel A), intermediate (panel B), or rapid (panel C) cryopreserved human

hepatocytes were cultured with varying concentrations of MelQx for 2 days, and

glucose- and serum-starved overnight. The cells were then incubated in a

gluconeogenic media containing 2 mM pyruvate, 0.5 mM lysine, 20 mM lactate,

and 5 mM glycerol for 24 hours. Media was collected, and extracellular glucose

was measured using a glucose oxidase-based assay. Glucose concentration was

normalized to total cell count and expressed as a percentage of the value found

in the vehicle-control cells. Bars represent mean \pm SEM. Statistical significance

was determined by one-way ANOVA followed by Dunnett's Comparison Test.

Significance of linear trend was determined using the post test for linear trend

(linear regression model). ***, $p < 0.001$; ****, $p < 0.0001$.

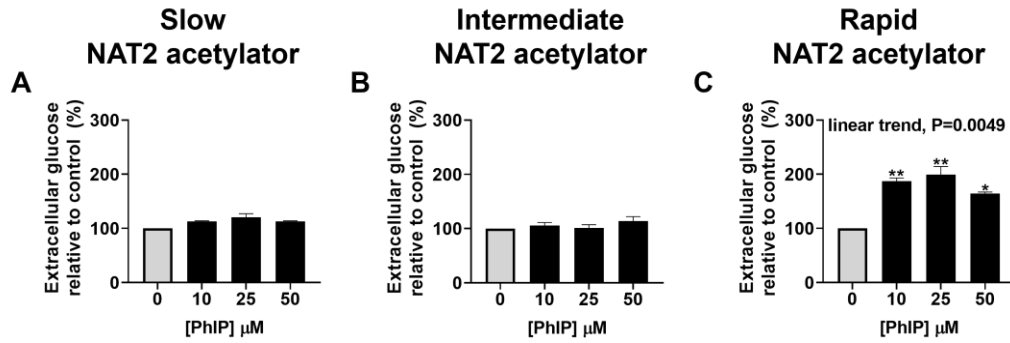


Figure 3.3. Glucose production in slow, intermediate, and rapid NAT2 acetylator cryopreserved human hepatocytes following PhIP treatment.

Slow (panel A), intermediate (panel B), or rapid (panel C) cryopreserved human hepatocytes were cultured with varying concentrations of PhIP for 2 days, and glucose- and serum-starved overnight. The cells were then incubated in a gluconeogenic media containing 2 mM pyruvate, 0.5 mM lysine, 20 mM lactate, and 5 mM glycerol for 24 hours. Media was collected, and extracellular glucose was measured using a glucose oxidase-based assay. Glucose concentration was normalized to total cell count and expressed as a percentage of the value found in the vehicle-control cells. Bars represent mean \pm SEM. Statistical significance was determined by one-way ANOVA followed by Dunnett's Comparison Test. Significance of linear trend was determined using the post test for linear trend (linear regression model). *, $p < 0.05$; **, $p < 0.01$.

DISCUSSION

Insulin resistance leads to defective glucose homeostasis, and subsequently, increased and sustained glucose production, which is a hallmark of type II diabetes [6]. We previously reported that HCAs cause increased glucose production in cryopreserved human hepatocytes [122]. In the current study, we investigated the role of hepatic metabolism on HCA-induced glucose production. It is well-known that mutagenicity of HCAs requires metabolism [72], but little is known about the role of HCA metabolism in the context of HCA-mediated insulin resistance and disruption of glucose homeostasis. Many HCAs are bioactivated by the phase II metabolic enzyme, NAT2, following *N*-hydroxylation by CYP1A2 [72]. As previously mentioned, NAT2 expresses a well-defined genetic polymorphism in humans, and the varying genotypes are highly correlated to categorized phenotypes, including rapid, intermediate, and slow acetylators who exhibit differential metabolism of aromatic amines and HCAs [113]. We measured glucose production in slow, intermediate, and rapid NAT2 acetylator cryopreserved human hepatocytes following HCA exposure and found that HCAs cause significant and most robust increases in glucose production in rapid NAT2 acetylators. In contrast, only marginal increases in glucose production occurred in intermediate NAT2 acetylators, and no change was observed in slow NAT2 acetylators. This indicates that, similar to metabolic biotransformation that leads to mutagenicity, HCA-mediated disruption of glucose homeostasis requires bioactivation by NAT2 that is modified by its genetic polymorphism.

Our previous report that HCAs cause a dose-dependent trend of increased glucose production but no statistical differences between control vs. treatment groups [122] can be explained by the findings presented here. Previous experiments utilized pooled cryopreserved human hepatocytes, which include a mixture of hepatocytes from 10 or 20 donors. It is likely that pooled vials of hepatocytes include a mixture of NAT2 acetylator phenotypes among donors, and thus the increased glucose production only apparent from rapid NAT2 acetylators was likely diminished by slow and intermediate NAT2 acetylators within the same vial of donors.

In summary, based on our findings, it is abundantly clear that metabolism of HCAs by NAT2 is required for their effects on glucose homeostasis. Accordingly, dysregulation of glucose homeostasis by HCAs was most robust in rapid NAT2 acetylators. These findings suggest that individuals with rapid NAT2 acetylator phenotypes may be at a greater risk of developing hyperglycemia and insulin resistance following dietary exposure to HCAs. Additional studies are needed to elucidate the precise mechanism by which HCAs and their metabolites lead to increased glucose production in hepatocytes.

CHAPTER 4

METABOLIC EFFECTS OF HETEROCYCLIC AMINES IS DEPENDENT ON *N*- ACETYLTRANSFERASE 2 GENETIC POLYMORPHISM IN HUMAN HEPATOCYTES

INTRODUCTION

Metabolic syndrome, commonly known as syndrome X, is characterized by a cluster of adverse health conditions that lead to increased risk of cardiovascular disease and other related health complications, including stroke, heart attack, and fatty liver [4]. Some of the medical conditions that constitute metabolic syndrome include insulin resistance and hyperglycemia, in addition to hypertension, central obesity, and abnormal cholesterol or triglyceride levels [1]. In the United States, it is estimated that more than one third of the U.S. adult population has metabolic syndrome, and cases of metabolic syndrome have been growing nationally and globally over the last several decades [2], [3]. Poor diet, lack of exercise, exposure to environmental pollutants, and genetic variants involved in glucose and lipid metabolism have been identified as some of the risk factors

for insulin resistance, type II diabetes, and metabolic syndrome [1], [119]–[121], [127].

Heterocyclic amines (HCAs) are mutagens and carcinogens [24], [84] primarily found in cooked meat, although they have also been identified in other products including cigarette smoke [25], [26]. Some of the most common HCAs found in cooked meat includes MeIQ (2-amino-3,4-dimethylimidazo[4,5-f]quinoline), MeIQx (2-amino-3,8-dimethylimidazo[4,5-f]quinoxaline), and PhIP (2-amino-1-methyl-6-phenylimidazo[4,5-b]pyridine) [112]. Thus far, most studies of HCAs have assessed their mutagenicity and carcinogenicity [24], [33], [37], [112]. However, a recent epidemiological study has linked dietary HCA exposure via cooked meat to the development of insulin resistance [43]. Furthermore, we have recently reported that HCAs induce insulin resistance and promote glucose production in human hepatocytes [127], suggesting that exposure to HCAs may contribute to the development of conditions associated with metabolic syndrome or type II diabetes.

Many HCAs require hepatic bioactivation to yield mutagenic and carcinogenic effects [72], [73], and the metabolic pathways of HCAs has been well characterized [110], [123]–[125]. In general, following *N*-hydroxylation mediated by Cytochrome P450 1A2 (CYP1A2) [72], HCAs are often *O*-acetylated by arylamine *N*-acetyltransferase 2 (NAT2). NAT2 is a xenobiotic- and drug-metabolizing enzyme that expresses a well-defined genetic polymorphism in humans [113]. Depending on the combination of *NAT2* alleles they carry, individuals can be categorized into rapid, intermediate, or slow acetylators who

exhibit differential metabolism of aromatic amines and HCAs [113]. We recently reported that induction of glucose production by HCAs is dependent on *NAT2* genetic polymorphism in human hepatocytes [128]. However, it is currently unknown if *NAT2* acetylator phenotype also alters the effects of HCAs on hepatic insulin sensitivity and gluconeogenic gene expression. In the present study, we investigated the contribution of *NAT2* genetic polymorphism to altered insulin sensitivity following exposure to HCAs in human hepatocytes.

MATERIALS AND METHODS

Heterocyclic amines (HCAs)

All HCAs were purchased from Toronto Research Chemicals. They were prepared into a solution with dimethyl sulfoxide (DMSO) at a stock concentration of 10 mM. The media containing the indicated concentration of HCAs used for experiments was prepared freshly using the stock solution at the time of experiment.

Cell culture

Cryopreserved human hepatocytes were purchased from BioIVT and stored in liquid nitrogen until use. Hepatocyte samples were collected from consenting donors under IRB approved protocols at the FDA licensed donor center at BioIVT (<http://www.bioivt.com/>). Hepatocytes were prepared from fresh human tissue and were isolated and frozen within 24 hours of organ removal by BioIVT. The hepatocytes are from human transplant rejected livers and tested negative for hepatitis B and C and HIV1 and 2. Hepatocytes were thawed according to the

manufacturer's instructions as previously reported [127]. Briefly, cells were thawed by warming a vial of the hepatocytes at 37 °C for 90 seconds and suspending them in InVitroGRO HT medium (BioIVT) containing 1 mL TORPEDO™ Antibiotic Mix (BioIVT) per 45 mL media, then plated on Biocoat® collagen-coated plates (Corning) and remained in an incubator with a humidified air (95%) and carbon dioxide (CO₂, 5%) condition at 37 °C.

Determination of NAT2 genotype and phenotype

Genomic DNA was isolated from cryopreserved human hepatocytes using the QIAamp DNA Mini Kit (QIAGEN) per manufacturer's instructions, and *NAT2* genotypes and deduced phenotypes were determined as previously described [126]. Individuals possessing two *NAT2* alleles associated with rapid acetylation activity (*NAT2*4*) were classified as rapid acetylators, and individuals possessing two *NAT2* alleles associated with slow acetylation activity (*NAT2*5B*) were classified as slow acetylators.

Western blot

Cryopreserved human hepatocytes were plated the day before the treatment and allowed to attach. Cells were incubated for 2 days with media containing indicated HCAs (PhIP, MeIQ, or MeIQx) at a concentration of 25 µM, then incubated overnight with serum-free DMEM containing indicated HCA treatment conditions. Prior to lysis, cells were treated with insulin (Sigma-Aldrich) at 100 nM (freshly prepared in PBS) for 10 minutes. The cells were lysed immediately in Laemmli buffer (50 mM Tris-Cl [pH 6.8], 2% sodium dodecyl sulfate [SDS; w/v],

0.1% bromophenol blue, 10% [v/v] glycerol) and boiled for 10 minutes. Protein concentrations were determined using Pierce BCA Assay kit (Thermo Scientific) per manufacturer's instructions. One to two μ L of 2-mercaptoethanol was added to each sample and boiled again for 5 minutes. Twenty-five μ g of protein per sample was loaded and separated on 4–12% gradient Bis-Tris Plus polyacrylamide gels (Invitrogen). The gel was transferred to a PVDF membrane and blocked in 5% (w/v) skim milk in tris-buffered saline containing 0.1% Tween 20 (TBST) for 30 minutes. Membranes were incubated with primary antibodies (1:2,000) overnight at 4°C, then washed 3 times for 5 minutes each with TBST. Membranes were incubated for 1 hour at room temperature with an HRP-conjugated secondary antibody (1:5,000), then washed with TBST 3 times. The protein-antibody complex was detected with chemiluminescent substrate (Thermo Scientific). Densitometry was performed using Image J analysis software (NIH). Insulin-stimulated phospho-AKT (p-AKT) (Ser473) protein band was quantified and normalized to total AKT. Values presented represent the p-AKT/total-AKT ratio in response to insulin following treatment with indicated HCAs, relative to the vehicle-treated control group. The following antibodies were purchased from Cell Signaling Technology: phosphorylated protein kinase B (p-AKT Ser473; Cat. No. 4060); and protein kinase B (AKT) (Cat. No. 4091); and anti-rabbit IgG, HRP-linked (Cat. No. 7074). Each experiment was conducted three times using three different donor batches.

Gene expression analysis by RT-qPCR

Cryopreserved human hepatocytes were plated the day before the treatment and allowed to attach. Cells were incubated for 3 days with media containing indicated HCAs (MeIQ, MeIQx, or PhIP) at a concentration of 25 μ M. RNA was isolated from the treated cells using E.Z.N.A. Total RNA Kit 1 (OmegaBiotek) per manufacturer's protocol. cDNA was synthesized using High-Capacity cDNA Reverse Transcriptase PCR (Thermo Scientific) per manufacturer's instructions. Gene-specific cDNA was amplified and detected using iTaq Universal SYBR Green Supermix (Bio-Rad), gene-specific primers, and StepOne real-time PCR system (Applied Biosystems). The following primers were used: *G6PC*, forward 5'-ACGAATCTACCTTGCTGCTCA-3'; reverse 5'-AAAATCCGATGGCGAAGCTG3'. *PCK1* or *PEPCK*, forward 5'-TGATGAGCCGCTAGCTTCAG-3'; reverse 5'-GCCTTTATGTTCTGCAGCCG-3'. *FOXO1*, forward 5'-AGTGGATGGTCAAGAGCGTG-3', reverse 5'-TTTGAGCTAGTTCGAGGGCG-3'. *PPAR α* (*PPARA*), forward 5'-GATTTTCGCAATCCATCGGCG-3', reverse 5'-AAACGAATCGCGTTGTGTGAC-3'. *PGC1 α* (*PPARGC1A*), forward 5'-CACGGACAGAACTGAGGGAC-3', reverse 5'-TTCGTTTGACCTGCGCAAAG-3'. *18S rRNA*, forward 5'-GGAAGGGCACCACCAGGAGT-3'; reverse 5'-TGCAGCCCCGGACATCTAAG-3'. *GAPDH*, forward 5'-GGTGAAGCAGGCGTCGGAGG-3'; reverse 5'-GAGGGCAATGCCAGCCCCAG-3'. Results were normalized to GAPDH. The relative fold change was calculated using the delta-delta Ct ($2^{-\Delta\Delta Ct}$) method with StepOne software (Applied Biosystems).

Statistical analysis

Differences in p-AKT/total AKT ratio between the treatment groups vs. control groups were tested for significance by one-way ANOVA followed by Dunnett's Comparison Test. Differences between relative gene expression of treatment groups vs. control groups were tested for significance by student's t-test. All statistical analyses were performed using GraphPad Prism v8.2.1 (GraphPad Software). The results are expressed as the mean \pm the standard error of the mean (SEM). Statistical significance was determined per the following p-values: * indicates $p < 0.05$, ** indicates $p < 0.01$, *** indicates $p < 0.001$, **** indicates $p < 0.0001$.

RESULTS

Decreased insulin signaling following HCA treatment in human

hepatocytes is dependent on NAT2 acetylator phenotype. Decreased insulin signaling is a fundamental characteristic of insulin resistance and type II diabetes [6]. AKT (protein kinase B) is a major downstream effector of insulin signaling and regulates many insulin-mediated responses, including suppression of gluconeogenesis and promotion of lipid synthesis [6], [87]. Therefore, the level of insulin-induced AKT phosphorylation is often used as an indicator of insulin sensitivity [87]. We previously reported that HCAs reduce AKT phosphorylation in HepG2 cells and pooled cryopreserved human hepatocytes, which contain hepatocytes from 10 to 20 donors [127]. Additionally, we reported that HCAs induce glucose production in human hepatocytes, and that this effect is dependent on *NAT2* genetic polymorphism [127], [128]. We found that HCA-induced glucose production was significantly greater in rapid *NAT2* acetylator

hepatocytes than in intermediate or slow NAT2 acetylators. However, it remains unknown if HCA-induced reduction of AKT phosphorylation is also dependent on *NAT2* genetic polymorphism.

To investigate if the rate of HCA metabolism by NAT2 alters the effects of HCAs on insulin sensitivity, we assessed insulin-induced phosphorylation of AKT at Ser473 following HCA treatment in cryopreserved human hepatocytes categorized according to NAT2 acetylator phenotype (i.e., slow or rapid). For all experiments reported in this study, rapid NAT2 acetylator hepatocytes possess two *NAT2*4* alleles, which are associated with rapid NAT2 activity, and slow NAT2 acetylator hepatocytes possess two *NAT2*5B* alleles, which are associated with slow NAT2 activity. Hepatocytes were treated with 25 μ M of MeIQ, MeIQx, or PhIP for 3 days prior to the insulin treatment. This HCA concentration was selected because it falls in the middle of our previously established dose-response, which ranged from 0 to 50 μ M, and is comparable to and often lower than concentrations of HCAs used to assess genotoxicity [128]–[131]. Phosphorylated AKT (at Ser473) and total AKT levels were measured using Western blot. In slow NAT2 acetylator human hepatocytes treated with MeIQ, there was no change in phosphorylated AKT to total AKT ratio (p-AKT/AKT) in response to insulin, compared to vehicle-control group (Fig. 4.1A). Similarly, there was no change in phosphorylated AKT to total AKT ratio (p-AKT/AKT) in response to insulin, compared to vehicle-control group, in slow NAT2 acetylator human hepatocytes treated with MeIQx (Fig. 4.1A). PhIP treatment on slow NAT2 acetylator human hepatocytes caused a marginal

decrease ($p < 0.05$) of 19% in phosphorylated AKT to total AKT ratio (p-AKT/AKT) in response to insulin, compared to vehicle-control group.

In contrast, each of the HCAs tested caused a statistically significant decrease in phosphorylated AKT to total AKT ratio (p-AKT/AKT) in response to insulin, compared to vehicle-control group, in rapid NAT2 acetylator human hepatocytes (Fig. 4.1B). There was a 27% ($p < 0.05$), 46.3% ($p < 0.01$), and 35.3% ($p < 0.01$) reduction in insulin-stimulated p-AKT/AKT following treatment with MeIQ, MeIQx, or PhIP, respectively (Fig. 4.1B). These results suggest that NAT2-mediated metabolism of HCAs is necessary for HCA-induced insulin resistance.

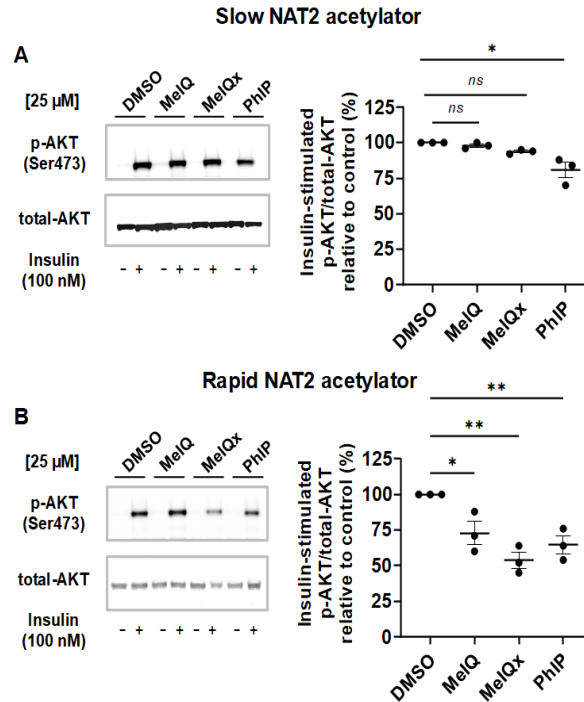


Figure 4.1. Insulin-induced AKT phosphorylation following HCA treatment in slow and rapid NAT2 acetylator cryopreserved human hepatocytes. Slow (panel A) and rapid (panel B) NAT2 acetylator cryopreserved human hepatocytes were cultured with DMSO or 25 μ M of MeIQ, MeIQx, or PhIP for 2 days, followed by a serum-starvation overnight. Prior to harvest, cells were treated with 100 nM insulin for 10 minutes. The relative levels of phospho-AKT (p-AKT) at Ser473 and total AKT (AKT) were measured using Western blot. The insulin-stimulated p-AKT/total-AKT ratio was expressed as a percentage of the DMSO-treated control cells. Statistical significance was determined by one-way ANOVA followed by Dunnett's Comparison Test. Data points represent results from three independent experiments, and the line and error bars represent mean \pm SEM. *, $p < 0.05$; **, $p < 0.01$.

Changes in expression of insulin receptor-target genes involved in gluconeogenesis following HCA treatment in hepatocytes is dependent on NAT2 acetylator phenotype. The liver facilitates regulation of glucose homeostasis by controlling many pathways involved in glucose metabolism, including glycogenolysis, glycolysis and gluconeogenesis [92]. Regulation of enzymes involved in these pathways is essential to maintain glucose homeostasis. The gluconeogenesis metabolic pathway produces glucose from non-carbohydrate carbon substrates, and the key regulatory enzymes in this pathway are glucose 6-phosphatase (G6PC) and phosphoenolpyruvate carboxykinase (PCK1; PEPCK) [92]. When insulin fails to properly phosphorylate AKT due to insulin resistance, dysregulation of gluconeogenic enzymes like G6PC and PCK1 often occurs [7], [87]. We previously reported that HCAs cause increased expression of *G6PC* and *PCK1* in HepG2 cells and pooled cryopreserved human hepatocytes [127]. However, it remains unknown if NAT2-mediated metabolism of HCAs alters this effect.

To investigate if the rate of HCA metabolism by NAT2 alters the effects of HCAs on expression of insulin receptor-target genes involved in gluconeogenesis, we measured expression of *G6PC* and *PCK1* following HCA treatment in cryopreserved human hepatocytes categorized according to NAT2 acetylator phenotype (i.e., slow or rapid). In slow NAT2 acetylator human hepatocytes, there were no changes in *G6PC* nor *PCK1* gene transcript levels following treatment with MeIQ (Fig. 4.2A-B). Similarly, no changes in *G6PC* or

PCK1 gene transcripts were observed in MeIQx- or PhIP-treated (Fig. 4.2A-B) slow NAT2 acetylator human hepatocytes.

In contrast, each of the HCAs tested caused a statistically significant increase in *G6PC* gene transcript levels, compared to the vehicle-control, in rapid NAT2 acetylator human hepatocytes (MeIQ, $p < 0.01$; MeIQx, $p < 0.001$; PhIP, $p < 0.01$) (Fig. 4.2A). Furthermore, each of the HCAs tested also caused a statistically significant increase in *PCK1* gene transcript levels, compared to the vehicle-control, in rapid NAT2 acetylator human hepatocytes (MeIQ, $p < 0.05$; MeIQx, $p < 0.01$; PhIP, $p < 0.05$) (Fig. 4.2B). These results suggest that, similarly to glucose production and insulin resistance, NAT2-mediated metabolism of HCAs is necessary for HCA-induced expression of insulin-target genes involved in gluconeogenesis.

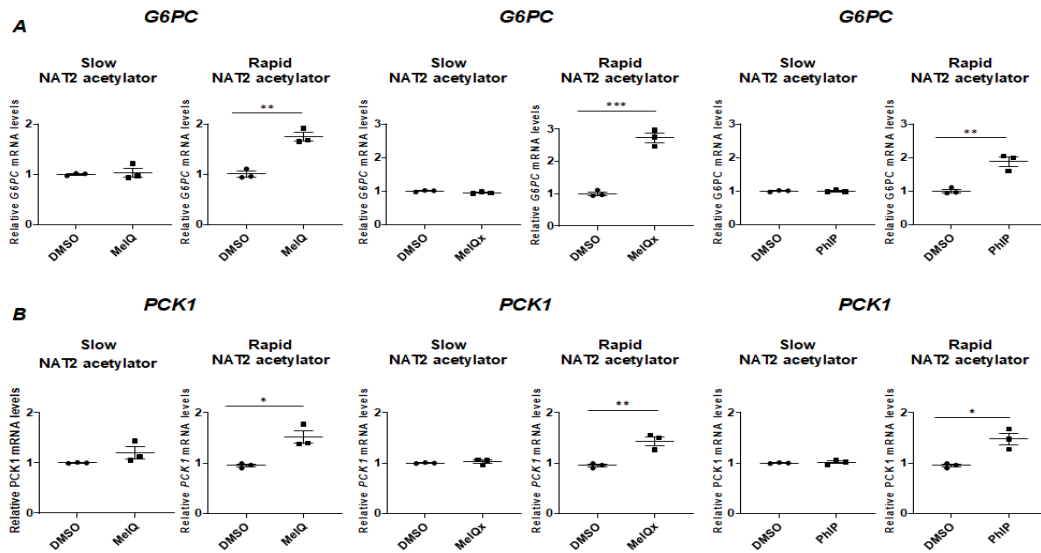


Figure 4.2. Changes in expression of insulin receptor-target genes involved in gluconeogenesis following HCA treatment in slow and rapid NAT2 acetylator cryopreserved human hepatocytes. Slow and rapid NAT2 acetylator cryopreserved human hepatocytes were cultured with DMSO or 25 μ M of the indicated HCA (MeIQ, MeIQx, or PhIP) for 3 days. The relative mRNA level of the indicated gene *G6PC* (panel A) or *PCK1* (panel B) was measured by RT-qPCR using GAPDH as an internal control. The mRNA levels were expressed as changes relative to that in the DMSO-control. Statistical significance was determined by Student's t-test. Data points represent the average from three independent experiments, and the line and error bars represent mean \pm SEM. *, $p < 0.05$; **, $p < 0.01$; ***, $p < 0.001$.

Changes in expression of genes involved in regulation of gluconeogenesis following HCA treatment in hepatocytes is dependent on NAT2 acetylator phenotype. We previously reported that, in addition to induced expression of *G6PC* and *PCK1* in cryopreserved human hepatocytes, HCAs also altered the expression of additional genes that regulate gluconeogenesis, including forkhead box O1 (*FOXO1*), peroxisome proliferator activated receptor alpha (*PPAR* α ; *PPARA*), and PPARG coactivator 1 alpha (*PGC1* α ; *PPARGC1A*) [127]. However, the effect of NAT2-mediated metabolism on these changes has yet to be investigated.

Forkhead box O1 (*FOXO1*) gene encodes a transcription factor protein that regulates metabolic homeostasis and insulin signaling [94]. Moreover, *FOXO1* regulates expression of gluconeogenic genes, *G6PC* and *PCK1*, and increased expression of *FOXO1* correlates with increased expression of *G6PC* and *PCK1* [95]. In slow NAT2 acetylator human hepatocytes, there was no change in *FOXO1* gene transcript levels following treatment with any of the HCAs tested (Fig. 4.3A). However, in rapid NAT2 acetylator human hepatocytes, there was a statistically significant increase ($p < 0.05$) in *FOXO1* gene transcript levels following treatment with MeIQ or MeIQx, although there was no change following treatment with PhIP.

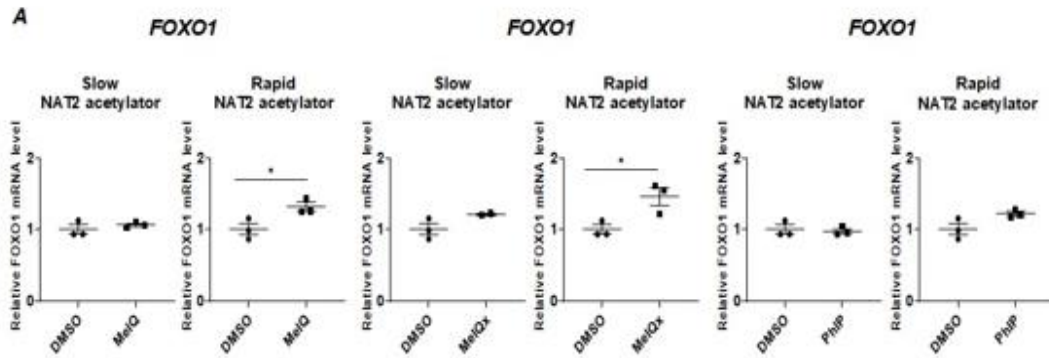


Figure 4.3. Changes in expression of the insulin receptor-target gene *FOXO1*, which regulates gluconeogenesis, following HCA treatment in slow and rapid NAT2 acetylator cryopreserved human hepatocytes. Slow and rapid NAT2 acetylator cryopreserved human hepatocytes were cultured with DMSO or 25 μ M of the indicated HCA (MeIQ, MeIQx, or PhIP) for 3 days. The relative mRNA level of the indicated gene *FOXO1* (panel A) was measured by RT-qPCR using GAPDH as an internal control. The mRNA levels were expressed as changes relative to that in the DMSO-control. Statistical significance was determined by Student's t-test. Data points represent the average from three independent experiments, and the line and error bars represent mean \pm SEM. *, $p < 0.05$.

Furthermore, peroxisome proliferator activated receptor alpha (*PPAR α*) regulates expression of genes involved in glucose and lipid metabolism and transport [96]. Like *FOXO1*, there was no change in *PPAR α* gene transcript levels following HCA treatment in slow NAT2 acetylator human hepatocytes (Fig. 4.4A). In rapid NAT2 acetylator human hepatocytes, however, there was a statistically significant increase ($p < 0.05$) in *PPAR α* gene transcript levels following treatment with MeIQ and PhIP, while there was no change following MeIQx treatment.

PPARG Coactivator 1 Alpha (*PGC1 α*) is a transcriptional co-activator that regulates expression of genes involved in glucose and fatty acid metabolism and is a known regulator of hepatic gluconeogenesis [97], [98]. Like *FOXO1* and *PPAR α* , there was no change in *PGC1 α* gene transcript levels following HCA treatment in slow NAT2 acetylator human hepatocytes (Fig. 4.4B). However, there was a statistically significant decrease ($p < 0.05$) in *PGC1 α* gene transcript levels following MeIQ or MeIQx treatment in rapid NAT2 acetylator human hepatocytes, while there was still no change after PhIP treatment (Fig. 4.4B). Taken together, these results indicate that, similar to our findings reported in Figure 4.3, metabolism of HCAs by NAT2 is necessary for HCA-mediated changes in expression of genes that regulate gluconeogenesis.

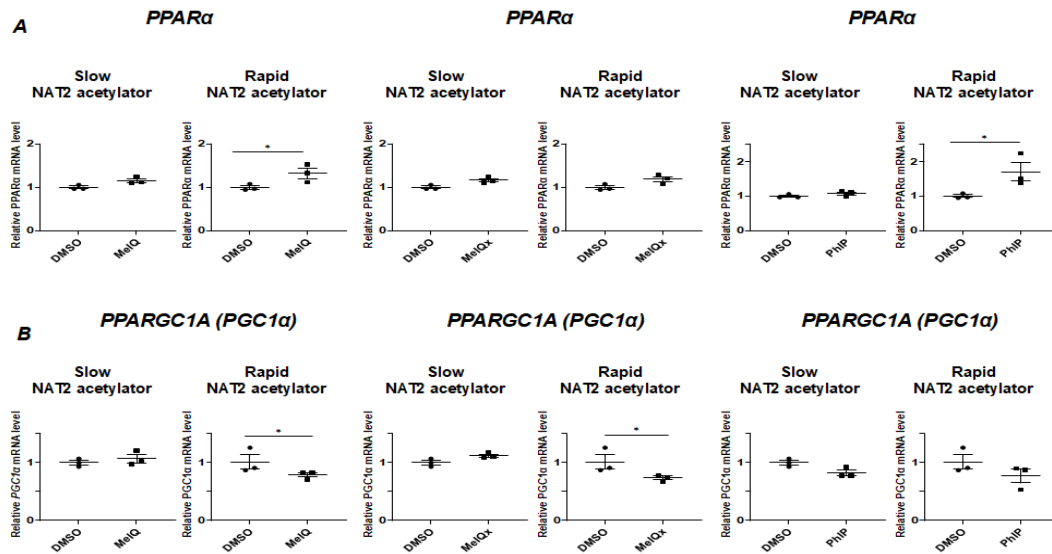


Figure 4.4. Changes in expression of additional genes that regulate gluconeogenesis following HCA treatment in slow and rapid NAT2 acetylator cryopreserved human hepatocytes. Slow and rapid NAT2 acetylator cryopreserved human hepatocytes were cultured with DMSO or 25 μ M of the indicated HCA (MeIQ, MeIQx, or PhIP) for 3 days. The relative mRNA level of the indicated gene *PPARα* (panel A), or *PPARGC1A* (panel B) was measured by RT-qPCR using GAPDH as an internal control. The mRNA levels were expressed as changes relative to that in the DMSO-control. Statistical significance was determined by Student's t-test. Data points represent the average from three independent experiments, and the line and error bars represent mean \pm SEM. *, $p < 0.05$.

DISCUSSION

Insulin resistance causes defective glucose homeostasis, and subsequently, increased and sustained glucose production, which is a hallmark of type II diabetes and metabolic syndrome [6]. These conditions significantly increase an individual's risk of other health complications like cardiovascular disease and fatty liver. We previously reported that HCAs cause insulin resistance, increased gluconeogenic gene expression, and increased glucose production in cryopreserved human hepatocytes [127], suggesting that exposure to HCAs via consumption of cooked meat can lead to development of hepatic metabolic dysregulation. In a follow-up study, we reported that induction of glucose production by HCAs is dependent on *NAT2* genetic polymorphism in cryopreserved human hepatocytes [128]. In the current study, we investigated the role of *NAT2*- mediated hepatic metabolism on HCA-induced insulin resistance and gluconeogenic gene expression.

It is well-known that mutagenicity and carcinogenicity of HCAs requires bioactivation [72], but little is known about the role of HCA metabolism in the context of HCA-mediated insulin resistance and disruption of hepatic glucose homeostasis. Many HCAs are bioactivated by the phase II metabolic enzyme, *NAT2*, following *N*-hydroxylation by *CYP1A2* [72]. As previously mentioned, *NAT2* expresses a well-defined genetic polymorphism in humans, and the subsequent genotypes are highly correlated to categorized phenotypes, including rapid, intermediate, and slow acetylators who exhibit differential metabolism of aromatic amines and HCAs [113]. In the present study, we measured insulin

signaling and expression of genes relating to gluconeogenesis in slow and rapid NAT2 acetylator cryopreserved human hepatocytes exposed to HCAs. We found that HCAs cause a significant reduction in insulin signaling and significant increase in expression of gluconeogenic genes in rapid NAT2 acetylator human hepatocytes, while little to no changes in insulin signaling or gene expression were detected in slow NAT2 acetylator human hepatocytes. Moreover, changes in expression of genes that regulate gluconeogenesis were observed in rapid NAT2 acetylators, while, again, no changes were seen in the slow NAT2 acetylators. This indicates that, like metabolic biotransformation that leads to mutagenicity, HCA-mediated disruption of insulin signaling and glucose homeostasis requires bioactivation by NAT2 that is modified by its genetic polymorphism.

The results presented here suggest that individuals with rapid NAT2 acetylator phenotype are at greater risk of developing insulin resistance and increased hepatic glucose production following exposure to HCAs. The allele associated with rapid NAT2 activity, *NAT2*4*, has highest frequency among Asian populations, accounting for roughly 50% of all *NAT2* allelic variations, although it is estimated that *NAT*4* makes up roughly 25% of alleles in Caucasians and 40% in African Americans [56]–[59]. Thus, the findings reported here are applicable to millions of people globally and provide greater insight into understanding an individual's risk of developing hepatic metabolic dysregulation after exposure to HCAs via consumption of cooked meat. The current study demonstrated the crucial need to consider the role of polymorphisms in genes

involved in metabolism when evaluating risk following exposure to toxicants. Additional studies should explore the mechanisms by which HCAs and their metabolites elicit changes to hepatic insulin signaling and glucose homeostasis.

CHAPTER 5
ACTIVATION OF C-JUN N-TERMINAL KINASE PROMOTES HETEROCYCLIC
AMINE-INDUCED INSULIN RESISTANCE IN HUMAN HEPATOCYTES

INTRODUCTION

Metabolic dysfunction-associated steatohepatitis (MASH), previously termed NAFLD, is the liver manifestation of metabolic syndrome, a condition in which an individual possesses a combination of health risk factors, including insulin resistance, hyperglycemia, hypertension, central obesity, and abnormal cholesterol or triglyceride levels [1], [132], [133]. In the United States, it is estimated that more than one third of the adult population has metabolic syndrome [2], [3], and these individuals are at an increased risk of severe health complications including, heart attack, fatty liver, and stroke [4]. Some have argued that insulin resistance may be the underlying etiology of metabolic syndrome [5]. Lifestyle choices like lack of exercise and poor diet are known to cause metabolic syndrome, but recently, additional precursors to developing conditions associated with metabolic syndrome have been identified, including

exposure to environmental pollutants and genetic variants involved in glucose and lipid metabolism [1], [119]–[122].

We recently reported that exposure to heterocyclic amines (HCAs) induced insulin resistance, gluconeogenic gene expression, and glucose production in human hepatocytes, identifying exposure to HCAs as a novel environmental risk factor for conditions associated with metabolic syndrome [127]. HCAs are mutagens and carcinogens formed from the high-temperature cooking of muscle meats, including poultry, beef, pork, and fish [112], although additional sources of HCAs include cigarette smoke and fumes generated from cooking oils [25], [26], [134]. While previous studies of HCAs have primarily assessed their mutagenic and carcinogenic properties, recent epidemiological studies have linked unhealthy cooking methods like grilling and frying, which favor production of HCAs, and dietary exposure to HCAs via cooked meat to the development of insulin resistance, type II diabetes, and MASLD/MASH [43], [44], [135]. Moreover, we recently reported that HCAs induce insulin resistance and glucose production [127] and lead to increased neutral lipids in human hepatocytes, further suggesting that HCA exposure may be an environmental risk factor contributing to the development of metabolic syndrome and underlying conditions associated with MASLD/MASH [127]. However, the mechanism by which HCAs lead to insulin resistance and disrupted energy homeostasis remains unknown.

cJun-N-terminal kinase (JNK) is a mitogen-activated protein kinase that is potently induced by cellular stress [136] and is one of the most investigated

molecules in obesity models of insulin resistance [137], [138]. JNK activity is known to disrupt insulin signaling by phosphorylating insulin receptor substrate 1 (IRS1) at Ser307, inhibiting phosphorylation of the tyrosine site and thus preventing downstream signaling [139], [140]. Reactive oxygen species (ROS), inflammation, endoplasmic reticulum stress (ER stress), and lipotoxicity are known to induce JNK activity, and each of these are also associated with insulin resistance [141]. In the present study, we investigated activation of JNK as a mechanism by which HCAs cause insulin resistance in human hepatocytes.

MATERIALS AND METHODS

Heterocyclic amines (HCAs)

MelQ, MelQx and PhIP were purchased from Toronto Research Chemicals and prepared into a solution with dimethyl sulfoxide (DMSO) at a stock concentration of 10 mM. MelQx and PhIP were diluted to 25 μ M working stock solutions prepared freshly in the cell culture media at the time of each experiment, as previously described.

Cell culture

Cryopreserved human hepatocytes were purchased from BioIVT and stored in liquid nitrogen. Hepatocyte samples were collected from consenting donors under IRB approved protocols at the FDA licensed donor center at BioIVT (<http://www.bioivt.com/>). Hepatocytes were prepared from fresh human tissue and were isolated and frozen within 24 hours of organ removal by BioIVT. The hepatocytes are from human transplant rejected livers and tested negative for

hepatitis B and C and HIV1 and 2. Hepatocytes were thawed according to the manufacturer's instructions as previously reported [127]. Briefly, cells were thawed by warming a vial of the hepatocytes at 37 °C for 90 seconds and suspending them in InVitroGRO HT medium (BioIVT) containing 1 mL TORPEDO™ Antibiotic Mix (BioIVT) per 45 mL media, then plated on Biocoat® collagen-coated plates (Corning) and remained in an incubator with a humidified air (95%) and carbon dioxide (CO₂, 5%) condition at 37 °C.

Western blot

Cryopreserved human hepatocytes were plated and allowed to attach for 4 hours. For experiments including JNK inhibitor, cells were pre-treated for 2 hours with 20 µM SP600125 (abcam). Cells were incubated for 24 hours with complete DMEM containing 25 µM of the indicated HCAs (MeIQ, MeIQx, or PhIP). For experiments containing insulin treatment, prior to lysis, cells were treated with insulin (Sigma-Aldrich) at 100 nM (freshly prepared in PBS) for 15 minutes. The cells were lysed immediately in Laemmli buffer (50 mM Tris-Cl [pH 6.8], 2% sodium dodecyl sulfate [SDS; w/v], 0.1% bromophenol blue, 10% [v/v] glycerol) and boiled for 10 minutes. Protein concentrations were determined using Pierce BCA Assay kit (Thermo Scientific) per manufacturer's instructions. One to two µL of 2-mercaptoethanol was added to each sample and boiled again for 5 minutes. Twenty-five to fifty µg of protein per sample was loaded and separated on 4–12% gradient Bis-Tris Plus polyacrylamide gels (Invitrogen) for JNK and AKT and 3–8% NuPAGE Tris-Acetate protein gels (Invitrogen) for IRS1. The gel was transferred to a PVDF membrane and blocked in 5% (w/v) skim milk in tris-

buffered saline containing 0.1% Tween 20 (TBST) for 30 minutes. Membranes were incubated with primary antibodies (1:2,000) overnight at 4°C. Membranes were washed 3 times for 5 minutes each with TBST. Membranes were incubated for 1 hour at room temperature with an HRP-conjugated secondary antibody (1:5,000) and washed with TBST 3 additional times, then protein-antibody complex was detected with chemiluminescent substrate (Thermo Scientific). Densitometry was performed using Image J analysis software (NIH). Phospho-JNK (p-JNK) (Thr183/Tyr185) protein band was quantified and normalized to total JNK. Insulin-stimulated phospho-IRS1 (p-IRS1) (Ser307) and phospho-AKT (p-AKT) (Ser473) protein band was quantified and normalized to total IRS1 and AKT, respectively. Values presented represent the p-IRS1/total-IRS1 and p-AKT/total-AKT ratio in response to insulin following treatment with indicated HCAs, relative to the vehicle-treated control group. The following antibodies were purchased from Cell Signaling Technology: phosphorylated JNK (Thr183/Tyr185) (Cat. No. 4668); and JNK (Cat. No. 9252); and phosphorylated IRS1 (Ser307) (Cat. No. 2381); and IRS1 (Cat. No. 2382); and phosphorylated protein kinase B (p-AKT Ser473; Cat. No. 4060); and protein kinase B (AKT) (Cat. No. 4091); and anti-rabbit IgG, HRP-linked (Cat. No. 7074).

Gene expression analysis by RT-qPCR

Cryopreserved human hepatocytes were plated and allowed to attach for 4 hours. Cells were incubated for 24 hours with media containing MeIQx or PhIP at a concentration of 25 µM. RNA was isolated from the treated cells using E.Z.N.A. Total RNA Kit 1 (Omegabiotek) per manufacturer's protocol. cDNA was

synthesized using High-Capacity cDNA Reverse Transcriptase PCR (Thermo Scientific) per manufacturer's instructions. Gene-specific cDNA was amplified and detected using iTaq Universal SYBR Green Supermix (Bio-Rad), gene-specific primers, and StepOne real-time PCR system (Applied Biosystems). The following predesigned primer was used: (Life Technologies, Grand Island, NY) Tumor necrosis factor alpha [Tnfa (Mm00443258_m1)]. Results were normalized to GAPDH, forward 5'-GGTGAAGCAGGCGTCGGAGG-3'; reverse 5'-GAGGGCAATGCCAGCCCCAG-3'. The relative fold change was calculated using the delta-delta Ct ($2^{-\Delta\Delta Ct}$) method with StepOne software (Applied Biosystems).

Reactive Oxygen Species

Cryopreserved human hepatocytes were plated and allowed to attach for 4 hours, then pre-treated with 20 μ M CM-H2DCFDA for 45 minutes according to manufacturer's protocol and then treated with DMSO or 25 or 50 μ M of the indicated HCA for 24 hours. Fluorescence intensity was measured at Ex/Em = 485/528 nm using a microplate reader. The relative ROS generation is expressed as a percentage relative to the control.

Neutral lipid measurements via BODIPY 493/503

Cryopreserved human hepatocytes were plated and treated as described above. At the completion of HCA treatment, cells were fixed with 3.7% formaldehyde for an incubation period of 10 minutes, washed twice with PBS, and stained with 2 μ M BODIPY 493/503 for 30 minutes. Cells were then washed twice with PBS, permeabilized with 0.25% Triton-X 100 for 5 minutes, washed 2 additional times

with PBS, counterstained with 300 nM DAPI solution for 5 minutes, and washed a final time with PBS. Cells were protected from light until imaged under fluorescent microscopy. FITC and DAPI channels using two fluorescence channels at 519 nm and 461 nm were used to capture BODIPY stained lipid droplets and DAPI stained nuclei, respectively. A subset of representative images was used for quantification according to the protocol described by Adomshick, Pu, and Veiga-Lopez [142]. Neutral lipid droplet measurements were normalized relative to cell count as determined by DAPI counterstain and expressed as a percentage relative to DMSO-treated control.

RNA-Seq library preparation & sequencing and downstream computation analysis

Hepatocytes were thawed and plated according to the manufacturer's instructions as previously reported [122]. After attachment, hepatocytes were treated with DMSO or 25 μ M of MeIQx or PhIP for 24 hours. RNA was isolated from the treated cells using E.Z.N.A. Total RNA Kit 1 (OmegaBiotek) per manufacturer's protocol. RNA-Seq libraries were prepared according to manufacturer's protocols using Illumina's TruSeq Stranded reference guide (document: 100000040498 v00; Illumina; San Diego, CA). Each sample consisted of 300 ng of RNA that was used for poly-A enrichment. First and second strand cDNA synthesis was completed followed by adapter and index ligation. mRNA libraries were prepared with Illumina's stranded mRNA prep ligation for 12 samples (catalog: 20040534; Illumina; San Diego, CA). Amplification of cDNA was performed according to manufacturer's protocol.

Library concentrations were assessed using a Qubit 4 fluorometer with dsRNA high sensitivity kit (catalog: Q33231; ThermoFisher; Madison, MI). Library size and fragment analysis was assessed on Agilent 4159 TapeStation System on a D5000 screen tape (catalog: 5067-5588; Agilent; Santa Clara, CA). Individual samples were then normalized to 10 nM prior to pooling and then quantified by Qubit analysis. Sequencing was performed on Illumina's NextSeq 2000 platform using a P3 100 cycle reagent kit and P3 flow cell. Libraries were then sequenced with a single 101 cycle read length with 2 indexes of 8bp each. FASTQ files were generated with BaseSpace DRAGEN analysis (v1.2.1). Raw gene counts were determined using HTSEQ-count (v0.10.0) using the Ensembl GRCm39 (v106) gene annotations.

Computational Downstream Analyses

Levels of differentially expressed genes in HCA-treated cells were transformed to \log_2 fold change relative to those in DMSO-treated control cells. RNA-Seq datasets were uploaded to MetaCore – Integrated pathway analysis for multi-Omics data software (Clarivate; St. Helier, Jersey, United Kingdom). Data was analyzed with MetaCore for network building and pathway analysis where only processes with a false discovery rate (FDR) ≤ 0.05 were accepted. Additionally, we analyzed our data through PANTHER Classification System and Gonet. These online algorithms provide gene function, ontology, pathways and statistical analysis tools.

Statistical analysis

Differences in relative gene expression, protein levels, ROS, and neutral lipid measurements between the treatment groups vs. control groups were tested for significance by one-way ANOVA followed by Dunnett's Comparison Test. All statistical analyses were performed using GraphPad Prism v8.2.1 (GraphPad Software). The results are expressed as the mean \pm the standard error of the mean (SEM). Statistical significance was determined per the following p-values: * indicates $p < 0.05$, ** indicates $p < 0.01$, *** indicates $p < 0.001$, **** indicates $p < 0.0001$.

RESULTS

HCA treatment induces phosphorylation of JNK in cryopreserved human hepatocytes. cJun-N-terminal kinase (JNK) is a mitogen-activated protein kinase that is potently induced by cellular stress [136]. It has been demonstrated that JNK activity leads to insulin resistance in hepatocytes by phosphorylating the serine-307 site of insulin receptor substrate 1 (IRS1), thereby blocking phosphorylation of the tyrosine site and preventing downstream signaling [139], [140]. We previously reported that HCAs induce insulin resistance in cryopreserved human hepatocytes [127], but the precise mechanism has not yet been investigated. To elucidate the mechanism by which HCAs induce insulin resistance in human hepatocytes, we interrogated the JNK-IRS1 pathway.

To investigate if HCAs lead to increased JNK activation, we treated cryopreserved human hepatocytes with DMSO or 25 μ M of the indicated HCA for 24 hours, then measured phosphorylated JNK (Thr183/Tyr185) and total JNK via

Western blot. JNK is phosphorylated sequentially at threonine and tyrosine residues within the activation loop, creating a functional active site by realigning the N- and C-terminal domains [143], [144], thus phosphorylation of JNK protein indicates increased JNK activity. We found that HCA treatment on human hepatocytes led to increased JNK phosphorylation, compared to the DMSO-treated control (Fig. 5.1). MeIQ treatment led to an average 6.4-fold significant increase ($p < 0.001$), and MeIQx treatment led to an average 8.6-fold significant increase ($p < 0.001$), compared to DMSO-treated control (Fig. 5.1). PhIP treatment caused an average 15.1-fold significant increase ($p < 0.0001$) in JNK phosphorylation (Fig. 5.1). These results indicate that HCA treatment on human hepatocytes leads to increased JNK activity.

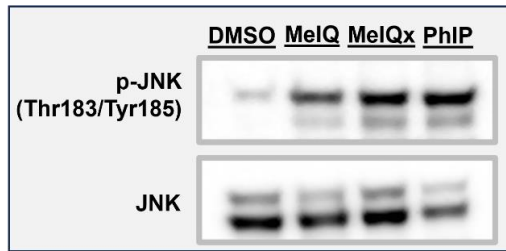
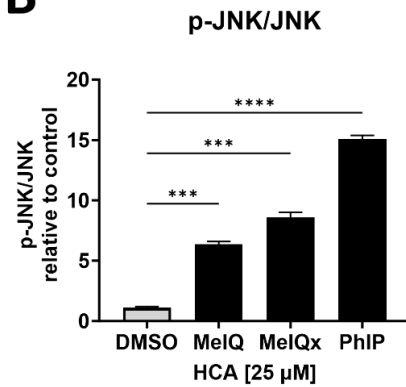
A**B**

Figure 5.1. HCA treatment induces phosphorylation of JNK in cryopreserved human hepatocytes. Cryopreserved human hepatocytes were treated with DMSO or 25 μ M of the indicated HCA for 24 hours. The relative levels of phospho-JNK (p-JNK) (Thr183/Tyr185) and total JNK (JNK) were measured using Western blot. The p-JNK/JNK ratio was expressed as a percentage of the DMSO-treated control cells. Bars represent mean \pm SEM. Statistical significance was determined using One-Way ANOVA followed by Dunnett's Comparisons Test. ***, $p < 0.001$; ****, $p < 0.0001$.

HCA treatment interferes with insulin signaling at IRS1 and AKT, but inhibiting JNK with SP600125 restores insulin signaling at both IRS1 and AKT in cryopreserved human hepatocytes. As previously mentioned, JNK activity leads to insulin resistance in hepatocytes by phosphorylating the serine-307 site of IRS1, thereby blocking phosphorylation of the tyrosine site and preventing downstream signaling [139], [140]. Since we found that HCAs caused increased JNK activity in hepatocytes, and JNK is known to disrupt IRS1 signaling, we investigated if HCAs disrupt insulin signaling at IRS1. Additionally, we used the JNK inhibitor SP600125 to investigate if blocking JNK activation affected IRS1 activity.

Cryopreserved human hepatocytes were pre-treated with DMSO or the JNK inhibitor SP600125 for 2 hours, then treated with DMSO or 25 μ M of the indicated HCA for 24 hours and stimulated with 100 nM insulin for 15 minutes prior to protein harvest for Western blot. We measured insulin-stimulated phosphorylation of IRS1 at Ser307 and total IRS1 protein, and results are presented as a phospho-IRS1/total-IRS1 ratio. HCA treatment led to significantly increased insulin-stimulated IRS1 phosphorylation at Ser307, compared to DMSO-treated control (MeIQx, $p < 0.05$; PhIP, $p < 0.001$) (Fig. 5.2A). However, inhibiting JNK activity with SP600125 led to decreased insulin-stimulated IRS1 phosphorylation (MeIQx, $p < 0.05$; PhIP, $p < 0.05$) (Fig. 5.2A), suggesting that JNK activity induced by HCA treatment is responsible for HCA-induced disruption of IRS1 signaling.

AKT (protein kinase B) is a major downstream effector of IRS1 in insulin signaling and regulates many insulin-mediated responses [6], and so insulin-induced AKT phosphorylation is often used as an indicator of insulin sensitivity [87]. We previously reported that HCAs induce insulin resistance in hepatocytes by reducing levels of insulin-induced AKT phosphorylation [127]. To investigate if increased JNK activity is responsible for HCA-induced disruption of AKT signaling, we treated hepatocytes as previously described and measured phosphorylated AKT (Ser473) and total AKT via Western blot. Consistent with previous findings, HCA treatment significantly decreased insulin-stimulated p-AKT/total AKT ratio (MeIQx, $p < 0.01$; PhIP, $p < 0.01$) (Fig. 5.2B). However, inhibition of JNK with SP600125 restored AKT activity. There was no significant difference in insulin-stimulated p-AKT/total AKT ratio in HCA-treated hepatocytes, compared to DMSO-treated control (Fig. 5.2B). These results indicate that, similar to IRS1, defective insulin signaling at AKT following HCA treatment is due to increased JNK activity.

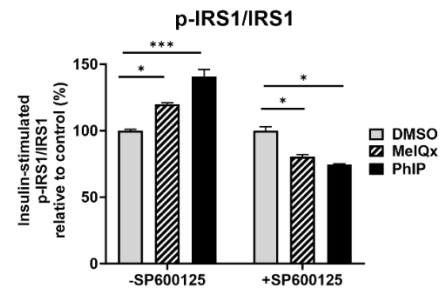
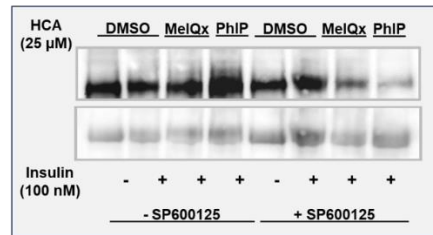
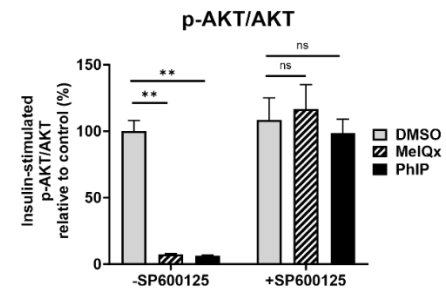
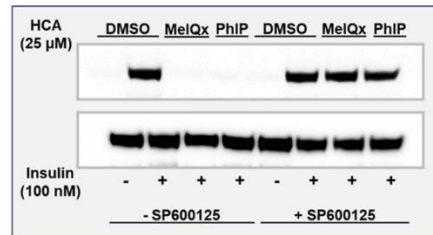
A**B**

Figure 5.2. HCA treatment interferes with insulin signaling at IRS1 and AKT, but inhibiting JNK with SP600125 restores insulin signaling at both IRS1 and AKT in cryopreserved human hepatocytes. Cryopreserved human hepatocytes were treated with DMSO or 25 μ M of the indicated HCA for 24 hours. Prior to harvesting cells for protein, hepatocytes were treated with 100 nM insulin for 15 minutes. The relative levels of phospho-IRS1 (p-IRS1) (Ser307) and total IRS1 (panel A) and phospho-AKT (p-AKT) (Ser473) and total AKT (panel B) were measured using Western blot. The insulin-stimulated p-IRS1/IRS and p-AKT/AKT ratios were expressed as a percentage of the DMSO-treated control cells. Bars represent mean \pm SEM. Statistical significance was determined using Two-Way ANOVA followed by Tukey's Comparisons Test. *, $p < 0.05$; **, $p < 0.01$; ***, $p < 0.001$.

HCA treatment leads to increased levels of ROS and increased expression of TNF in cryopreserved human hepatocytes. Since HCA treatment led to increased JNK activity in hepatocytes, and this increased JNK activity was responsible for disrupted insulin signaling following HCA treatment, we next investigated potential causes of HCA-induced JNK activation. Reactive oxygen species (ROS), inflammation, ER stress, and excess free fatty acids have been reported to induce JNK [145]. HCAs have been shown to cause ROS in Chinese hamster ovary cells [111]. To investigate if ROS is a potential cause of HCA-induced hepatic JNK activation and subsequent insulin resistance, we pre-treated cryopreserved human hepatocytes for 45 minutes with CM-H₂DCFDA and then treated the cells for 24 hours with DMSO or 25 μ M or 50 μ M of the indicated HCA. ROS was quantified by measuring fluorescence intensity at Ex/Em = 485/528 nm using a microplate reader. MelQx treatment increased ROS levels significantly ($p < 0.05$) by an average 217% and 267% at 25 μ M and 50 μ M, respectively (Fig. 5.3A). PhIP treatment also significantly increased ROS levels, compared to DMSO-treated control, by an average 250% ($p < 0.05$) at 25 μ M and 333% ($p < 0.01$) at 50 μ M (Fig. 5.3A). These results indicate that HCA treatment led to increased overall ROS levels in hepatocytes, suggesting that ROS may contribute to HCA-induced JNK activation.

Oxidative stress caused by ROS is often linked to inflammation [146]. The proinflammatory cytokine TNF is commonly used an indicator of inflammation in hepatocytes [147]. To investigate if HCAs cause inflammation, we treated cryopreserved human hepatocytes with DMSO or 25 μ M of the indicated HCA for

24 hours and measured gene expression of *TNF* via qRT-PCR. Both MeIQx and PhIP significantly increased relative *TNF* gene expression levels (MeIQx, $p < 0.01$; PhIP, $p < 0.001$) (Fig. 5.3B). These results indicate that HCAs may lead to inflammation in hepatocytes, although other markers of inflammation should be investigated further. Taken together, it is likely that ROS and inflammation are involved in HCA-induced JNK activation in human hepatocytes.

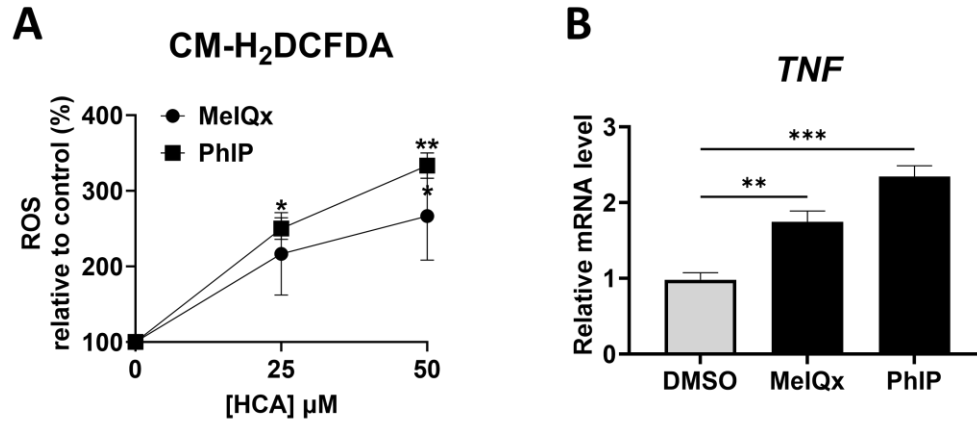


Figure 5.3. HCA treatment leads to increased levels of ROS and increased expression of TNF in cryopreserved human hepatocytes. For ROS measurements (panel A), hepatocytes were pre-treated with 20 μ M CM-H₂DCFDA for 45 minutes, then treated with DMSO or 25 or 50 μ M of the indicated HCA for 24 hours. Fluorescence intensity was measured at Ex/Em = 485/528 nm using a microplate reader. The relative ROS generation is expressed as a percentage relative to the control. For relative mRNA levels of TNF (panel B), hepatocytes were treated with DMSO or 25 μ M of the indicated HCA for 24 hours, and mRNA levels were measured via qRT-PCR. The relative mRNA levels are normalized to GAPDH and expressed relative to the DMSO-control. Data points (panel A) or bars (panel B) represent mean \pm SEM. Statistical significance was determined using One-Way ANOVA followed by Dunnett's Comparisons Test. *, $p < 0.05$; **, $p < 0.01$; ***, $p < 0.001$.

HCA treatment leads to neutral lipid accumulation in cryopreserved human hepatocytes. As previously mentioned, in addition to ROS, and inflammation, excess free fatty acids and lipotoxicity have been reported to induce JNK [148], [149]. To investigate if HCAs lead to lipid accumulation, cryopreserved human hepatocytes were treated with DMSO or 25 μ M of the indicated HCA, then fixed, permeabilized, and stained with BODIPY 493/503 and counterstained with DAPI. We automatically analyzed fluorescence via the Cytation5 imager. MeIQx treatment on hepatocytes significantly ($p < 0.05$) increased neutral lipids, compared to DMSO-treated control, by an average 230% (Fig. 5.4). PhIP treatment on hepatocytes also significantly ($p < 0.01$) increased neutral lipids by an average 245%, compared to DMSO-treated control (Fig. 5.4). These findings confirm that HCAs lead to neutral lipid accumulation in hepatocytes, suggesting that lipotoxicity may be an additional factor contributing to HCA-induced JNK activation.

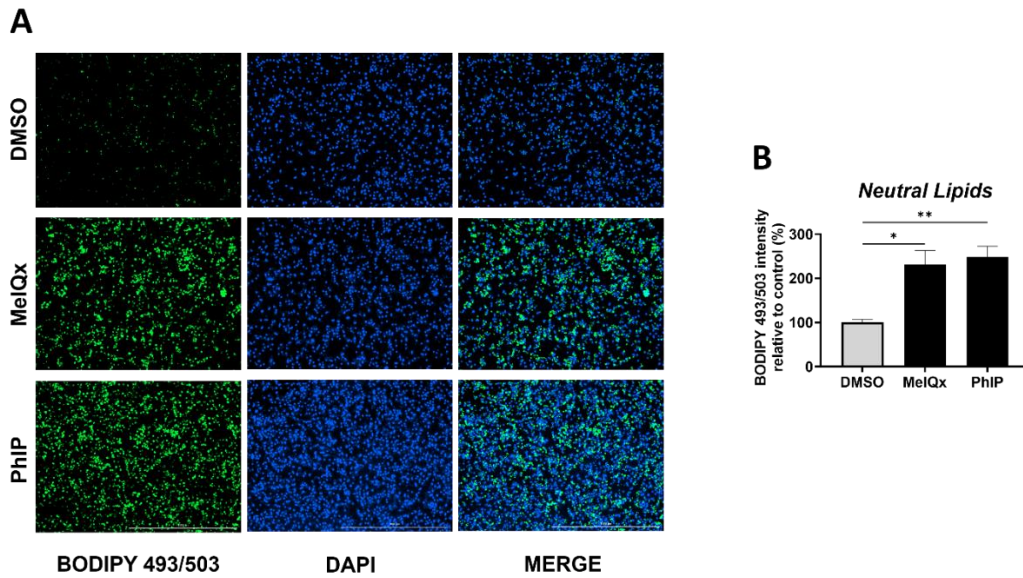


Figure 5.4. HCA treatment leads to neutral lipid accumulation in cryopreserved human hepatocytes. Hepatocytes were treated with DMSO or 25 μ M of the indicated HCA for 24 hours. Cells were then fixed, permeabilized, and stained with BODIPY 493/503 and DAPI. Cells were imaged under microscopy (panel A) and quantified using CellProfiler 4.2.5 (panel B). Neutral lipid droplet measurements were normalized relative to cell count as determined by DAPI counterstain and expressed as a percentage relative to DMSO-treated control. Statistical significance was determined by One-Way ANOVA followed by Dunnett's Comparisons Test. Bars represent mean \pm SEM. *, $p < 0.05$; **, $p < 0.01$.

Gene Ontology (GO) biological processes, molecular functions, and cellular components significantly enriched among genes upregulated by PhIP treatment in cryopreserved human hepatocytes include indicators of endoplasmic reticulum stress. To better explore the mechanisms by which HCAs disrupt insulin signaling and energy homeostasis in hepatocytes, we conducted an unbiased analysis and comparison of genomes of hepatocytes treated with MelQx or PhIP. The enrichment analysis of genes upregulated by PhIP treatment identified the gene ontology biological process “response to endoplasmic reticulum stress” (GO:0034976) and multiple related pathways involved in this category (Fig. 5.5A). Among them includes “regulation of response to endoplasmic reticulum stress” (GO:1905897), “ERAD pathway” (GO:0036503), “response to topologically incorrect protein” (GO:0035966), “response to unfolded protein” (GO:006986), and “‘de novo’ protein folding (GO:006458). Moreover, enrichment analysis of genes upregulated by PhIP treatment identified the following gene ontology cellular component terms: ER subcompartment (GO:0098827), ER membrane (GO:0005789), nuclear outer membrane-ER membrane network (GO:0042175), ER protein-containing complex (GO:0140534), and ER chaperone complex (GO:0034663) (Fig. 5.5B). Endoplasmic reticulum (ER) stress is caused by proteotoxicity, lipotoxicity, and glucotoxicity and is known to cause cellular dysfunction [150]. ER stress can lead to insulin resistance via JNK activation and is associated with obesity and diabetes [151]. Interestingly, the ER-stress mediated JNK activation pathway of insulin resistance involves IRE1 α , and the enrichment analysis identified the

reactome pathway “IRE1alpha activates chaperones” (R-HSA-381070), in addition to pathways relating to oxidative stress and unfolded protein response (Fig. 5.6A). Figure 5.6B depicts a proposed potential mechanism by which HCAs induce insulin resistance, including ER stress mediated JNK activation. This novel proposal requires further interrogation of the ER stress response following HCA treatment and validation of gene expression by qRT-PCR.

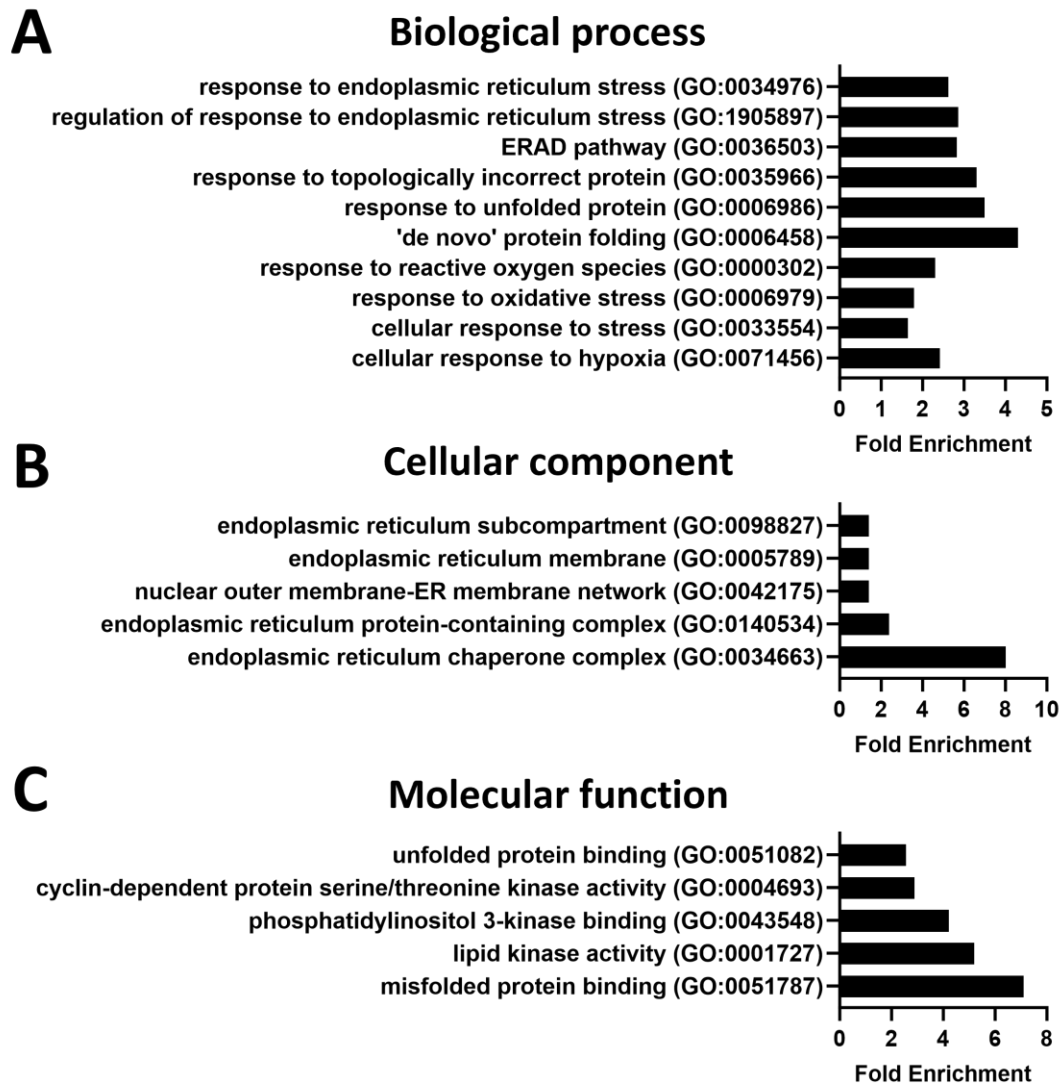


Figure 5.5. Gene Ontology (GO) biological processes, cellular components, and molecular functions significantly enriched among genes upregulated by PhIP treatment in cryopreserved human hepatocytes include indicators of endoplasmic reticulum stress. Panels A, B, and C show fold enrichment for selected GO biological processes, cellular component, and molecular function terms enriched among the *upregulated* genes, respectively.

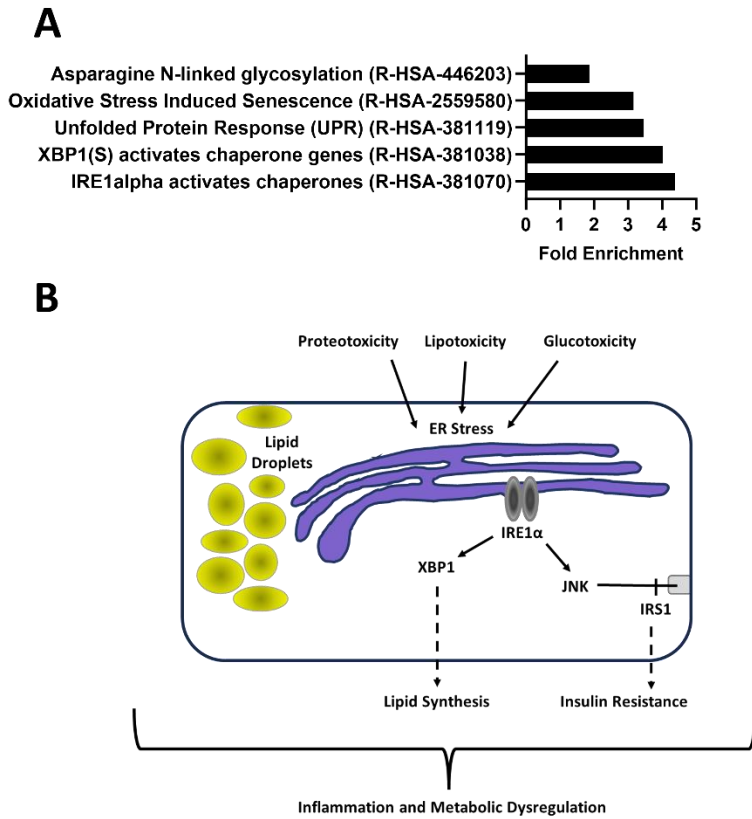


Figure 5.6. Reactome pathways significantly enriched among genes upregulated by PhIP treatment in cryopreserved human hepatocytes. Panel A shows fold enrichment for selected reactome pathways significantly enriched among upregulated genes. Panel B shows a proposed mechanism for ER stress and JNK-activated induction of insulin resistance.

DISCUSSION

The current study demonstrated, for the first time, that common HCAs found in cooked meat led to increased JNK protein activation. Moreover, inhibition of JNK activation with SP600125 restored insulin signaling at IRS1 and AKT in HCA-treated hepatocytes. Additionally, we showed that HCAs cause increased ROS, lipids, and expression of the inflammatory gene *TNF*. Lastly, an RNA-sequencing study showed that the GO biological processes, molecular functions, and cellular components enriched by genes upregulated by PhIP treatment in hepatocytes related to ER stress and the unfolded protein response. Taken together, these data provide insight into the potential mechanisms by which HCAs lead to insulin resistance and dysregulation of metabolism.

One well documented molecular mechanism of insulin resistance in hepatocytes includes ER stress resulting from proteotoxicity, lipotoxicity, and glucotoxicity. Downstream of ER stress, JNK activation disrupts insulin signaling at IRS1 by phosphorylation at the Ser307 site, disrupting downstream signaling and leading to insulin resistance [139], [140]. We've shown that HCA treatment on human hepatocytes reduces AKT phosphorylation at Ser473 and increases IRS1 phosphorylation at Ser307, indicating that HCAs cause insulin resistance. However, blocking JNK activation with SP600125 in HCA-treated hepatocytes restored insulin signaling at both IRS1 and AKT. These findings indicate clearly that activation of JNK is responsible for decreased insulin sensitivity in hepatocytes exposed to HCAs.

ROS are prominent molecules involved in cell signaling, and it is well known that increased ROS in the cell results in ER stress and UPR activation. However, it is important to note that many downstream activities of the UPR signal transducers generate ROS [152]. Increased cytosolic concentration of Ca^{2+} induces ROS production [153]. We showed that HCAs lead to increased ROS, and although not addressed in the confines of this study, our RNA-sequencing experiment indicated alterations in calcium storage. Although we've demonstrated that HCA treatment ultimately led to increased ROS, additional studies are needed to determine if ROS is the source or product of ER stress. Future studies should also investigate the potential role of calcium transport and storage in ER stress activation following HCA treatment.

In addition to ROS, ER stress-mediated IRE1 signaling can generate a key inflammatory signaling pathway via JNK activation or other pathways, which can activate inflammatory genes, ultimately disrupting metabolic function [154]. We showed that HCAs increased expression of the key inflammatory gene *TNF*, suggesting inflammation may be involved in HCA-induced insulin resistance. Additional cytokines and chemokines should be investigated to corroborate inflammation from HCAs. Moreover, The IRE1 α /XBP1 pathway contributes significantly to lipogenesis, and we've shown that HCAs lead to increased neutral lipids in human hepatocytes and that this pathway was identified by enrichment of genes upregulated by PhIP treatment. This suggests that lipotoxicity may also be a source or product of ER stress, and thus, the role of disrupted lipid homeostasis from HCAs should be interrogated further.

In summary, HCAs commonly found in cooked meat increase JNK activation in human hepatocytes, and blocking JNK activation restores HCA-induced insulin resistance. ROS, inflammation, and lipotoxicity have been proposed as potentially involved in HCA-mediated disruption of energy homeostasis, and an RNA-sequencing experiment implicated ER stress and the UPR pathway. Taken together, these results provide insight into some of the first ever proposed mechanisms for HCA-induced insulin resistance and metabolic diseases.

CHAPTER 6

HETEROCYCLIC AMINES DISRUPT LIPID HOMEOSTASIS IN HUMAN HEPATOCTES

INTRODUCTION

Metabolic dysfunction associated steatotic liver disease (MASLD)/metabolic dysfunction-associated steatohepatitis (MASH) previously termed NAFLD is a spectrum of conditions that are characterized by evidence of hepatic steatosis in the absence of excess alcohol consumption [133], and it is estimated that it is present in 20 to 30% of individuals in western countries [155]. MASH is the liver manifestation of metabolic syndrome, a term used to describe a condition where an individual possesses a combination of health risk factors, including insulin resistance, hyperglycemia, hypertension, dyslipidemia, and obesity [132]. Metabolic syndrome is a growing epidemic in the United States and worldwide, affecting an estimated 20 to 25% of the adult population [1], [156]. While it was historically believed that lifestyle choices like poor diet and lack of exercise were the primary precursors to developing conditions associated with metabolic syndrome, genetic and environmental risk factors have recently

been identified, including environmental pollutant exposure and genetic variants involved in glucose and lipid metabolism [1], [119]–[121], [127], [128]. We recently reported that exposure to heterocyclic amines (HCAs) induced insulin resistance, gluconeogenic gene expression, and glucose production in human hepatocytes, identifying exposure to HCAs as a novel environmental risk factor for conditions associated with metabolic syndrome [127].

HCAs are primarily formed from the high-temperature cooking of muscle meats, including poultry, beef, pork, and fish [112], although other sources include cigarette smoke and fumes generated from cooking oils. [25], [26], [134]. MeIQx (2-amino-3,8-dimethylimidazo[4,5-f]quinoxaline) and PhIP (2-amino-1-methyl-6-phenylimidazo[4,5-b]pyridine) are the most abundant HCAs formed in grilled beef, poultry, fish, and bacon [37], and these HCAs are highly mutagenic and carcinogenic [24], [33], [37], [112]. Cooking meat at high temperatures or for a prolonged period of time favors HCA formation, so grilling, broiling, or frying cooking methods enhance exposure to HCAs [112]. Previous studies of HCAs have primarily assessed their mutagenic and carcinogenic properties. However, recent epidemiological studies have linked unhealthy cooking methods like grilling and frying, which favor production of HCAs, and dietary exposure to HCAs via cooked meat to the development of insulin resistance, type II diabetes, and MASLD/MASH [43], [44], [135]. Moreover, we recently reported that HCAs induce insulin resistance and glucose production in human hepatocytes, further suggesting that HCA exposure may be an environmental risk factor contributing

to the development of metabolic syndrome and underlying conditions associated with MASLD/MASH [127].

In addition to insulin resistance and hyperglycemia, abnormal cholesterol and triglyceride levels are some of the medical conditions associated with metabolic syndrome [1], [132]. In fact, it has been reported that hyperglycemia and lipid abnormalities, mainly hypertriglyceridemia, develop as a result of impaired sensitivity to insulin [157]. Although we have reported that HCAs cause insulin resistance and increased glucose production in hepatocytes, the effects of HCAs on lipid homeostasis have yet to be investigated. In the current study, we examined neutral lipid accumulation, triglycerides, cholesterol, free fatty acids, and expression of genes involved in lipid metabolism and transport in human hepatocytes exposed to HCAs to assess the effects of HCAs on hepatic lipid homeostasis.

MATERIALS AND METHODS

Heterocyclic amines (HCAs)

MeIQx and PhIP were purchased from Toronto Research Chemicals and prepared into a solution with dimethyl sulfoxide (DMSO) at a stock concentration of 10 mM. MeIQx and PhIP were diluted to 25 μ M working stock solutions prepared freshly in the cell culture media at the time of each experiment.

Cell culture

Cryopreserved human hepatocytes were purchased from BioIVT and stored in liquid nitrogen. Hepatocyte samples were collected from consenting donors

under IRB approved protocols at the FDA licensed donor center at BioIVT (<http://www.bioivt.com/>). Hepatocytes were prepared from fresh human tissue and were isolated and frozen within 24 hours of organ removal by BioIVT. The hepatocytes are from human transplant rejected livers and tested negative for hepatitis B and C and HIV1 and 2. Hepatocytes were thawed according to the manufacturer's instructions as previously reported [127]. Briefly, cells were thawed by warming a vial of the hepatocytes at 37 °C for 90 seconds and suspending them in InVitroGRO HT medium (BioIVT) containing 1 mL TORPEDO™ Antibiotic Mix (BioIVT) per 45 mL media, then plated on Biocoat® collagen-coated plates (Corning) and remained in an incubator with a humidified air (95%) and carbon dioxide (CO₂, 5%) condition at 37 °C.

Gene expression analysis by RT-qPCR

Cryopreserved human hepatocytes were plated and allowed to attach for 4 hours. Cells were incubated for 24 hours with media containing MeIQx or PhIP at a concentration of 25 µM. RNA was isolated from the treated cells using E.Z.N.A. Total RNA Kit 1 (Omegabiotek) per manufacturer's protocol. cDNA was synthesized using High-Capacity cDNA Reverse Transcriptase PCR (Thermo Scientific) per manufacturer's instructions. Gene-specific cDNA was amplified and detected using iTaq Universal SYBR Green Supermix (Bio-Rad), gene-specific primers, and StepOne real-time PCR system (Applied Biosystems). The following primers were used: PNPLA3, forward 5'-TCTGGATTCTTCCCCGGAGT-3'; reverse 5'-CTGGAAGCCATGTCACCAGT-3'. HSD17B13, forward 5'-AATTTGCCGCTGTTGGCTTT-3'; reverse 5'-

ATTTTGTGGCCAACCACTGC-3'. PLIN2, forward 5'-
AGTCTTGGGGAGTCGGATGA-3'; reverse 5'-CACGGGAGTGAAGCTTGGTA-
3'. PON1, forward 5'-GACCATGGCGAAGCTGATTG-3'; reverse 5'-
CCAGGACTGTTGGGGTTGAA-3'. DGAT1, forward 5'-
GTATGGCCACACCCACAAGG-3'; reverse 5'-TGCCCAGGTTCCAAGTGAAG-
3'. DGAT2, forward 5'-TGTCTGGAGGTATCTGCCCT-3'; reverse 5'-
ACAACAGTGGTGATGGGCTT-3'. CD36, forward 5'-
TGATGTGCAAAATCCACAGGAA-3'; reverse 5'-
ACCATTGGGCTGCAGGAAAG-3'. FASN, forward 5'-
CCGCTTCCGAGATTCCATCC-3'; reverse 5'-TGGCAAACACACCCTCCTTC-3'.
CPT1A, forward 5'-GATGAGTCGTGCCACCAAGA-3'; reverse 5'-
GCTCTTGCTGCCTGAATGTG-3'. SCD1, forward 5'-
GCAGCCGAGCTTTGTAAGAG-3'; reverse 5'-GTTCTACACCTGGCTTTGGG-3'.
GAPDH, forward 5'-GGTGAAGCAGGCGTCGGAGG-3'; reverse 5'-
GAGGGCAATGCCAGCCCCAG-3'. Results were normalized to GAPDH. The
relative fold change was calculated using the delta-delta Ct ($2^{-\Delta\Delta Ct}$) method
with StepOne software (Applied Biosystems).

Neutral lipid measurements via BODIPY 493/503

Cryopreserved human hepatocytes were plated and treated as described in section 2.3. At the completion of HCA treatment, cells were fixed with 3.7% formaldehyde for an incubation period of 10 minutes, washed twice with PBS, and stained with 2 μ M BODIPY 493/503 for 30 minutes. Cells were then washed twice with PBS, permeabilized with 0.25% Triton-X 100 for 5 minutes, washed 2

additional times with PBS, counterstained with 300 nM DAPI solution for 5 minutes, and washed a final time with PBS. Cells were protected from light until imaged under fluorescent microscopy. FITC and DAPI channels using two fluorescence channels at 519 nm and 461 nm were used to capture BODIPY stained lipid droplets and DAPI stained nuclei, respectively. A subset of representative images was used for quantification according to the protocol described by Adomshick, Pu, and Veiga-Lopez [142]. Neutral lipid droplet measurements were normalized relative to cell count as determined by DAPI counterstain and expressed as a percentage relative to DMSO-treated control.

Neutral lipid measurements via Oil Red O

Cryopreserved human hepatocytes were plated and treated as described in section 2.3. At the completion of HCA treatment, cells were fixed with 3.7% formaldehyde as described in section 2.4. and stained with freshly filtered 0.2% Oil Red O for 30 minutes. Cells were washed 5 times with distilled water, and the dye was eluted with 100% 2-propanol after a 10-minute incubation. The eluate was transferred to a 96-well plate in duplicate, and absorption was read at 510 nm using a microplate reader. The cells on the original plate were permeabilized and counterstained with DAPI solution as described in section 2.4. The absorbance readings were averaged and normalized relative to cell count as determined by DAPI counterstain. Results are expressed as a percentage relative to the DMSO-treated control.

Cholesterol measurements

Cryopreserved human hepatocytes were plated and treated as described in section 2.3. Following treatment, cells were fixed, stained, and analyzed using a total cholesterol assay kit (Abcam) according to manufacturer's instructions.

Triglyceride and free fatty acid measurements

Cryopreserved human hepatocytes were plated and treated as described in section 2.3. For endogenous triglycerides, after treatment, cells were harvested, homogenized, and analyzed via a fluorometric triglyceride assay kit (Abcam) per manufacturer's instructions. For extracellular free fatty acids, media was collected after treatment and analyzed via a fluorometric free fatty acid kit (Abcam) per manufacturer's instructions.

Statistical analysis

Differences in neutral lipids, relative gene expression, cholesterol, triglycerides, and free fatty acids between the treatment groups vs. control groups were tested for significance by one-way ANOVA followed by Dunnett's Comparison Test. All statistical analyses were performed using GraphPad Prism v8.2.1 (GraphPad Software). The results are expressed as the mean \pm the standard error of the mean (SEM) and represent the averages of three independent experiments. Statistical significance was determined per the following p-values: * indicates $p < 0.05$, ** indicates $p < 0.01$, *** indicates $p < 0.001$, **** indicates $p < 0.0001$.

RESULTS

HCAs cause neutral lipid accumulation in cryopreserved human hepatocytes. Lipid droplets are metabolically active organelles enclosed by a

phospholipid monolayer that contains proteins responsible for neutral lipid synthesis or metabolism [158]. Accumulation of lipid droplets in the liver is an adaptive response to increased free fatty acids and de novo lipogenesis in hepatocytes, and dysregulation of lipid droplet biogenesis and degradation can cause intracellular lipid accumulation [159]. Lipid droplet accumulation is a key characteristic of MASLD/MASH, a condition also associated with dietary HCA exposure [43].

To investigate if HCAs cause lipid droplet accumulation, we treated cryopreserved human hepatocytes with DMSO or 25 μ M MeIQx or PhIP for 24 hours, then fixed and stained the cells for neutral lipids. Neutral lipids were stained using BODIPY 493/503 dye or Oil Red O, and DAPI was used to counterstain the nuclei. BODIPY 493/503 and DAPI-stained cells were imaged under fluorescent microscopy and quantified using CellProfiler 4.2.5. Oil Red O dye was eluted from the cells and quantified by reading absorbance at 510 nm. Neutral lipid droplet measurements were normalized relative to cell count as determined by DAPI counterstain and expressed as a percentage relative to DMSO-treated control. MeIQx treatment on hepatocytes caused an average 237% significant increase ($p < 0.01$) in neutral lipid accumulation as measured by the BODIPY 493/503 stain, and PhIP treatment caused an average 24% significant increase ($p < 0.01$) (Fig. 6.1A-B). Consistent with these findings, both HCAs caused increased neutral lipid accumulation when measured using Oil Red O dye. MeIQx treatment caused an average 446% significant increase ($p < 0.001$) and PhIP treatment caused an average 600% significant increase ($p <$

0.0001) in neutral lipids compared to the DMSO-treated control (Fig. 6.1C). Moreover, hepatocytes stained with BODIPY 493/503 and DAPI were imaged and quantified automatically using a Biotek Cytation 5 imager, and similar results were observed (data not shown). These results indicate that HCAs lead to neutral lipid accumulation in human hepatocytes.

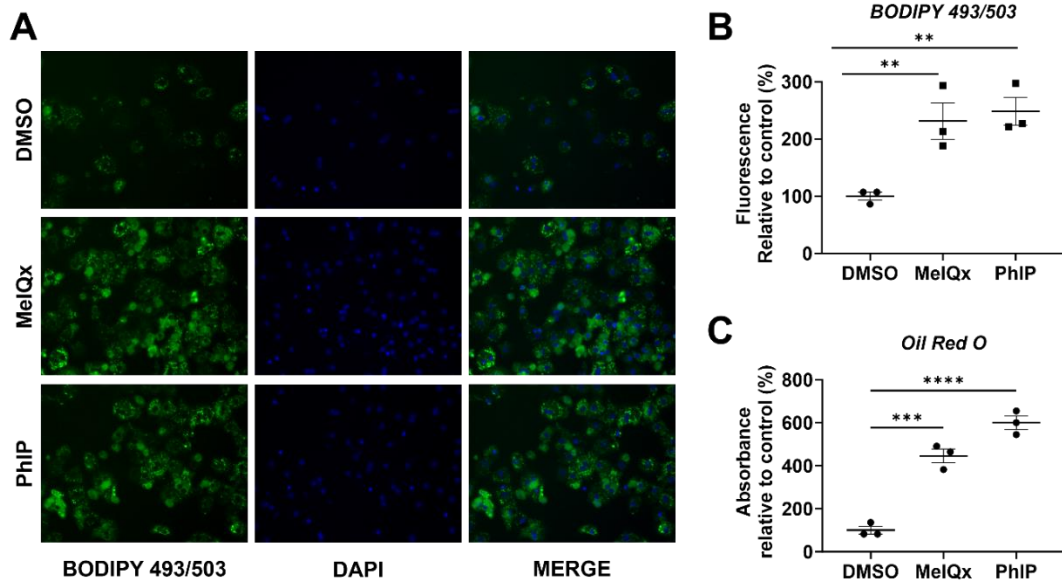


Figure 6.1. Neutral lipid accumulation following HCA treatment in cryopreserved human hepatocytes. Cryopreserved human hepatocytes were treated with DMSO or 25 μ M of the indicated HCA for 24 hours. Cells were then fixed, permeabilized, and stained with the indicated dye. BODIPY 493/503 and DAPI-stained cells were imaged under microscopy (panel A) and quantified using CellProfiler 4.2.5 (panel B). Oil Red O-stained cells were quantified by reading absorbance at 510 nm (panel C). Neutral lipid droplet measurements were normalized relative to cell count as determined by DAPI counterstain and expressed as a percentage relative to DMSO-treated control. Statistical significance was determined by one-way ANOVA followed by Dunnett's Comparisons Test. Data points represent the averages of three independent experiments, and line and error bars represent mean \pm SEM. **, $p < 0.01$; ***, $p < 0.001$; ****, $p < 0.0001$.

HCAs cause increased expression of lipid droplet-associated genes in cryopreserved human hepatocytes. To further investigate the effects of HCAs on lipid accumulation, we measured changes in expression of genes associated with lipid droplets in hepatocytes following treatment with HCAs. Cryopreserved human hepatocytes were treated with DMSO or 25 μ M MelQx or PhIP for 24 hours. The mRNA levels were measured via qRT-PCR and expressed relative to the DMSO-treated control. We measured three commonly investigated genes known to be expressed in hepatic lipid droplets, including patatin-like phospholipase domain-containing protein 3 (*PNPLA3*), hydroxysteroid 17-beta dehydrogenase 13 (*HSD17B13*), and perilipin 2 (*PLIN2*).

PNPLA3 is a lipid regulator located in the lipid droplets of hepatocytes, hydrolyzing triglycerides and catalyzing the transfer of polyunsaturated fatty acids from di- and tri-acylglycerols to phosphocholines [160]. Its primary function is to remodel phospholipids of lipid droplets. High glucose and lipotoxic conditions have been shown to induce expression of *PNPLA3*, and sustained increased expression of *PNPLA3* is associated with fatty liver [161]. We found that PhIP treatment on cryopreserved human hepatocytes significantly increased ($p < 0.05$) expression of *PNPLA3*, while MelQx treatment had no effect (Fig. 6.2A). Since there are multiple mechanisms for transcriptional regulation of *PNPLA3*, including nutrient availability and genetic polymorphisms [161], it is unclear at this time the precise mechanism by which PhIP induces expression of *PNPLA3*. However, increased expression of *PNPLA3* in hepatocytes is highly correlated with

increased lipid droplets [161], and so this finding for PhIP is consistent with the results presented in Figure 6.1.

In addition to *PNPLA3*, we investigated if HCA treatment on hepatocytes affected the expression of an additional gene, *HSD17B13*, which is a recently identified liver-enriched and hepatocyte-specific lipid droplet-associated gene. *HSD17B13* has been reported to be strongly associated with the development and progression of MASLD/MASH in both mice and humans [162], [163]. Like our findings with *PNPLA3*, PhIP treatment on hepatocytes significantly increased ($p < 0.05$) expression of *HSD17B13*, while MelQx treatment had no effect (Fig. 6.2B).

The final lipid-associated gene we investigated is *PLIN2*, which is a constitutive and ubiquitously expressed lipid droplet gene encoding for a protein often used as a marker for lipid droplets [164]. *PLIN2* expression levels are known to correlate with triglyceride content and lipid droplet density [165]. Each of the HCAs tested significantly increased the expression of *PLIN2*, compared to the DMSO-treated control (MelQx, $p < 0.001$; PhIP, $p < 0.001$) (Fig. 6.2C). These findings are consistent with the results presented in Figure 5.1, further indicating that HCAs lead to neutral lipid droplet accumulation in human hepatocytes.

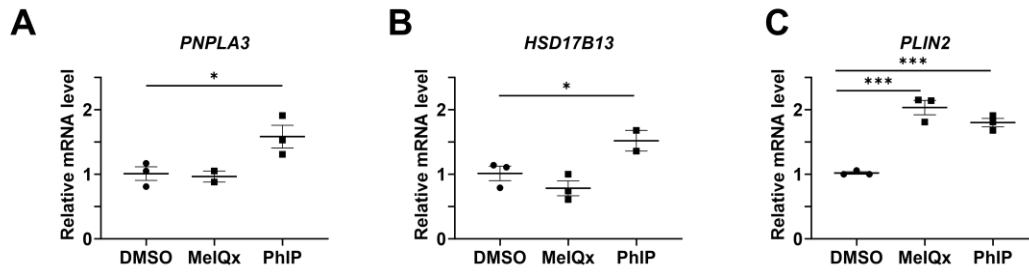


Figure 6.2. Increases in expression of lipid droplet genes following HCA treatment in cryopreserved human hepatocytes. Cryopreserved human hepatocytes were treated with DMSO or 25 μ M of the indicated HCA for 24 hours. The mRNA levels were measured via qRT-PCR using GAPDH as an internal control and are expressed relative to the DMSO-treated control. Statistical significance was determined by one-way ANOVA followed by Dunnett's Comparison Test. Data points represent the averages of three independent experiments, and line and error bars represent mean \pm SEM. *, $p < 0.05$; ***, $p < 0.001$.

HCA treatment causes increased total cholesterol and decreased expression of *PON1* in cryopreserved human hepatocytes.

Cholesterol homeostasis is essential to maintain proper cellular functions, and cellular cholesterol levels reflect the balance between biosynthesis, uptake, export and esterification [166].

Dysregulation of cholesterol homeostasis is associated with increased risk of fatty liver diseases and cardiovascular diseases [166], [167]. In fact, excess lipids in hepatic steatosis are primarily neutral lipids, including triglycerides and cholesterol esters [167]. Since HCA treatment in hepatocytes caused increased neutral lipids, we next investigated if HCAs altered cholesterol levels in hepatocytes. Cryopreserved human hepatocytes were treated with DMSO or 25 μ M MeIQx or PhIP for 24 hours, then total cholesterol was measured using a fluorometric cholesterol assay kit (Abcam). MeIQx treatment significantly increased ($p < 0.05$) total cholesterol levels by an average of 17.8% in cryopreserved human hepatocytes, and PhIP treatment significantly increased ($p < 0.001$) total cholesterol levels by an average of 45.3% (Fig. 6.3A).

Additionally, we investigated if HCA treatment altered the expression of paraoxonase-1 (*PON1*), which is a gene encoding for a protein that stimulates cholesterol efflux and is speculated to play a role in several conditions associated with NAFLD and related diseases [168]. Recently, it was stated that *PON1* is linked to a reduction in oxidative stress and inflammation [169], and epidemiological studies have demonstrated that low *PON1* activity is associated with increased risk of cardiovascular events [170]. HCA treatment on

cryopreserved human hepatocytes significantly decreased the expression of *PON1* (MeIQx, $p < 0.0001$; PhIP, $p < 0.0001$) (Fig. 6.3B).

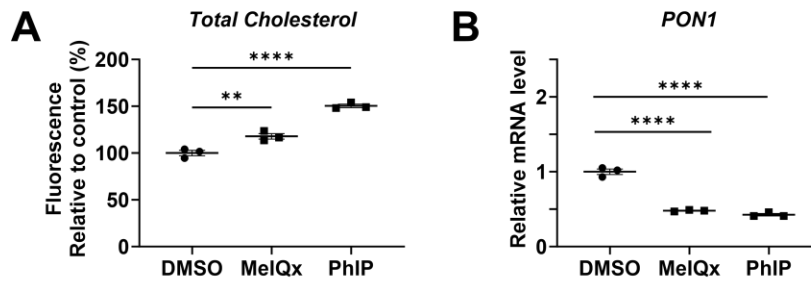


Figure 6.3. Increased cholesterol and decreased expression of *PON1* following HCA treatment in cryopreserved human hepatocytes.

Cryopreserved human hepatocytes were treated with DMSO or 25 μ M of the indicated HCA for 24 hours. Cholesterol was measured using a fluorescent dye kit (panel A), and mRNA levels were measured via qRT-PCR (panel B) using GAPDH as an internal control and are expressed relative to the DMSO-treated control. Statistical significance was determined by one-way ANOVA followed by Dunnett's Comparison Test. Bars represent mean \pm SEM (panel A). Data points represent the averages of three independent experiments, and line and error bars represent mean \pm SEM (panel B). **, $p < 0.01$; ****, $p < 0.0001$.

HCAs cause increased endogenous triglycerides and increased expression of genes involved in triglyceride synthesis in cryopreserved human

hepatocytes. The hallmark of MASLD/MASH is triglyceride accumulation in hepatocytes that arises from an imbalance between lipid acquisition via fatty acid uptake and de novo lipogenesis and lipid removal by mitochondrial fatty acid oxidation and export [171]. As mentioned in section 3.3., excess lipids in hepatic steatosis are primarily neutral lipids, including triglycerides and cholesterol esters [167]. Since HCA treatment on hepatocytes led to increased neutral lipids and increased total cholesterol, we next examined if HCAs also increased triglycerides. Cryopreserved human hepatocytes were treated with DMSO or 25 μ M MeIQx or PhIP for 24 hours, then endogenous triglycerides were measured using a fluorometric triglyceride assay kit (Abcam). MeIQx did not alter triglyceride levels in hepatocytes, but PhIP significantly increased ($p < 0.001$) triglycerides by an average of 54.6% (Fig. 6.4A).

To better understand the source of increased triglycerides from HCA treatment, we next investigated if HCAs altered expression of genes involved in triglyceride synthesis, including diacylglycerol *O*-acyltransferase 1 (*DGAT1*) and diacylglycerol *O*-acyltransferase 2 (*DGAT2*). The final and only committed step in the biosynthesis of triglycerides is catalyzed by the *DGAT1* and *DGAT2* enzymes [172]. While there are a variety of mechanisms by which *DGAT1* and *DGAT2* are transcriptionally and post-transcriptionally regulated, it is known that both of these enzymes are involved in energy metabolism, particularly triglyceride homeostasis [172]. While both HCAs caused a slight increase in expression of

DGAT1, neither were statistically significant (Fig. 6.4B). However, both MeIQx and PhIP treatment on cryopreserved human hepatocytes caused a statistically significant increase in *DGAT2* expression, compared to DMSO-treated control (MeIQx, $p < 0.05$; PhIP, $p < 0.0001$) (Fig. 6.4C). These findings indicate that HCAs cause dysregulation of triglyceride homeostasis, and that HCA-induced triglyceride accumulation may in-part be due to increased triglyceride synthesis.

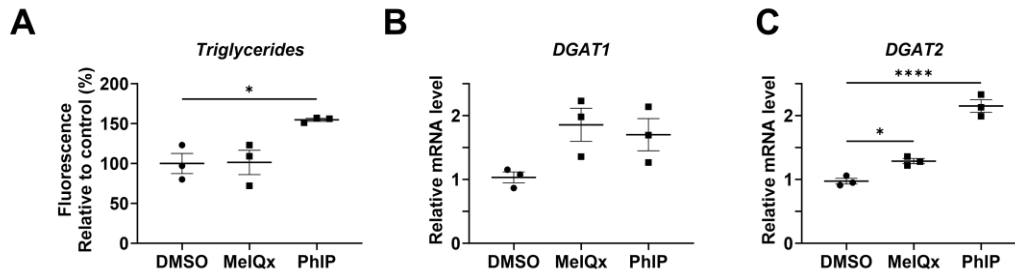


Figure 6.4. Increased triglycerides and increased expression of genes involved in triglyceride synthesis following HCA treatment in cryopreserved human hepatocytes. Cryopreserved human hepatocytes were treated with DMSO or 25 μ M of the indicated HCA for 24 hours. Triglycerides were measured using a fluorescent dye kit (panel A), and mRNA levels were measured via qRT-PCR (panels B-C) using GAPDH as an internal control and are expressed relative to the DMSO-treated control. Statistical significance was determined by one-way ANOVA followed by Dunnett's Comparison Test. Bars represent mean \pm SEM (panel A). Data points represent the averages of three independent experiments, and line and error bars represent mean \pm SEM (panel B). *, $p < 0.05$; ****, $p < 0.0001$.

HCAs cause increased extracellular free fatty acids and dysregulated expression of genes involved in free fatty acid uptake and metabolism in cryopreserved human hepatocytes. Hepatic lipotoxicity occurs when the liver's ability to use, store and export free fatty acids as triglycerides is overwhelmed by a free fatty acid flux, often caused by increased hepatic de novo lipogenesis, a hallmark of insulin resistance and MASLD/MASH [173]. Excess free fatty acids leads to ER and oxidative stress, autophagy, lipoapoptosis and inflammation, and free fatty acid levels are correlated with many disease severities [174], [175]. Insulin resistance is known to cause increased circulation of free fatty acids, which is often accompanied by increased cholesterol and triglycerides [176]. Since HCAs induce insulin resistance and increase cholesterol and triglyceride levels in human hepatocytes, we next investigated if HCAs also alter free fatty acids. Cryopreserved human hepatocytes were treated with DMSO or 25 μ M MeIQx or PhIP for 24 hours, then extracellular long-chain free fatty acids were measured using a fluorometric free fatty acid assay kit (Abcam). MeIQx significantly increased ($p < 0.01$) extracellular free fatty acid levels in hepatocytes by an average of 69.7% compared to the DMSO-treated control group (Fig. 6.5A). PhIP also significantly increased ($p < 0.05$) extracellular free fatty acid levels to approximately double that of the DMSO-treated control by an average of a 105% increase (Fig. 6.5A).

In addition to free fatty acid levels, we also measured changes in expression of genes involved in free fatty acid uptake and metabolism, including cluster of differentiation 36 (*CD36*), fatty acid synthase (*FASN*), carnitine

palmitoyltransferase 1A (*CPT1A*), and stearoyl-CoA desaturase (*SCD1*), to better understand the mechanism by which HCAs lead to increased extracellular free fatty acid levels in human hepatocytes. CD36 is a fatty acid translocase responsible for fatty acid uptake and triglyceride storage and export, and this protein has been implicated in playing a role in lipid accumulation, inflammatory signaling, energy reprogramming, and oxidative stress [177]. There are many mechanisms by which expression of *CD36* in hepatocytes is increased, but regardless of the mechanism, increased expression of CD36 tends to correlate with increased lipid accumulation and development of MASLD/MASH [173], [177]. Cryopreserved human hepatocytes treated with 25 μ M PhIP for 24 hours showed a significant increase ($p < 0.01$) in expression of *CD36*, compared to DMSO- treated control, while MeIQx-treated hepatocytes showed a slight increase in *CD36* expression, although not statistically significant (Fig. 6.5B).

Additionally, we evaluated changes in expression of *FASN*, which catalyzes the last step in fatty acid biosynthesis, and thus is considered a major determinant of the maximal hepatic capacity to generate fatty acids by de novo lipogenesis [178]. Increased *FASN* expression in hepatocytes is correlated with increased free fatty acids. We found that MeIQx treatment on hepatocytes caused a slight increase in expression of *FASN*, although not statistically significant, while PhIP treatment significantly increased ($p < 0.05$) *FASN* expression (Fig. 6.5C).

Next, we examined expression of *CPT1A*, which is responsible for the transport of long-chain fatty acids into the mitochondria and serves as the rate-

limiting enzyme for β -oxidation [179]. Deficiency or abnormal regulation of *CPT1A* can lead to metabolic disorders, but increasing expression of *CPT1A* in patients with metabolic syndrome has been shown to drastically lower triglyceride levels and improve other lipid metabolism abnormalities [180]. In cryopreserved human hepatocytes treated with HCAs, there was a significant decrease ($p < 0.01$) in expression of *CPT1A* following PhIP treatment, while MelQx did not affect *CPT1A* expression (Fig. 6.5D). These results suggest that increased extracellular free fatty acids induced by PhIP exposure in hepatocytes could be partly due to inefficient transport into the mitochondria. However, due to the complex transcriptional, post-transcriptional, and genetic regulation of *CPT1A*, this mechanism needs to be further evaluated.

Lastly, we measured changes in expression of *SCD1*, a key enzyme in lipid metabolism involved in the regulation of triglyceride synthesis and fatty acid oxidation in hepatocytes [181], [182]. Previous studies reported that *SCD1* activity was increased in MASLD/MASH patients, and that deletion of *SCD1* decreased liver lipid synthesis [183], [184]. MelQx treatment on hepatocytes significantly increased ($p < 0.05$) expression of *SCD1*, while PhIP treatment did not (Fig. 6.5E).

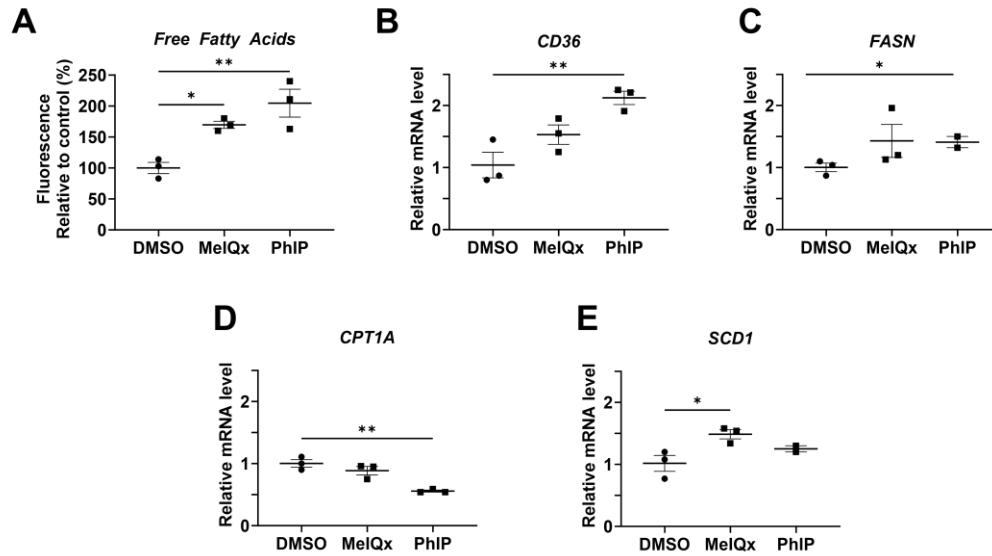


Figure 6.5. Increased free fatty acids and dysregulated expression of genes involved in free fatty acid uptake and metabolism following HCA treatment in cryopreserved human hepatocytes.

Cryopreserved human hepatocytes were treated with DMSO or 25 μ M of the indicated HCA for 24 hours.

Extracellular free fatty acids were measured using a fluorescent dye kit (panel A), and mRNA levels were measured via qRT-PCR (panels B-E) using GAPDH as an internal control and are expressed relative to the DMSO-treated control.

Statistical significance was determined by one-way ANOVA followed by

Dunnett's Comparison Test. Bars represent mean \pm SEM (panel A). Data points represent the averages of three independent experiments, and line and error

bars represent mean \pm SEM (panel B). *, $p < 0.05$; **, $p < 0.01$.

DISCUSSION

The current study demonstrates, for the first time, that the most common HCAs found in cooked meat can lead to dysregulation of hepatic lipid homeostasis, a condition associated with metabolic syndrome and MASLD/MASH. The findings presented here indicate that HCAs can lead to increased neutral lipids and free fatty acids and dysregulation of several key genes involved in lipid metabolism and transport in human hepatocytes. These findings support a previous epidemiological study that documented an association between consumption of unhealthily cooked meat, which favors HCA formation, with MASLD/MASH [43].

One interesting observation from the current study is that PhIP displays a greater effect than MeIQx on dysregulation of lipid homeostasis. While each HCA caused an increase in neutral lipids compared to the DMSO-control as measured by Oil Red O staining, the increase in neutral lipids in PhIP-treated hepatocytes was significantly greater ($p = 0.0197$) than in MeIQx-treated hepatocytes. Furthermore, PhIP treatment led to increased expression of several key genes associated with lipid droplets in hepatocytes, including *PNPLA3*, *HSD17B13*, and *PLIN2*, while MeIQx treatment only increased expression of *PLIN2*. Similarly, each HCA tested led to increased cholesterol and free fatty acids, compared to the DMSO-treated control, but PhIP treatment exhibited an average 27.5% and 35.0% increase, respectively, greater than MeIQx treatment. Furthermore, key enzymes involved in free fatty acid uptake and metabolism, including *CD36*, *FASN*, and *CPT1A*, are dysregulated by PhIP treatment but unaffected by MeIQx

treatment. Additionally, PhIP treatment increased triglyceride levels, while MeIQx treatment exhibited no effect. Although MeIQx did in fact lead to dysregulation of some components of lipid homeostasis, including increased neutral lipids and free fatty acids, the effects of PhIP on lipid homeostasis are more apparent and robust. Interestingly, this finding is inversely correlated to the findings previously reported on HCA-mediated insulin resistance and dysregulated glucose homeostasis in hepatocytes. We previously reported that MeIQx caused a dose-dependent reduction in insulin sensitivity and a dose-dependent increase in glucose production, while the effects of PhIP were either not dose-dependent or absent [127]. The structural differences between PhIP and MeIQx and their subsequent differences in metabolism were proposed as potential explanations for the differences in altered insulin sensitivity and glucose production that was reported previously, and these structural and metabolic differences may also be responsible for the differences in dysregulation of lipid homeostasis reported here. The potential role of HCA metabolism in dysregulation of lipid homeostasis should be explored further.

Of note, HCAs often require hepatic bioactivation to yield mutagenic and carcinogenic effects [56], [72], [73], [110], [115], [118], [124]. Many HCAs are bioactivated via *O*-acetylation by the phase II metabolic enzyme *N*-acetyltransferase 2 (NAT2) following *N*-hydroxylation mediated by Cytochrome P450 1A2 (CYP1A2) [72]. *NAT2* exhibits a genetic polymorphism in humans that correlates to acetylation activity, and individuals can be phenotyped as slow, intermediate, or rapid NAT2 acetylators based on their *NAT2* genotype [52],

which exhibit differential metabolism of HCAs, and subsequently, differential risk of genotoxicity [52], [124]. In addition to genotoxicity, we recently reported that induction of glucose production by HCAs is dependent on *NAT2* genetic polymorphism [128]. We also recently reported that *NAT2* genetic polymorphism affects HCA-induced insulin resistance and increased gluconeogenesis (in review). Since defective insulin signaling is associated with dysregulation of both glucose and lipid homeostasis, it is important that future studies investigate if *NAT2* genetic polymorphism plays a role in HCA-mediated dysregulation of hepatic lipids.

In addition to the potential role of *NAT2* genetic polymorphism, future studies should include investigation of the underlying mechanisms by which HCAs dysregulate hepatic lipid homeostasis and the subsequent downstream manifestations of lipotoxicity. Hepatic lipid accumulation is primarily induced by increased hepatic uptake of circulating fatty acids, increased hepatic de novo fatty acid synthesis, decreased hepatic β -oxidation, and decreased hepatic lipid export [185], and some of the downstream lipotoxic consequences include ER stress, mitochondrial dysfunction, and insulin resistance [186]. Increased fatty acid and triglyceride uptake and synthesis and impaired β -oxidation is known to result from elevated extracellular glucose and free fatty acids [187], and since HCAs have been shown to increase both extracellular glucose [127] and free fatty acids, this is one potential underlying mechanism of HCA-mediated dysregulated lipid homeostasis and subsequent lipid accumulation. Additionally, PhIP increased expression of *CD36* and *FASN*, suggesting that PhIP treatment

in hepatocytes led to increased free fatty acid uptake and synthesis, which may be an additional partial underlying source of lipid dysregulation. Future studies should continue to explore mechanisms of dysregulated hepatic lipids and their subsequent lipotoxicity.

In summary, some of the most common HCAs found in cooked meat caused dysregulation of lipid homeostasis in cryopreserved human hepatocytes, as evident by increased neutral lipids and free fatty acids and dysregulation of key genes involved in lipid metabolism, storage, uptake, and transport. These findings suggest that exposure to HCAs by cooked meat consumption may lead to fat accumulation in the liver, contributing to conditions associated with metabolic syndrome and MASLD/MASH. Future studies should continue to explore the underlying mechanisms that elicit the effects reported here in addition to the role of *NAT2* genetic polymorphisms.

CHAPTER 7

SUMMARY AND CONCLUSIONS

This study provides evidence for the first time that HCAs lead to insulin resistance and dysregulation of energy homeostasis, including increased glucose production and lipid accumulation, in human hepatocytes, and this association is independent of meat consumption. Moreover, this study indicates that these outcomes are differentially affected by *NAT2* genetic polymorphism. Our findings propose potential mechanisms of HCA-mediated disruption of insulin signaling and energy homeostasis, including ER stress, JNK activation, ROS, and lipotoxicity.

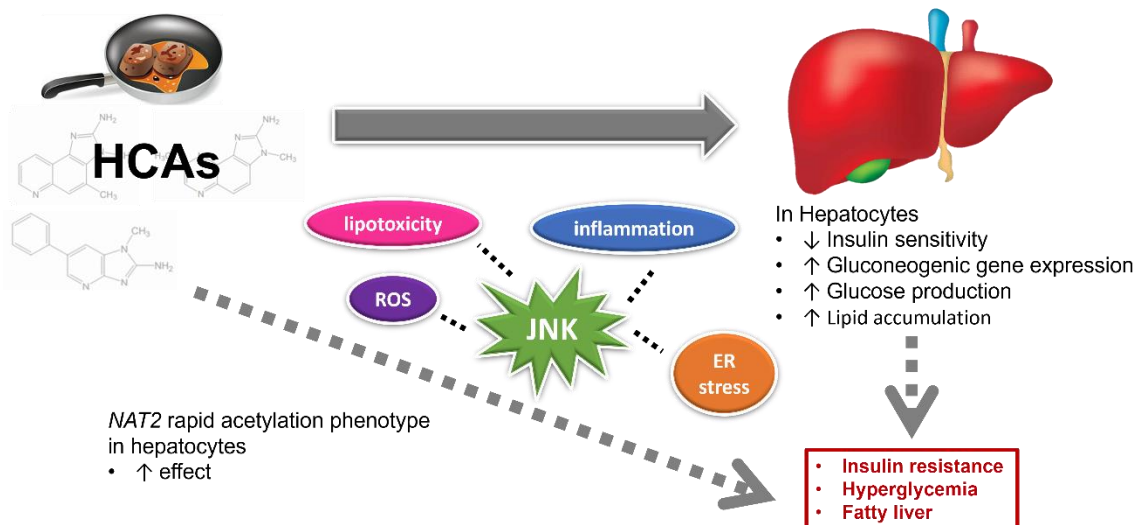


Figure 7.1. Summary of dissertation findings.

In Chapter 2 of this work, we provide evidence that HCAs commonly found in cooked meat caused insulin resistance and increased glucose production in HepG2 and human hepatocytes. We also show that insulin receptor-target genes involved in gluconeogenesis, including *G6PC* and *PCK1*, are upregulated in human hepatocytes following exposure to HCAs, indicating that upregulation in gluconeogenesis may, at least in part, contribute to HCA-induced increase in glucose production. The findings reported in Chapter 2 imply that, independent of meat consumption, dietary exposure to HCAs contribute to pathogenesis of insulin resistance and hyperglycemia.

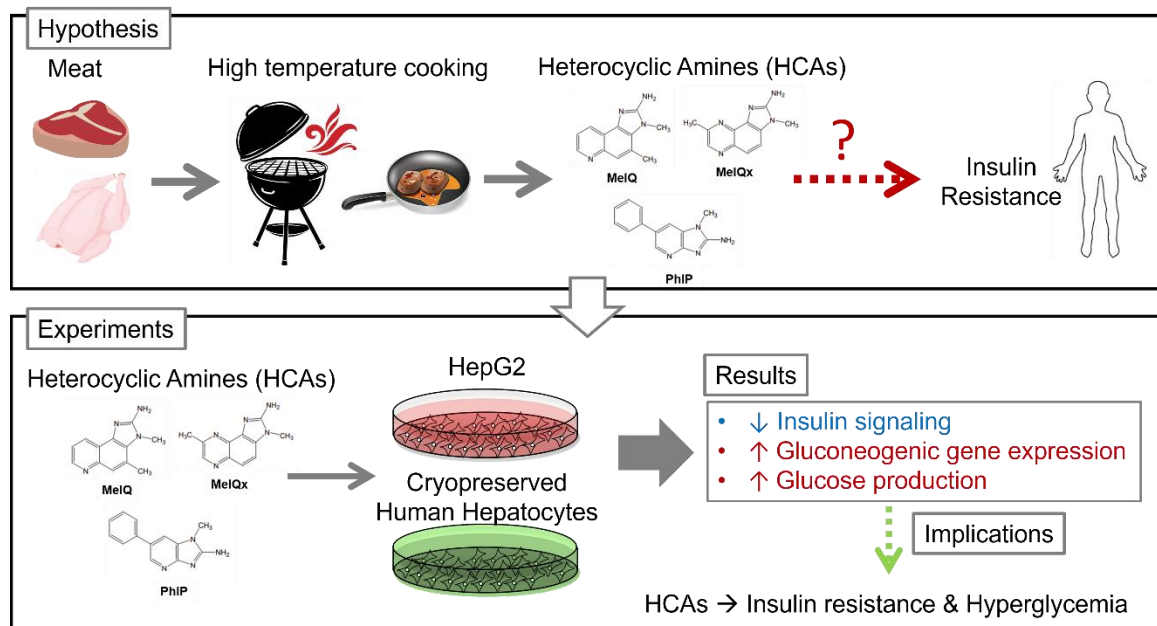


Figure 7.2. Summary of Chapter 2.

In Chapter 3, we investigated the contribution of *NAT2* genetic polymorphism to increased glucose production in hepatocytes following exposure to HCAs. We found that metabolism of HCAs by *NAT2* is required for their effects on glucose homeostasis, suggesting that individuals with rapid *NAT2* acetylator phenotypes may be at a greater risk of developing hyperglycemia and insulin resistance following dietary exposure to HCAs.

Moreover, Chapter 4 explored the role of *NAT2* genetic polymorphism on additional aspects of HCA-mediated disruption of energy homeostasis, including insulin signaling and insulin receptor-target genes involved in gluconeogenesis. Like our findings reported in Chapter 3, we found that individuals with rapid *NAT2* acetylator phenotype are at greater risk of developing insulin resistance and increased hepatic glucose production following exposure to HCAs. This study demonstrated the crucial need to consider the role of polymorphisms in genes involved in metabolism when evaluating risk following exposure to toxicants.

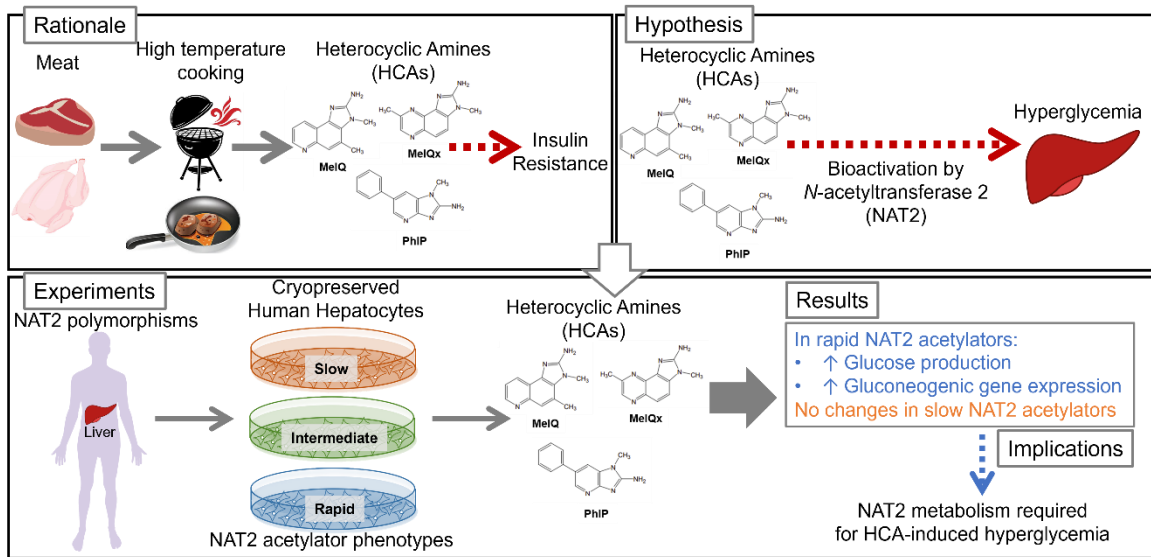


Figure 7.3. Summary of Chapters 3 and 4.

Chapter 5 explored potential mechanisms by which HCAs dysregulate energy homeostasis. We found that HCAs lead to JNK activation and blocking JNK restored insulin signaling in HCA-treated hepatocytes. Chapter 5 also shows that HCAs caused ROS, inflammation, and lipid accumulation. Moreover, enrichment analysis from an RNA-sequencing experiment where cryopreserved human hepatocytes were treated with HCAs identified “response to endoplasmic reticulum stress” (GO:0034976) and multiple related pathways involved in this category, which is of particular interest since ER stress is known to lead to JNK activation and subsequent insulin resistance. These findings implicate ER stress and JNK protein activity in HCA-induced insulin resistance.

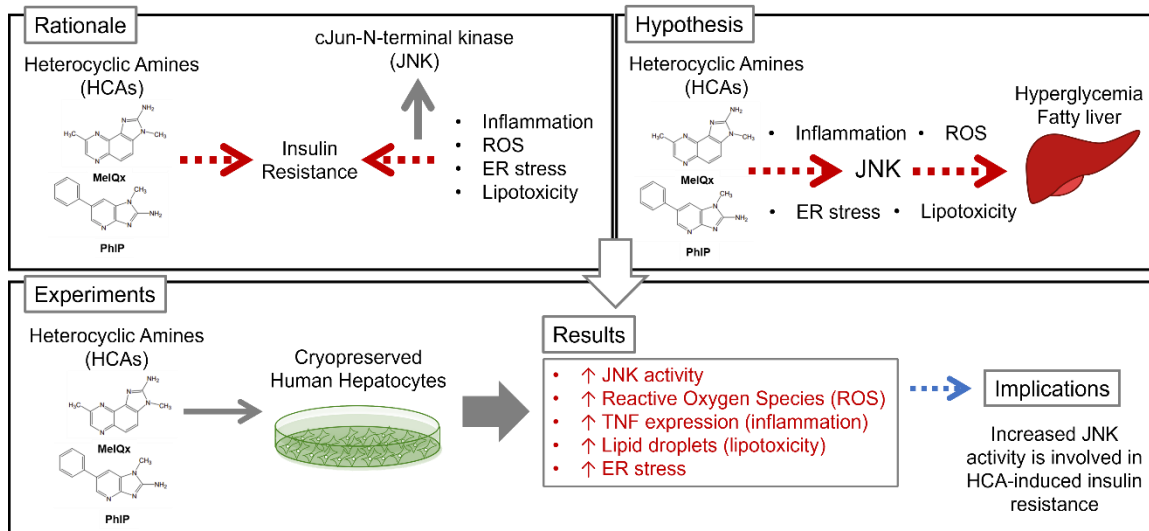


Figure 7.4. Summary of Chapter 5.

Chapter 6 investigated disruption of lipid homeostasis following treatment of HCAs in cryopreserved human hepatocytes. We found that HCAs caused increased lipid accumulation, triglycerides, cholesterol, and free fatty acids. Additionally, disruption of several key genes involved in lipid homeostasis was reported. The results in Chapter 6 suggest that, in addition to changes in insulin sensitivity and glucose homeostasis, HCAs dysregulate lipid homeostasis as well. These findings suggest that exposure to HCAs by cooked meat consumption may lead to fat accumulation in the liver, contributing to conditions associated with metabolic syndrome and MASLD/MASH.

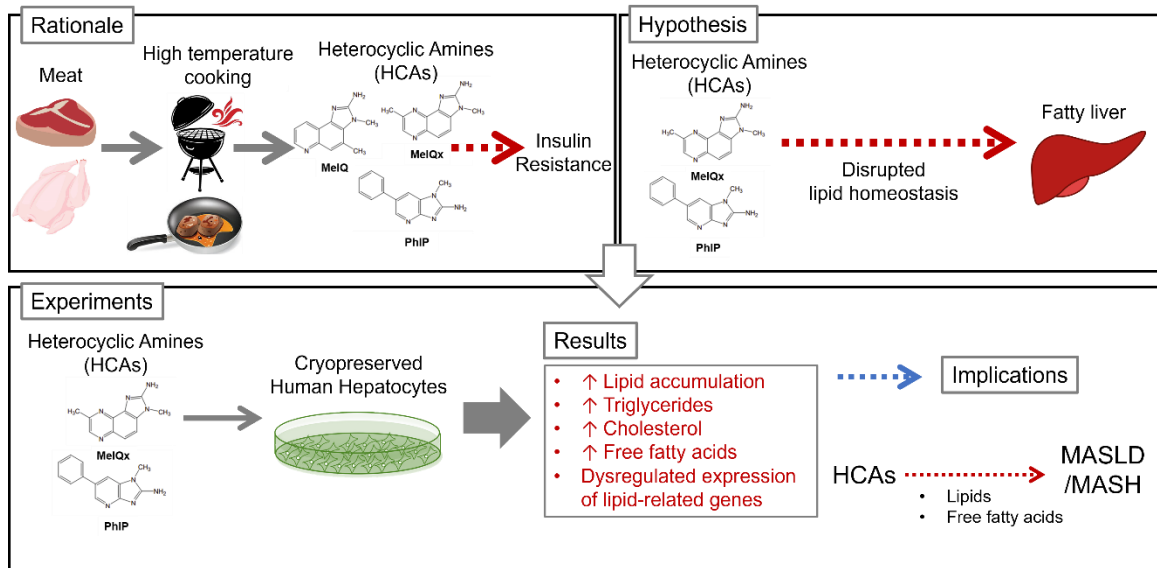


Figure 7.5. Summary of Chapter 6.

In total, the work described in this dissertation identifies a novel role for HCAs in the pathogenesis of hepatic insulin resistance and increased glucose and lipids in human hepatocytes. We've also indicated a clear role of *NAT2* genetic polymorphism in the bioactivation of these compounds that is required for them to mediate these effects. The work reported in this dissertation will aid to elucidate risks associated with development of conditions associated with metabolic syndrome and insulin resistance, specifically with a focus on the role of gene-environmental interactions in the context of metabolic disorders.

STRENGTHS AND LIMITATIONS

STRENGTHS

The work presented here is, to our knowledge, the first comprehensive experimental study of HCA-induced disruption of energy homeostasis. Previous work in the field of HCAs has primarily focused on their genotoxic effects. Although recent epidemiological studies have documented an association between HCAs and insulin resistance, the work of this dissertation is the first to investigate this potentially novel link.

The sheer novelty of the work serves as a major strength of this dissertation. No previous studies of HCAs have investigated their impact on energy homeostasis. This dissertation examines altered insulin signaling and glucose and lipid homeostasis following HCA treatment. An RNA sequencing analysis also provides insight into the mechanisms by which HCAs may mediate these effects. Moreover, we considered the role of *NAT2* genetic polymorphism,

allowing us to investigate a gene-environmental interaction in the context of HCA-mediated disruption of energy homeostasis. This entirely novel study also sheds light on the newly recognized necessity of considering genetics when investigating risk associated with metabolic diseases.

An additional major strength of these studies is the use of cryopreserved human hepatocytes. Cryopreserved human hepatocytes are the gold standard model for *in vitro* hepatic toxicology research and allowed us to also consider the role of NAT2 metabolism in our studies, as cryopreserved human hepatocytes express normal levels of metabolic enzymes and were genotyped and phenotyped for NAT2 activity. The abundant use of this cell culture model affirms the relevance of reported findings.

LIMITATIONS

Major limitations of this work include the narrow range of HCA doses and treatment times. While it is difficult to determine precise HCA exposure levels in the human population, future studies could include a wider range of doses. The doses selected for these studies were based on the literature reports of HCA doses used in genotoxicity studies. However, exposure levels needed to mediate the effects reported here may vary. Additionally, the use of cryopreserved human hepatocytes limits the length of time for HCA treatment. The studies here included treatment that varied from 24 to 72 hours. Using a model that allowed

for repeated low-dose treatments over an extended period could provide a more realistic model of human exposure.

An additional limitation includes the lack of *in vivo* studies. We did not yet utilize a mouse model for these studies because mice provide a poor model system for investigating NAT2 metabolism. It is believed that mouse Nat1 is homologous to human NAT2, so Nat1 KO mice have been used as a surrogate for studying the effects of human NAT2, but this presents major limitations. As previously reviewed [188], the mouse Nat1 coding sequence is only slightly more homologous to human NAT2 than to human NAT1, and for amino acid homology, mouse Nat1 is actually more homologous to human NAT1 (73%) than human NAT2 (72%). Additionally, mouse Nat1 is expressed across every tissue examined [189], whereas human NAT2 expression is largely limited to liver and GI tract. Additionally, the substrate profiles of mouse Nat1 and human NAT2 are less similar than previously believed [190]. Therefore, it is likely that mouse Nat1 and human NAT2 do not share identical roles. Despite this, *in vivo* studies of HCA-mediated insulin resistance and metabolic effects could be useful. Understanding the whole-organ and whole-body effects of HCAs on hepatic energy homeostasis could provide greater insight into the physiological effects of HCAs. Although overcoming the obstacle of investigating NAT2 metabolism in mouse models may be challenging, future *in vivo* studies could utilize HCA metabolites instead of parent compounds. Additionally, humanized Nat mouse models could be used.

FUTURE DIRECTIONS

Future directions should include experiments using lower HCA concentrations and longer treatment times to model physiologically relevance. Additionally, the use of animal models to characterize the novel link between HCAs and insulin resistance should be pursued. Finally, additional potential mechanisms of disrupted energy homeostasis by HCAs should also be explored.

REFERENCES

- [1] M. G. Saklayen, “The Global Epidemic of the Metabolic Syndrome,” *Curr. Hypertens. Rep.*, vol. 20, no. 2, p. 12, Feb. 2018, doi: 10.1007/s11906-018-0812-z.
- [2] Y.-W. Park, S. Zhu, L. Palaniappan, S. Heshka, M. R. Carnethon, and S. B. Heymsfield, “The metabolic syndrome: prevalence and associated risk factor findings in the US population from the Third National Health and Nutrition Examination Survey, 1988-1994,” *Arch. Intern. Med.*, vol. 163, no. 4, pp. 427–436, Feb. 2003, doi: 10.1001/archinte.163.4.427.
- [3] L. Yang and G. A. Colditz, “Prevalence of Overweight and Obesity in the United States, 2007-2012,” *JAMA Intern. Med.*, vol. 175, no. 8, pp. 1412–1413, Aug. 2015, doi: 10.1001/jamainternmed.2015.2405.
- [4] S. Mottillo *et al.*, “The metabolic syndrome and cardiovascular risk a systematic review and meta-analysis,” *J. Am. Coll. Cardiol.*, vol. 56, no. 14, pp. 1113–1132, Sep. 2010, doi: 10.1016/j.jacc.2010.05.034.
- [5] C. K. Roberts, A. L. Hevener, and R. J. Barnard, “Metabolic syndrome and insulin resistance: underlying causes and modification by exercise training,” *Compr. Physiol.*, vol. 3, no. 1, pp. 1–58, Jan. 2013, doi: 10.1002/cphy.c110062.

- [6] M. C. Petersen and G. I. Shulman, "Mechanisms of Insulin Action and Insulin Resistance," *Physiol. Rev.*, vol. 98, no. 4, pp. 2133–2223, Oct. 2018, doi: 10.1152/physrev.00063.2017.
- [7] D. Santoleri and P. M. Titchenell, "Resolving the Paradox of Hepatic Insulin Resistance," *Cell. Mol. Gastroenterol. Hepatol.*, vol. 7, no. 2, pp. 447–456, 2019, doi: 10.1016/j.jcmgh.2018.10.016.
- [8] H. V. Lin and D. Accili, "Hormonal regulation of hepatic glucose production in health and disease," *Cell Metab.*, vol. 14, no. 1, pp. 9–19, Jul. 2011, doi: 10.1016/j.cmet.2011.06.003.
- [9] M. S. Brown and J. L. Goldstein, "Selective versus total insulin resistance: a pathogenic paradox," *Cell Metab.*, vol. 7, no. 2, pp. 95–96, Feb. 2008, doi: 10.1016/j.cmet.2007.12.009.
- [10] C. M. Taniguchi, B. Emanuelli, and C. R. Kahn, "Critical nodes in signalling pathways: insights into insulin action," *Nat. Rev. Mol. Cell Biol.*, vol. 7, no. 2, pp. 85–96, Feb. 2006, doi: 10.1038/nrm1837.
- [11] P. Gual, Y. Le Marchand-Brustel, and J.-F. Tanti, "Positive and negative regulation of insulin signaling through IRS-1 phosphorylation," *Biochimie*, vol. 87, no. 1, pp. 99–109, Jan. 2005, doi: 10.1016/j.biochi.2004.10.019.
- [12] M. F. White, "IRS proteins and the common path to diabetes," *Am. J. Physiol.-Endocrinol. Metab.*, vol. 283, no. 3, pp. E413–E422, Sep. 2002, doi: 10.1152/ajpendo.00514.2001.

- [13] G. S. Hotamisligil, "Inflammation and metabolic disorders," *Nature*, vol. 444, no. 7121, Art. no. 7121, Dec. 2006, doi: 10.1038/nature05485.
- [14] C. de Luca and J. M. Olefsky, "Inflammation and insulin resistance," *FEBS Lett.*, vol. 582, no. 1, pp. 97–105, Jan. 2008, doi: 10.1016/j.febslet.2007.11.057.
- [15] P. Sangwung, K. F. Petersen, G. I. Shulman, and J. W. Knowles, "Mitochondrial Dysfunction, Insulin Resistance, and Potential Genetic Implications," *Endocrinology*, vol. 161, no. 4, Apr. 2020, doi: 10.1210/endocr/bqaa017.
- [16] L. Salvadó, X. Palomer, E. Barroso, and M. Vázquez-Carrera, "Targeting endoplasmic reticulum stress in insulin resistance," *Trends Endocrinol. Metab.*, vol. 26, no. 8, pp. 438–448, Aug. 2015, doi: 10.1016/j.tem.2015.05.007.
- [17] T. C. Alves *et al.*, "Regulation of hepatic fat and glucose oxidation in rats with lipid-induced hepatic insulin resistance," *Hepatol. Baltim. Md*, vol. 53, no. 4, pp. 1175–1181, Apr. 2011, doi: 10.1002/hep.24170.
- [18] N. Houstis, E. D. Rosen, and E. S. Lander, "Reactive oxygen species have a causal role in multiple forms of insulin resistance," *Nature*, vol. 440, no. 7086, pp. 944–948, Apr. 2006, doi: 10.1038/nature04634.
- [19] I. A. Leclercq, G. C. Farrell, J. Field, D. R. Bell, F. J. Gonzalez, and G. R. Robertson, "CYP2E1 and CYP4A as microsomal catalysts of lipid peroxides in murine nonalcoholic steatohepatitis," *J. Clin. Invest.*, vol. 105, no. 8, pp. 1067–1075, Apr. 2000, doi: 10.1172/JCI8814.

- [20] J. M. Schattenberg *et al.*, “Jnk1 but not jnk2 promotes the development of steatohepatitis in mice,” *Hepatology*, vol. 43, no. 1, pp. 163–172, 2006, doi: 10.1002/hep.20999.
- [21] J. M. Schattenberg, Y. Wang, R. Singh, R. M. Rigoli, and M. J. Czaja, “Hepatocyte CYP2E1 overexpression and steatohepatitis lead to impaired hepatic insulin signaling,” *J. Biol. Chem.*, vol. 280, no. 11, pp. 9887–9894, Mar. 2005, doi: 10.1074/jbc.M410310200.
- [22] J. K. Kim *et al.*, “Tissue-specific overexpression of lipoprotein lipase causes tissue-specific insulin resistance,” *Proc. Natl. Acad. Sci. U. S. A.*, vol. 98, no. 13, pp. 7522–7527, Jun. 2001, doi: 10.1073/pnas.121164498.
- [23] V. T. Samuel *et al.*, “Mechanism of hepatic insulin resistance in non-alcoholic fatty liver disease,” *J. Biol. Chem.*, vol. 279, no. 31, pp. 32345–32353, Jul. 2004, doi: 10.1074/jbc.M313478200.
- [24] J. S. Felton, M. G. Knize, F. T. Hatch, M. J. Tanga, and M. E. Colvin, “Heterocyclic amine formation and the impact of structure on their mutagenicity,” *Cancer Lett.*, vol. 143, no. 2, pp. 127–134, Sep. 1999, doi: 10.1016/s0304-3835(99)00141-x.
- [25] L. Zhang *et al.*, “Evaluation of Tobacco Smoke and Diet as Sources of Exposure to Two Heterocyclic Aromatic Amines for the U.S. Population: NHANES 2013-2014,” *Cancer Epidemiol. Biomark. Prev. Publ. Am. Assoc. Cancer Res. Cosponsored Am. Soc. Prev. Oncol.*, vol. 29, no. 1, pp. 103–111, Jan. 2020, doi: 10.1158/1055-9965.EPI-19-0169.

- [26] L. Zhang, D. L. Ashley, and C. H. Watson, "Quantitative analysis of six heterocyclic aromatic amines in mainstream cigarette smoke condensate using isotope dilution liquid chromatography-electrospray ionization tandem mass spectrometry," *Nicotine Tob. Res. Off. J. Soc. Res. Nicotine Tob.*, vol. 13, no. 2, pp. 120–126, Feb. 2011, doi: 10.1093/ntr/ntq219.
- [27] G. Eisenbrand and W. Tang, "Food-borne heterocyclic amines. Chemistry, formation, occurrence and biological activities. A literature review," *Toxicology*, vol. 84, no. 1–3, pp. 1–82, Nov. 1993, doi: 10.1016/0300-483x(93)90109-6.
- [28] C. M. Lan, T. H. Kao, and B. H. Chen, "Effects of heating time and antioxidants on the formation of heterocyclic amines in marinated foods," *J. Chromatogr. B Analyt. Technol. Biomed. Life. Sci.*, vol. 802, no. 1, pp. 27–37, Mar. 2004, doi: 10.1016/j.jchromb.2003.09.025.
- [29] R. Zamora and F. J. Hidalgo, "Formation of heterocyclic aromatic amines with the structure of aminoimidazoazarenes in food products," *Food Chem.*, vol. 313, p. 126128, May 2020, doi: 10.1016/j.foodchem.2019.126128.
- [30] F. Toribio, E. Moyano, L. Puignou, and M. T. Galceran, "Ion-trap tandem mass spectrometry for the determination of heterocyclic amines in food," *J. Chromatogr. A*, vol. 948, no. 1–2, pp. 267–281, Mar. 2002, doi: 10.1016/s0021-9673(01)01476-5.
- [31] M. Murkovic, "Formation of heterocyclic aromatic amines in model systems," *J. Chromatogr. B Analyt. Technol. Biomed. Life. Sci.*, vol. 802, no. 1, pp. 3–10, Mar. 2004, doi: 10.1016/j.jchromb.2003.09.026.

- [32] K. Skog, A. Solyakov, and M. Jägerstad, "Effects of heating conditions and additives on the formation of heterocyclic amines with reference to amino-carbolines in a meat juice model system," *Food Chem.*, vol. 68, no. 3, pp. 299–308, Feb. 2000, doi: 10.1016/S0308-8146(99)00195-8.
- [33] M. G. Knize, F. A. Dolbeare, P. L. Cunningham, and J. S. Felton, "Mutagenic activity and heterocyclic amine content of the human diet," *Princess Takamatsu Symp.*, vol. 23, pp. 30–38, 1995.
- [34] C. Dennis, F. Karim, and J. S. Smith, "Evaluation of maillard reaction variables and their effect on heterocyclic amine formation in chemical model systems," *J. Food Sci.*, vol. 80, no. 2, pp. T472-478, Feb. 2015, doi: 10.1111/1750-3841.12737.
- [35] M. Jägerstad *et al.*, "Creatin(in)e and Maillard reaction products as precursors of mutagenic compounds: Effects of various amino acids," *Food Chem.*, vol. 12, no. 4, pp. 255–264, Jan. 1983, doi: 10.1016/0308-8146(83)90014-6.
- [36] R. J. Turesky, J. Taylor, L. Schnackenberg, J. P. Freeman, and R. D. Holland, "Quantitation of carcinogenic heterocyclic aromatic amines and detection of novel heterocyclic aromatic amines in cooked meats and grill scrapings by HPLC/ESI-MS," *J. Agric. Food Chem.*, vol. 53, no. 8, pp. 3248–3258, Apr. 2005, doi: 10.1021/jf048290g.
- [37] K. I. Skog, M. A. Johansson, and M. I. Jägerstad, "Carcinogenic heterocyclic amines in model systems and cooked foods: a review on formation, occurrence and intake," *Food Chem. Toxicol. Int. J. Publ. Br.*

- Ind. Biol. Res. Assoc.*, vol. 36, no. 9–10, pp. 879–896, Oct. 1998, doi: 10.1016/s0278-6915(98)00061-1.
- [38] P. Arvidsson, M. a. j. s. Van Boekel, K. Skog, and M. Jägerstad, “Kinetics of Formation of Polar Heterocyclic Amines in a Meat Model System,” *J. Food Sci.*, vol. 62, no. 5, pp. 911–916, 1997, doi: 10.1111/j.1365-2621.1997.tb15005.x.
- [39] T. K. Lam *et al.*, “Intakes of Red Meat, Processed Meat, and Meat Mutagens Increase Lung Cancer Risk,” *Cancer Res.*, vol. 69, no. 3, pp. 932–939, Jan. 2009, doi: 10.1158/0008-5472.CAN-08-3162.
- [40] C. Potera, “Red Meat and Colorectal Cancer: Exploring the Potential HCA Connection,” *Environ. Health Perspect.*, vol. 124, no. 10, p. A189, Oct. 2016, doi: 10.1289/ehp.124-A189.
- [41] S. E. Steck *et al.*, “Nucleotide excision repair gene polymorphisms, meat intake and colon cancer risk,” *Mutat. Res. Mol. Mech. Mutagen.*, vol. 762, pp. 24–31, Apr. 2014, doi: 10.1016/j.mrfmmm.2014.02.004.
- [42] L. I. Mignone *et al.*, “Meat consumption, heterocyclic amines, NAT2, and the risk of breast cancer,” *Nutr. Cancer*, vol. 61, no. 1, pp. 36–46, 2009, doi: 10.1080/01635580802348658.
- [43] S. Zelber-Sagi *et al.*, “High red and processed meat consumption is associated with non-alcoholic fatty liver disease and insulin resistance,” *J. Hepatol.*, vol. 68, no. 6, pp. 1239–1246, Jun. 2018, doi: 10.1016/j.jhep.2018.01.015.

- [44] G. Liu *et al.*, “Meat Cooking Methods and Risk of Type 2 Diabetes: Results From Three Prospective Cohort Studies,” *Diabetes Care*, vol. 41, no. 5, pp. 1049–1060, May 2018, doi: 10.2337/dc17-1992.
- [45] G. Liu, G. Zong, F. B. Hu, W. C. Willett, D. M. Eisenberg, and Q. Sun, “Cooking Methods for Red Meats and Risk of Type 2 Diabetes: A Prospective Study of U.S. Women,” *Diabetes Care*, vol. 40, no. 8, pp. 1041–1049, Aug. 2017, doi: 10.2337/dc17-0204.
- [46] E. Sim, A. Abuhammad, and A. Ryan, “Arylamine N-acetyltransferases: from drug metabolism and pharmacogenetics to drug discovery,” *Br. J. Pharmacol.*, vol. 171, no. 11, pp. 2705–2725, Jun. 2014, doi: 10.1111/bph.12598.
- [47] D. W. Hein, M. A. Doll, and M. R. Habil, “Human N-Acetyltransferase 1 and 2 Differ in Affinity Towards Acetyl-Coenzyme A Cofactor and N-Hydroxy-Arylamine Carcinogens,” *Front. Pharmacol.*, vol. 13, p. 821133, 2022, doi: 10.3389/fphar.2022.821133.
- [48] A. Husain, X. Zhang, M. A. Doll, J. C. States, D. F. Barker, and D. W. Hein, “Identification of N-acetyltransferase 2 (NAT2) transcription start sites and quantitation of NAT2-specific mRNA in human tissues,” *Drug Metab. Dispos. Biol. Fate Chem.*, vol. 35, no. 5, pp. 721–727, May 2007, doi: 10.1124/dmd.106.014621.
- [49] K. Fukunaga *et al.*, “Functional Characterization of the Effects of N-acetyltransferase 2 Alleles on N-acetylation of Eight Drugs and Worldwide

- Distribution of Substrate-Specific Diversity,” *Front. Genet.*, vol. 12, p. 652704, Mar. 2021, doi: 10.3389/fgene.2021.652704.
- [50] D. W. Nebert, “Role of genetics and drug metabolism in human cancer risk,” *Mutat. Res.*, vol. 247, no. 2, pp. 267–281, Apr. 1991, doi: 10.1016/0027-5107(91)90022-g.
- [51] A. Woziwodzka, M. Tarasewicz, and J. Piosik, “[Heterocyclic aromatic amines, food-derived mutagens: metabolism and relevance to cancer susceptibility],” *Postepy Biochem.*, vol. 56, no. 4, pp. 435–446, 2010.
- [52] D. W. Hein, “Molecular genetics and function of NAT1 and NAT2: role in aromatic amine metabolism and carcinogenesis,” *Mutat. Res. Mol. Mech. Mutagen.*, vol. 506–507, pp. 65–77, Sep. 2002, doi: 10.1016/S0027-5107(02)00153-7.
- [53] B. S. Shastry, “SNPs: Impact on Gene Function and Phenotype,” in *Single Nucleotide Polymorphisms: Methods and Protocols*, A. A. Komar, Ed., in *Methods in Molecular Biology*TM. , Totowa, NJ: Humana Press, 2009, pp. 3–22. doi: 10.1007/978-1-60327-411-1_1.
- [54] D. W. Hein, S. Boukouvala, D. M. Grant, R. F. Minchin, and E. Sim, “Changes in consensus arylamine N-acetyltransferase gene nomenclature,” *Pharmacogenet. Genomics*, vol. 18, no. 4, p. 367, Apr. 2008, doi: 10.1097/FPC.0b013e3282f60db0.
- [55] K. Walker, G. Ginsberg, D. Hattis, D. O. Johns, K. Z. Guyton, and B. Sonawane, “Genetic polymorphism in N-Acetyltransferase (NAT): Population distribution of NAT1 and NAT2 activity,” *J. Toxicol. Environ.*

Health B Crit. Rev., vol. 12, no. 5–6, pp. 440–472, 2009, doi:

10.1080/10937400903158383.

- [56] C.-C. Huang *et al.*, “NAT2 fast acetylator genotype is associated with an increased risk of colorectal cancer in Taiwan,” *Dis. Colon Rectum*, vol. 50, no. 7, pp. 981–989, Jul. 2007, doi: 10.1007/s10350-007-0230-9.
- [57] A. Koizumi *et al.*, “Evidence on N-acetyltransferase allele-associated metabolism of hydrazine in Japanese workers,” *J. Occup. Environ. Med.*, vol. 40, no. 3, pp. 217–222, Mar. 1998, doi: 10.1097/00043764-199803000-00003.
- [58] B. Zhao, A. Seow, E. J. Lee, and H. P. Lee, “Correlation between acetylation phenotype and genotype in Chinese women,” *Eur. J. Clin. Pharmacol.*, vol. 56, no. 9–10, pp. 689–692, Dec. 2000, doi: 10.1007/s002280000203.
- [59] A. Sabbagh, A. Langaney, P. Darlu, N. Gérard, R. Krishnamoorthy, and E. S. Poloni, “Worldwide distribution of NAT2 diversity: implications for NAT2 evolutionary history,” *BMC Genet.*, vol. 9, p. 21, Feb. 2008, doi: 10.1186/1471-2156-9-21.
- [60] M. Chen *et al.*, “N-acetyltransferase 2 slow acetylator genotype associated with adverse effects of sulfasalazine in the treatment of inflammatory bowel disease,” *Can. J. Gastroenterol.*, vol. 21, no. 3, pp. 155–158, Mar. 2007.
- [61] R. P. Tiis, L. P. Osipova, D. V. Lichman, E. N. Voronina, and M. L. Filipenko, “Studying polymorphic variants of the NAT2 gene (NAT2*5 and

- NAT2*7) in Nenets populations of Northern Siberia,” *BMC Genet.*, vol. 21, no. Suppl 1, p. 115, Oct. 2020, doi: 10.1186/s12863-020-00909-4.
- [62] I. Metushi, J. Uetrecht, and E. Phillips, “Mechanism of isoniazid-induced hepatotoxicity: then and now,” *Br. J. Clin. Pharmacol.*, vol. 81, no. 6, pp. 1030–1036, Jun. 2016, doi: 10.1111/bcp.12885.
- [63] R. L. de F. Teixeira *et al.*, “Genetic polymorphisms of NAT2, CYP2E1 and GST enzymes and the occurrence of antituberculosis drug-induced hepatitis in Brazilian TB patients,” *Mem. Inst. Oswaldo Cruz*, vol. 106, no. 6, pp. 716–724, Sep. 2011, doi: 10.1590/s0074-02762011000600011.
- [64] M. Richardson, J. Kirkham, K. Dwan, D. J. Sloan, G. Davies, and A. L. Jorgensen, “NAT2 variants and toxicity related to anti-tuberculosis agents: a systematic review and meta-analysis,” *Int. J. Tuberc. Lung Dis. Off. J. Int. Union Tuberc. Lung Dis.*, vol. 23, no. 3, pp. 293–305, Mar. 2019, doi: 10.5588/ijtld.18.0324.
- [65] J. A. Timbrell, S. J. Harland, and V. Facchini, “Polymorphic acetylation of hydralazine,” *Clin. Pharmacol. Ther.*, vol. 28, no. 3, pp. 350–355, Sep. 1980, doi: 10.1038/clpt.1980.173.
- [66] D. W. Hein *et al.*, “Metabolic activation and deactivation of arylamine carcinogens by recombinant human NAT1 and polymorphic NAT2 acetyltransferases,” *Carcinogenesis*, vol. 14, no. 8, pp. 1633–1638, Aug. 1993, doi: 10.1093/carcin/14.8.1633.
- [67] M. García-Closas *et al.*, “NAT2 slow acetylation, GSTM1 null genotype, and risk of bladder cancer: results from the Spanish Bladder Cancer Study

- and meta-analyses,” *Lancet Lond. Engl.*, vol. 366, no. 9486, pp. 649–659, Aug. 2005, doi: 10.1016/S0140-6736(05)67137-1.
- [68] P. M. Marcus, P. Vineis, and N. Rothman, “NAT2 slow acetylation and bladder cancer risk: a meta-analysis of 22 case-control studies conducted in the general population,” *Pharmacogenetics*, vol. 10, no. 2, pp. 115–122, Mar. 2000, doi: 10.1097/00008571-200003000-00003.
- [69] T. D. da Silva, A. V. Felipe, J. M. de Lima, C. T. F. Oshima, and N. M. Forones, “N-Acetyltransferase 2 genetic polymorphisms and risk of colorectal cancer,” *World J. Gastroenterol.*, vol. 17, no. 6, pp. 760–765, Feb. 2011, doi: 10.3748/wjg.v17.i6.760.
- [70] C. Lilla *et al.*, “Effect of NAT1 and NAT2 genetic polymorphisms on colorectal cancer risk associated with exposure to tobacco smoke and meat consumption,” *Cancer Epidemiol. Biomark. Prev. Publ. Am. Assoc. Cancer Res. Cosponsored Am. Soc. Prev. Oncol.*, vol. 15, no. 1, pp. 99–107, Jan. 2006, doi: 10.1158/1055-9965.EPI-05-0618.
- [71] H. Wang *et al.*, “Interaction between Red Meat Intake and NAT2 Genotype in Increasing the Risk of Colorectal Cancer in Japanese and African Americans,” *PloS One*, vol. 10, no. 12, p. e0144955, 2015, doi: 10.1371/journal.pone.0144955.
- [72] H. C. Chou, N. P. Lang, and F. F. Kadlubar, “Metabolic activation of N-hydroxy arylamines and N-hydroxy heterocyclic amines by human sulfotransferase(s),” *Cancer Res.*, vol. 55, no. 3, pp. 525–529, Feb. 1995.

- [73] F. P. Guengerich, "Metabolic activation of carcinogens," *Pharmacol. Ther.*, vol. 54, no. 1, pp. 17–61, 1992, doi: 10.1016/0163-7258(92)90050-a.
- [74] H. Ohgaki, H. Hasegawa, M. Suenaga, S. Sato, S. Takayama, and T. Sugimura, "Carcinogenicity in mice of a mutagenic compound, 2-amino-3,8-dimethylimidazo[4,5-f]quinoxaline (MeIQx) from cooked foods," *Carcinogenesis*, vol. 8, no. 5, pp. 665–668, May 1987, doi: 10.1093/carcin/8.5.665.
- [75] M. A. Butler, M. Iwasaki, F. P. Guengerich, and F. F. Kadlubar, "Human cytochrome P-450PA (P-450IA2), the phenacetin O-deethylase, is primarily responsible for the hepatic 3-demethylation of caffeine and N-oxidation of carcinogenic arylamines," *Proc. Natl. Acad. Sci. U. S. A.*, vol. 86, no. 20, pp. 7696–7700, Oct. 1989, doi: 10.1073/pnas.86.20.7696.
- [76] D. W. Hein, "N-acetyltransferase 2 genetic polymorphism: effects of carcinogen and haplotype on urinary bladder cancer risk," *Oncogene*, vol. 25, no. 11, pp. 1649–1658, Mar. 2006, doi: 10.1038/sj.onc.1209374.
- [77] M. Fathzadeh, D. W. Hein, and J. W. Knowles, "The Human Arylamine N-Acetyltransferase Type 2 Gene: Genomics and Cardiometabolic Risk," in *Arylamine N-Acetyltransferases in Health and Disease*, WORLD SCIENTIFIC, 2017, pp. 43–67. doi: 10.1142/9789813232013_0002.
- [78] J. W. Knowles *et al.*, "Identification and validation of N-acetyltransferase 2 as an insulin sensitivity gene," *J. Clin. Invest.*, vol. 125, no. 4, pp. 1739–1751, Apr. 2015, doi: 10.1172/JCI74692.

- [79] P. Marzuillo *et al.*, “Novel association between the nonsynonymous A803G polymorphism of the N-acetyltransferase 2 gene and impaired glucose homeostasis in obese children and adolescents,” *Pediatr. Diabetes*, vol. 18, no. 6, pp. 478–484, 2017, doi: 10.1111/pedi.12417.
- [80] T. M. Teslovich *et al.*, “Biological, clinical and population relevance of 95 loci for blood lipids,” *Nature*, vol. 466, no. 7307, pp. 707–713, Aug. 2010, doi: 10.1038/nature09270.
- [81] J. P. Camporez, Y. Wang, K. Faarkrog, N. Chukijrungroat, K. F. Petersen, and G. I. Shulman, “Mechanism by which arylamine N-acetyltransferase 1 ablation causes insulin resistance in mice,” *Proc. Natl. Acad. Sci. U. S. A.*, vol. 114, no. 52, pp. E11285–E11292, Dec. 2017, doi: 10.1073/pnas.1716990115.
- [82] I. Chennamsetty *et al.*, “Nat1 deficiency is associated with mitochondrial dysfunction and exercise intolerance in mice,” *Cell Rep.*, vol. 17, no. 2, pp. 527–540, Oct. 2016, doi: 10.1016/j.celrep.2016.09.005.
- [83] E. Cecchin and G. Stocco, “Pharmacogenomics and Personalized Medicine,” *Genes*, vol. 11, no. 6, Jun. 2020, doi: 10.3390/genes11060679.
- [84] K.-W. Cheng, F. Chen, and M. Wang, “Heterocyclic amines: chemistry and health,” *Mol. Nutr. Food Res.*, vol. 50, no. 12, pp. 1150–1170, Dec. 2006, doi: 10.1002/mnfr.200600086.
- [85] A. Orzechowski, D. Schrenk, B. S. Bock-Hennig, and K. W. Bock, “Glucuronidation of carcinogenic arylamines and their N-hydroxy derivatives by rat and human phenol UDP-glucuronosyltransferase of the

- UGT1 gene complex," *Carcinogenesis*, vol. 15, no. 8, pp. 1549–1553, Aug. 1994, doi: 10.1093/carcin/15.8.1549.
- [86] S. Knasmüller *et al.*, "Genotoxic effects of heterocyclic aromatic amines in human derived hepatoma (HepG2) cells," *Mutagenesis*, vol. 14, no. 6, pp. 533–540, Nov. 1999, doi: 10.1093/mutage/14.6.533.
- [87] Z. Zhang, H. Liu, and J. Liu, "Akt activation: A potential strategy to ameliorate insulin resistance," *Diabetes Res. Clin. Pract.*, vol. 156, p. 107092, Oct. 2019, doi: 10.1016/j.diabres.2017.10.004.
- [88] R. W. Mackenzie and B. T. Elliott, "Akt/PKB activation and insulin signaling: a novel insulin signaling pathway in the treatment of type 2 diabetes," *Diabetes Metab. Syndr. Obes. Targets Ther.*, vol. 7, pp. 55–64, 2014, doi: 10.2147/DMSO.S48260.
- [89] E. Gonzalez and T. E. McGraw, "Insulin-modulated Akt subcellular localization determines Akt isoform-specific signaling," *Proc. Natl. Acad. Sci. U. S. A.*, vol. 106, no. 17, pp. 7004–7009, Apr. 2009, doi: 10.1073/pnas.0901933106.
- [90] S. Sefried, H.-U. Häring, C. Weigert, and S. S. Eckstein, "Suitability of hepatocyte cell lines HepG2, AML12 and THLE-2 for investigation of insulin signalling and hepatokine gene expression," *Open Biol.*, vol. 8, no. 10, p. 180147, Oct. 2018, doi: 10.1098/rsob.180147.
- [91] W.-M. Yang, K.-H. Min, and W. Lee, "MiR-1271 upregulated by saturated fatty acid palmitate provokes impaired insulin signaling by repressing INSR and IRS-1 expression in HepG2 cells," *Biochem. Biophys. Res. Commun.*,

vol. 478, no. 4, pp. 1786–1791, Sep. 2016, doi:
10.1016/j.bbrc.2016.09.029.

- [92] H.-S. Han, G. Kang, J. S. Kim, B. H. Choi, and S.-H. Koo, “Regulation of glucose metabolism from a liver-centric perspective,” *Exp. Mol. Med.*, vol. 48, p. e218, Mar. 2016, doi: 10.1038/emm.2015.122.
- [93] P. Puigserver *et al.*, “Insulin-regulated hepatic gluconeogenesis through FOXO1-PGC-1alpha interaction,” *Nature*, vol. 423, no. 6939, pp. 550–555, May 2003, doi: 10.1038/nature01667.
- [94] Y. Xing, A. Li, Y. Yang, X. Li, L. Zhang, and H. Guo, “The regulation of FOXO1 and its role in disease progression,” *Life Sci.*, vol. 193, pp. 124–131, Jan. 2018, doi: 10.1016/j.lfs.2017.11.030.
- [95] D. N. Gross, A. P. J. van den Heuvel, and M. J. Birnbaum, “The role of FoxO in the regulation of metabolism,” *Oncogene*, vol. 27, no. 16, pp. 2320–2336, Apr. 2008, doi: 10.1038/onc.2008.25.
- [96] S. Kersten and R. Stienstra, “The role and regulation of the peroxisome proliferator activated receptor alpha in human liver,” *Biochimie*, vol. 136, pp. 75–84, May 2017, doi: 10.1016/j.biochi.2016.12.019.
- [97] J. C. Yoon *et al.*, “Control of hepatic gluconeogenesis through the transcriptional coactivator PGC-1,” *Nature*, vol. 413, no. 6852, pp. 131–138, Sep. 2001, doi: 10.1038/35093050.
- [98] S. Goffart and R. J. Wiesner, “Regulation and Co-Ordination of Nuclear Gene Expression During Mitochondrial Biogenesis,” *Exp. Physiol.*, vol. 88, no. 1, pp. 33–40, 2003, doi: 10.1113/eph8802500.

- [99] J. Westerbacka *et al.*, “Genes involved in fatty acid partitioning and binding, lipolysis, monocyte/macrophage recruitment, and inflammation are overexpressed in the human fatty liver of insulin-resistant subjects,” *Diabetes*, vol. 56, no. 11, pp. 2759–2765, Nov. 2007, doi: 10.2337/db07-0156.
- [100] M. Ahrens *et al.*, “DNA methylation analysis in nonalcoholic fatty liver disease suggests distinct disease-specific and remodeling signatures after bariatric surgery,” *Cell Metab.*, vol. 18, no. 2, pp. 296–302, Aug. 2013, doi: 10.1016/j.cmet.2013.07.004.
- [101] C. Koliaki *et al.*, “Adaptation of hepatic mitochondrial function in humans with non-alcoholic fatty liver is lost in steatohepatitis,” *Cell Metab.*, vol. 21, no. 5, pp. 739–746, May 2015, doi: 10.1016/j.cmet.2015.04.004.
- [102] T. C. Leone *et al.*, “PGC-1alpha deficiency causes multi-system energy metabolic derangements: muscle dysfunction, abnormal weight control and hepatic steatosis,” *PLoS Biol.*, vol. 3, no. 4, p. e101, Apr. 2005, doi: 10.1371/journal.pbio.0030101.
- [103] J. L. Estall *et al.*, “Sensitivity of lipid metabolism and insulin signaling to genetic alterations in hepatic peroxisome proliferator-activated receptor-gamma coactivator-1alpha expression,” *Diabetes*, vol. 58, no. 7, pp. 1499–1508, Jul. 2009, doi: 10.2337/db08-1571.
- [104] E. M. Morris *et al.*, “PGC-1 α overexpression results in increased hepatic fatty acid oxidation with reduced triacylglycerol accumulation and

- secretion,” *Am. J. Physiol. Gastrointest. Liver Physiol.*, vol. 303, no. 8, pp. G979-992, Oct. 2012, doi: 10.1152/ajpgi.00169.2012.
- [105] W. Zhang *et al.*, “FoxO1 regulates multiple metabolic pathways in the liver: effects on gluconeogenic, glycolytic, and lipogenic gene expression,” *J. Biol. Chem.*, vol. 281, no. 15, pp. 10105–10117, Apr. 2006, doi: 10.1074/jbc.M600272200.
- [106] H. Kamata, S.-I. Honda, S. Maeda, L. Chang, H. Hirata, and M. Karin, “Reactive oxygen species promote TNF α -induced death and sustained JNK activation by inhibiting MAP kinase phosphatases,” *Cell*, vol. 120, no. 5, pp. 649–661, Mar. 2005, doi: 10.1016/j.cell.2004.12.041.
- [107] P. Storz and A. Toker, “Protein kinase D mediates a stress-induced NF- κ B activation and survival pathway,” *EMBO J.*, vol. 22, no. 1, pp. 109–120, Jan. 2003, doi: 10.1093/emboj/cdg009.
- [108] P. Gual, Y. Le Marchand-Brustel, and J.-F. Tanti, “Positive and negative regulation of insulin signaling through IRS-1 phosphorylation,” *Biochimie*, vol. 87, no. 1, pp. 99–109, Jan. 2005, doi: 10.1016/j.biochi.2004.10.019.
- [109] A. M. Carvalho, A. M. Miranda, F. A. Santos, A. P. M. Loureiro, R. M. Fisberg, and D. M. Marchioni, “High intake of heterocyclic amines from meat is associated with oxidative stress,” *Br. J. Nutr.*, vol. 113, no. 8, pp. 1301–1307, Apr. 2015, doi: 10.1017/S0007114515000628.
- [110] K. J. Metry *et al.*, “Effect of rapid human N-acetyltransferase 2 haplotype on DNA damage and mutagenesis induced by 2-amino-3-methylimidazo-[4,5-f]quinoline (IQ) and 2-amino-3,8-dimethylimidazo-[4,5-f]quinoxaline

- (MelQx),” *Mutat. Res.*, vol. 684, no. 1–2, pp. 66–73, Feb. 2010, doi: 10.1016/j.mrfmmm.2009.12.001.
- [111] D. W. Hein, R. A. Salazar-González, M. A. Doll, and Y. Zang, “The effect of the rs1799931 G857A (G286E) polymorphism on N-acetyltransferase 2-mediated carcinogen metabolism and genotoxicity differs with heterocyclic amine exposure,” *Arch. Toxicol.*, vol. 97, no. 10, pp. 2697–2705, Oct. 2023, doi: 10.1007/s00204-023-03577-2.
- [112] R. J. Turesky, “Formation and biochemistry of carcinogenic heterocyclic aromatic amines in cooked meats,” *Toxicol. Lett.*, vol. 168, no. 3, pp. 219–227, Feb. 2007, doi: 10.1016/j.toxlet.2006.10.018.
- [113] D. W. Hein, “Molecular genetics and function of NAT1 and NAT2: role in aromatic amine metabolism and carcinogenesis,” *Mutat. Res.*, vol. 506–507, pp. 65–77, Sep. 2002, doi: 10.1016/s0027-5107(02)00153-7.
- [114] K. U. Hong, R. A. Salazar-González, K. M. Walls, and D. W. Hein, “Transcriptional Regulation of Human Arylamine N-Acetyltransferase 2 Gene by Glucose and Insulin in Liver Cancer Cell Lines,” *Toxicol. Sci. Off. J. Soc. Toxicol.*, vol. 190, no. 2, pp. 158–172, Nov. 2022, doi: 10.1093/toxsci/kfac103.
- [115] S. Langouët *et al.*, “Metabolism of 2-amino-3,8-dimethylimidazo[4,5-f]quinoxaline in human hepatocytes: 2-amino-3-methylimidazo[4,5-f]quinoxaline-8-carboxylic acid is a major detoxification pathway catalyzed by cytochrome P450 1A2,” *Chem. Res. Toxicol.*, vol. 14, no. 2, pp. 211–221, Feb. 2001, doi: 10.1021/tx000176e.

- [116] D. Gu *et al.*, "A comprehensive approach to the profiling of the cooked meat carcinogens 2-amino-3,8-dimethylimidazo[4,5-f]quinoxaline, 2-amino-1-methyl-6-phenylimidazo[4,5-b]pyridine, and their metabolites in human urine," *Chem. Res. Toxicol.*, vol. 23, no. 4, pp. 788–801, Apr. 2010, doi: 10.1021/tx900436m.
- [117] S. Kimura *et al.*, "Carcinogenesis of the food mutagen PhIP in mice is independent of CYP1A2," *Carcinogenesis*, vol. 24, no. 3, pp. 583–587, Mar. 2003, doi: 10.1093/carcin/24.3.583.
- [118] K. J. Metry, J. R. Neale, J. Bendaly, N. B. Smith, W. M. Pierce, and D. W. Hein, "Effect of N-acetyltransferase 2 polymorphism on tumor target tissue DNA adduct levels in rapid and slow acetylator congenic rats administered 2-amino-1-methyl-6-phenylimidazo[4,5-b]pyridine or 2-amino-3,8-dimethylimidazo-[4,5-f]quinoxaline," *Drug Metab. Dispos. Biol. Fate Chem.*, vol. 37, no. 11, pp. 2123–2126, Nov. 2009, doi: 10.1124/dmd.109.029512.
- [119] A. E. Brown and M. Walker, "Genetics of Insulin Resistance and the Metabolic Syndrome," *Curr. Cardiol. Rep.*, vol. 18, no. 8, p. 75, Aug. 2016, doi: 10.1007/s11886-016-0755-4.
- [120] J. Ruzzin *et al.*, "Persistent Organic Pollutant Exposure Leads to Insulin Resistance Syndrome," *Environ. Health Perspect.*, vol. 118, no. 4, pp. 465–471, Apr. 2010, doi: 10.1289/ehp.0901321.
- [121] R. M. Sargis *et al.*, "The novel endocrine disruptor tolylfluanid impairs insulin signaling in primary rodent and human adipocytes through a reduction in insulin receptor substrate-1 levels," *Biochim. Biophys. Acta*

BBA - Mol. Basis Dis., vol. 1822, no. 6, pp. 952–960, Jun. 2012, doi:
10.1016/j.bbadis.2012.02.015.

- [122] K. M. Walls, K. U. Hong, and D. W. Hein, “Heterocyclic amines reduce insulin-induced AKT phosphorylation and induce gluconeogenic gene expression in human hepatocytes,” *Arch. Toxicol.*, Apr. 2023, doi: 10.1007/s00204-023-03488-2.
- [123] J. Bendaly *et al.*, “2-Amino-3,8-dimethylimidazo-[4,5-f]quinoxaline-induced DNA adduct formation and mutagenesis in DNA repair-deficient Chinese hamster ovary cells expressing human cytochrome P4501A1 and rapid or slow acetylator N-acetyltransferase 2,” *Cancer Epidemiol. Biomark. Prev. Publ. Am. Assoc. Cancer Res. Cosponsored Am. Soc. Prev. Oncol.*, vol. 16, no. 7, pp. 1503–1509, Jul. 2007, doi: 10.1158/1055-9965.EPI-07-0305.
- [124] K. J. Metry *et al.*, “2-amino-1-methyl-6-phenylimidazo [4,5-b] pyridine-induced DNA adducts and genotoxicity in chinese hamster ovary (CHO) cells expressing human CYP1A2 and rapid or slow acetylator N-acetyltransferase 2,” *Mol. Carcinog.*, vol. 46, no. 7, pp. 553–563, Jul. 2007, doi: 10.1002/mc.20302.
- [125] R. J. Turesky and L. Le Marchand, “Metabolism and biomarkers of heterocyclic aromatic amines in molecular epidemiology studies: lessons learned from aromatic amines,” *Chem. Res. Toxicol.*, vol. 24, no. 8, pp. 1169–1214, Aug. 2011, doi: 10.1021/tx200135s.
- [126] M. A. Doll and D. W. Hein, “Comprehensive human NAT2 genotype method using single nucleotide polymorphism-specific polymerase chain

- reaction primers and fluorogenic probes,” *Anal. Biochem.*, vol. 288, no. 1, pp. 106–108, Jan. 2001, doi: 10.1006/abio.2000.4892.
- [127] K. M. Walls, K. U. Hong, and D. W. Hein, “Heterocyclic amines reduce insulin-induced AKT phosphorylation and induce gluconeogenic gene expression in human hepatocytes,” *Arch. Toxicol.*, vol. 97, no. 6, pp. 1613–1626, Jun. 2023, doi: 10.1007/s00204-023-03488-2.
- [128] K. M. Walls, K. U. Hong, and D. W. Hein, “Induction of glucose production by heterocyclic amines is dependent on N-acetyltransferase 2 genetic polymorphism in cryopreserved human hepatocytes,” *Toxicol. Lett.*, vol. 383, pp. 192–195, Jul. 2023, doi: 10.1016/j.toxlet.2023.07.002.
- [129] S. Knasmüller *et al.*, “Genotoxic effects of heterocyclic aromatic amines in human derived hepatoma (HepG2) cells,” *Mutagenesis*, vol. 14, no. 6, pp. 533–540, Nov. 1999, doi: 10.1093/mutage/14.6.533.
- [130] O. Viegas *et al.*, “Protective effects of xanthohumol against the genotoxicity of heterocyclic aromatic amines MeIQx and PhIP in bacteria and in human hepatoma (HepG2) cells,” *Food Chem. Toxicol.*, vol. 50, no. 3, pp. 949–955, Mar. 2012, doi: 10.1016/j.fct.2011.11.031.
- [131] M. Pezdirc, B. Žegura, and M. Filipič, “Genotoxicity and induction of DNA damage responsive genes by food-borne heterocyclic aromatic amines in human hepatoma HepG2 cells,” *Food Chem. Toxicol.*, vol. 59, pp. 386–394, Sep. 2013, doi: 10.1016/j.fct.2013.06.030.
- [132] K. G. M. M. Alberti *et al.*, “Harmonizing the metabolic syndrome: a joint interim statement of the International Diabetes Federation Task Force on

Epidemiology and Prevention; National Heart, Lung, and Blood Institute; American Heart Association; World Heart Federation; International Atherosclerosis Society; and International Association for the Study of Obesity,” *Circulation*, vol. 120, no. 16, pp. 1640–1645, Oct. 2009, doi: 10.1161/CIRCULATIONAHA.109.192644.

- [133] P. Kudaravalli and S. John, “Nonalcoholic Fatty Liver,” in *StatPearls*, Treasure Island (FL): StatPearls Publishing, 2023. Accessed: Oct. 02, 2023. [Online]. Available: <http://www.ncbi.nlm.nih.gov/books/NBK541033/>
- [134] Y. Xian *et al.*, “Modified QuEChERS purification and Fe₃O₄ nanoparticle decoloration for robust analysis of 14 heterocyclic aromatic amines and acrylamide in coffee products using UHPLC-MS/MS,” *Food Chem.*, vol. 285, pp. 77–85, Jul. 2019, doi: 10.1016/j.foodchem.2019.01.132.
- [135] G. Liu, G. Zong, F. B. Hu, W. C. Willett, D. M. Eisenberg, and Q. Sun, “Cooking Methods for Red Meats and Risk of Type 2 Diabetes: A Prospective Study of U.S. Women,” *Diabetes Care*, vol. 40, no. 8, pp. 1041–1049, Aug. 2017, doi: 10.2337/dc17-0204.
- [136] L. Chang and M. Karin, “Mammalian MAP kinase signalling cascades,” *Nature*, vol. 410, no. 6824, pp. 37–40, Mar. 2001, doi: 10.1038/35065000.
- [137] M. Pal, M. A. Febbraio, and G. I. Lancaster, “The roles of c-Jun NH₂-terminal kinases (JNKs) in obesity and insulin resistance,” *J. Physiol.*, vol. 594, no. 2, pp. 267–279, Jan. 2016, doi: 10.1113/JP271457.
- [138] G. Solinas and M. Karin, “JNK1 and IKKbeta: molecular links between obesity and metabolic dysfunction,” *FASEB J. Off. Publ. Fed. Am. Soc.*

Exp. Biol., vol. 24, no. 8, pp. 2596–2611, Aug. 2010, doi: 10.1096/fj.09-151340.

- [139] V. Aguirre, E. D. Werner, J. Giraud, Y. H. Lee, S. E. Shoelson, and M. F. White, “Phosphorylation of Ser307 in Insulin Receptor Substrate-1 Blocks Interactions with the Insulin Receptor and Inhibits Insulin Action,” *J. Biol. Chem.*, vol. 277, no. 2, pp. 1531–1537, Jan. 2002, doi: 10.1074/jbc.M101521200.
- [140] V. Aguirre, T. Uchida, L. Yenush, R. Davis, and M. F. White, “The c-Jun NH2-terminal Kinase Promotes Insulin Resistance during Association with Insulin Receptor Substrate-1 and Phosphorylation of Ser307,” *J. Biol. Chem.*, vol. 275, no. 12, pp. 9047–9054, Mar. 2000, doi: 10.1074/jbc.275.12.9047.
- [141] S. A. Litwak *et al.*, “JNK Activation of BIM Promotes Hepatic Oxidative Stress, Steatosis, and Insulin Resistance in Obesity,” *Diabetes*, vol. 66, no. 12, pp. 2973–2986, Dec. 2017, doi: 10.2337/db17-0348.
- [142] V. Adomshick, Y. Pu, and A. Veiga-Lopez, “Automated Lipid Droplet Quantification System for Phenotypic Analysis of Adipocytes using CellProfiler,” *Toxicol. Mech. Methods*, vol. 30, no. 5, pp. 378–387, Jun. 2020, doi: 10.1080/15376516.2020.1747124.
- [143] R. J. Davis, “Signal transduction by the JNK group of MAP kinases,” *Cell*, vol. 103, no. 2, pp. 239–252, Oct. 2000, doi: 10.1016/s0092-8674(00)00116-1.

- [144] C. Tournier, A. J. Whitmarsh, J. Cavanagh, T. Barrett, and R. J. Davis, "The MKK7 gene encodes a group of c-Jun NH2-terminal kinase kinases," *Mol. Cell. Biol.*, vol. 19, no. 2, pp. 1569–1581, Feb. 1999, doi: 10.1128/MCB.19.2.1569.
- [145] S. Win, T. A. Than, J. Zhang, C. Oo, R. W. M. Min, and N. Kaplowitz, "New insights into the role and mechanism of c-Jun-N-terminal kinase signaling in the pathobiology of liver diseases," *Hepatol. Baltim. Md*, vol. 67, no. 5, p. 2013, May 2018, doi: 10.1002/hep.29689.
- [146] M. Mittal, M. R. Siddiqui, K. Tran, S. P. Reddy, and A. B. Malik, "Reactive Oxygen Species in Inflammation and Tissue Injury," *Antioxid. Redox Signal.*, vol. 20, no. 7, pp. 1126–1167, Mar. 2014, doi: 10.1089/ars.2012.5149.
- [147] G. Tiegs and A. K. Horst, "TNF in the liver: targeting a central player in inflammation," *Semin. Immunopathol.*, vol. 44, no. 4, p. 445, 2022, doi: 10.1007/s00281-022-00910-2.
- [148] H. Malhi, S. F. Bronk, N. W. Werneburg, and G. J. Gores, "Free fatty acids induce JNK-dependent hepatocyte lipoapoptosis," *J. Biol. Chem.*, vol. 281, no. 17, pp. 12093–12101, Apr. 2006, doi: 10.1074/jbc.M510660200.
- [149] P. Puri *et al.*, "Activation and dysregulation of the unfolded protein response in nonalcoholic fatty liver disease," *Gastroenterology*, vol. 134, no. 2, pp. 568–576, Feb. 2008, doi: 10.1053/j.gastro.2007.10.039.

- [150] J. Han and R. J. Kaufman, "The role of ER stress in lipid metabolism and lipotoxicity," *J. Lipid Res.*, vol. 57, no. 8, pp. 1329–1338, Aug. 2016, doi: 10.1194/jlr.R067595.
- [151] G. S. Hotamisligil, "Role of endoplasmic reticulum stress and c-Jun NH2-terminal kinase pathways in inflammation and origin of obesity and diabetes," *Diabetes*, vol. 54 Suppl 2, pp. S73-78, Dec. 2005, doi: 10.2337/diabetes.54.suppl_2.s73.
- [152] T. A. Riaz, R. P. Junjappa, M. Handigund, J. Ferdous, H.-R. Kim, and H.-J. Chae, "Role of Endoplasmic Reticulum Stress Sensor IRE1 α in Cellular Physiology, Calcium, ROS Signaling, and Metaflammation," *Cells*, vol. 9, no. 5, May 2020, doi: 10.3390/cells9051160.
- [153] L. D. Ly *et al.*, "Oxidative stress and calcium dysregulation by palmitate in type 2 diabetes," *Exp. Mol. Med.*, vol. 49, no. 2, p. e291, Feb. 2017, doi: 10.1038/emm.2016.157.
- [154] F. Urano *et al.*, "Coupling of stress in the ER to activation of JNK protein kinases by transmembrane protein kinase IRE1," *Science*, vol. 287, no. 5453, pp. 664–666, Jan. 2000, doi: 10.1126/science.287.5453.664.
- [155] S. Milić and D. Stimac, "Nonalcoholic fatty liver disease/steatohepatitis: epidemiology, pathogenesis, clinical presentation and treatment," *Dig. Dis. Basel Switz.*, vol. 30, no. 2, pp. 158–162, 2012, doi: 10.1159/000336669.
- [156] S. M. Grundy, "Metabolic syndrome pandemic," *Arterioscler. Thromb. Vasc. Biol.*, vol. 28, no. 4, pp. 629–636, Apr. 2008, doi: 10.1161/ATVBAHA.107.151092.

- [157] P. Dobrowolski *et al.*, “Metabolic syndrome – a new definition and management guidelines,” *Arch. Med. Sci. AMS*, vol. 18, no. 5, pp. 1133–1156, Aug. 2022, doi: 10.5114/aoms/152921.
- [158] E. Scorletti and R. M. Carr, “A new perspective on NAFLD: Focusing on lipid droplets,” *J. Hepatol.*, vol. 76, no. 4, pp. 934–945, Apr. 2022, doi: 10.1016/j.jhep.2021.11.009.
- [159] D. G. Mashek, “Hepatic lipid droplets: A balancing act between energy storage and metabolic dysfunction in NAFLD,” *Mol. Metab.*, vol. 50, p. 101115, Aug. 2021, doi: 10.1016/j.molmet.2020.101115.
- [160] P. K. Luukkonen *et al.*, “Human PNPLA3-I148M variant increases hepatic retention of polyunsaturated fatty acids,” *JCI Insight*, vol. 4, no. 16, pp. e127902, 127902, Aug. 2019, doi: 10.1172/jci.insight.127902.
- [161] F. V. Bruschi, M. Tardelli, M. Herac, T. Claudel, and M. Trauner, “Metabolic regulation of hepatic PNPLA3 expression and severity of liver fibrosis in patients with NASH,” *Liver Int.*, vol. 40, no. 5, pp. 1098–1110, May 2020, doi: 10.1111/liv.14402.
- [162] W. Su *et al.*, “Comparative proteomic study reveals 17 β -HSD13 as a pathogenic protein in nonalcoholic fatty liver disease,” *Proc. Natl. Acad. Sci. U. S. A.*, vol. 111, no. 31, pp. 11437–11442, Aug. 2014, doi: 10.1073/pnas.1410741111.
- [163] H. Zhang, W. Su, H. Xu, X. Zhang, and Y. Guan, “HSD17B13: A Potential Therapeutic Target for NAFLD,” *Front. Mol. Biosci.*, vol. 8, p. 824776, Jan. 2022, doi: 10.3389/fmolb.2021.824776.

- [164] D. L. Brasaemle, T. Barber, N. E. Wolins, G. Serrero, E. J. Blanchette-Mackie, and C. Londos, "Adipose differentiation-related protein is an ubiquitously expressed lipid storage droplet-associated protein," *J. Lipid Res.*, vol. 38, no. 11, pp. 2249–2263, Nov. 1997.
- [165] M. Imamura *et al.*, "ADRP stimulates lipid accumulation and lipid droplet formation in murine fibroblasts," *Am. J. Physiol. Endocrinol. Metab.*, vol. 283, no. 4, pp. E775-783, Oct. 2002, doi: 10.1152/ajpendo.00040.2002.
- [166] J. Luo, H. Yang, and B.-L. Song, "Mechanisms and regulation of cholesterol homeostasis," *Nat. Rev. Mol. Cell Biol.*, vol. 21, no. 4, Art. no. 4, Apr. 2020, doi: 10.1038/s41580-019-0190-7.
- [167] N. L. Gluchowski, M. Becuwe, T. C. Walther, and R. V. Farese, "Lipid droplets and liver disease: from basic biology to clinical implications," *Nat. Rev. Gastroenterol. Hepatol.*, vol. 14, no. 6, pp. 343–355, Jun. 2017, doi: 10.1038/nrgastro.2017.32.
- [168] N. Shunmoogam, P. Naidoo, and R. Chilton, "Paraoxonase (PON)-1: a brief overview on genetics, structure, polymorphisms and clinical relevance," *Vasc. Health Risk Manag.*, vol. 14, pp. 137–143, 2018, doi: 10.2147/VHRM.S165173.
- [169] A. Mahrooz, M. Mackness, A. Bagheri, M. Ghaffari-Cherati, and P. Masoumi, "The epigenetic regulation of paraoxonase 1 (PON1) as an important enzyme in HDL function: The missing link between environmental and genetic regulation," *Clin. Biochem.*, vol. 73, pp. 1–10, Nov. 2019, doi: 10.1016/j.clinbiochem.2019.07.010.

- [170] Y. Ikeda, M. Inoue, T. Suehiro, K. Arai, Y. Kumon, and K. Hashimoto, "Low human paraoxonase predicts cardiovascular events in Japanese patients with type 2 diabetes," *Acta Diabetol.*, vol. 46, no. 3, pp. 239–242, Sep. 2009, doi: 10.1007/s00592-008-0066-3.
- [171] Y. Kawano and D. E. Cohen, "Mechanisms of hepatic triglyceride accumulation in non-alcoholic fatty liver disease," *J. Gastroenterol.*, vol. 48, no. 4, pp. 434–441, Apr. 2013, doi: 10.1007/s00535-013-0758-5.
- [172] C.-L. E. Yen, S. J. Stone, S. Koliwad, C. Harris, and R. V. Farese, "DGAT enzymes and triacylglycerol biosynthesis," *J. Lipid Res.*, vol. 49, no. 11, pp. 2283–2301, Nov. 2008, doi: 10.1194/jlr.R800018-JLR200.
- [173] P. Rada, Á. González-Rodríguez, C. García-Monzón, and Á. M. Valverde, "Understanding lipotoxicity in NAFLD pathogenesis: is CD36 a key driver?," *Cell Death Dis.*, vol. 11, no. 9, Art. no. 9, Sep. 2020, doi: 10.1038/s41419-020-03003-w.
- [174] C. García-Monzón *et al.*, "Hepatic insulin resistance is associated with increased apoptosis and fibrogenesis in nonalcoholic steatohepatitis and chronic hepatitis C," *J. Hepatol.*, vol. 54, no. 1, pp. 142–152, Jan. 2011, doi: 10.1016/j.jhep.2010.06.021.
- [175] A. E. Feldstein *et al.*, "Hepatocyte apoptosis and fas expression are prominent features of human nonalcoholic steatohepatitis," *Gastroenterology*, vol. 125, no. 2, pp. 437–443, Aug. 2003, doi: 10.1016/s0016-5085(03)00907-7.

- [176] A. Arvind, S. A. Osganian, D. E. Cohen, and K. E. Corey, "Lipid and Lipoprotein Metabolism in Liver Disease," in *Endotext*, K. R. Feingold, B. Anawalt, M. R. Blackman, A. Boyce, G. Chrousos, E. Corpas, W. W. de Herder, K. Dhatariya, K. Dungan, J. Hofland, S. Kalra, G. Kaltsas, N. Kapoor, C. Koch, P. Kopp, M. Korbonits, C. S. Kovacs, W. Kuohung, B. Laferrère, M. Levy, E. A. McGee, R. McLachlan, M. New, J. Purnell, R. Sahay, A. S. Shah, F. Singer, M. A. Sperling, C. A. Stratakis, D. L. Trencé, and D. P. Wilson, Eds., South Dartmouth (MA): MDText.com, Inc., 2000. Accessed: Sep. 27, 2023. [Online]. Available: <http://www.ncbi.nlm.nih.gov/books/NBK326742/>
- [177] Y. Feng *et al.*, "Biological Mechanisms and Related Natural Inhibitors of CD36 in Nonalcoholic Fatty Liver," *Drug Des. Devel. Ther.*, vol. 16, pp. 3829–3845, Nov. 2022, doi: 10.2147/DDDT.S386982.
- [178] C. Dorn *et al.*, "Expression of fatty acid synthase in nonalcoholic fatty liver disease," *Int. J. Clin. Exp. Pathol.*, vol. 3, no. 5, pp. 505–514, Mar. 2010.
- [179] J. D. McGarry, K. F. Woeltje, M. Kuwajima, and D. W. Foster, "Regulation of ketogenesis and the renaissance of carnitine palmitoyltransferase," *Diabetes. Metab. Rev.*, vol. 5, no. 3, pp. 271–284, May 1989, doi: 10.1002/dmr.5610050305.
- [180] A. Deprince, J. T. Haas, and B. Staels, "Dysregulated lipid metabolism links NAFLD to cardiovascular disease," *Mol. Metab.*, vol. 42, p. 101092, Dec. 2020, doi: 10.1016/j.molmet.2020.101092.

- [181] L. Hodson and B. A. Fielding, "Stearoyl-CoA desaturase: rogue or innocent bystander?," *Prog. Lipid Res.*, vol. 52, no. 1, pp. 15–42, Jan. 2013, doi: 10.1016/j.plipres.2012.08.002.
- [182] A. M. ALJohani, D. N. Syed, and J. M. Ntambi, "Insights into Stearoyl-CoA Desaturase-1 Regulation of Systemic Metabolism," *Trends Endocrinol. Metab. TEM*, vol. 28, no. 12, pp. 831–842, Dec. 2017, doi: 10.1016/j.tem.2017.10.003.
- [183] A. Kotronen *et al.*, "Hepatic stearoyl-CoA desaturase (SCD)-1 activity and diacylglycerol but not ceramide concentrations are increased in the nonalcoholic human fatty liver," *Diabetes*, vol. 58, no. 1, pp. 203–208, Jan. 2009, doi: 10.2337/db08-1074.
- [184] J. M. Ntambi *et al.*, "Loss of stearoyl-CoA desaturase-1 function protects mice against adiposity," *Proc. Natl. Acad. Sci. U. S. A.*, vol. 99, no. 17, pp. 11482–11486, Aug. 2002, doi: 10.1073/pnas.132384699.
- [185] C. E. Geisler and B. J. Renquist, "Hepatic lipid accumulation: cause and consequence of dysregulated glucoregulatory hormones," *J. Endocrinol.*, vol. 234, no. 1, pp. R1–R21, Jul. 2017, doi: 10.1530/JOE-16-0513.
- [186] Y. Geng, K. N. Faber, V. E. de Meijer, H. Blokzijl, and H. Moshage, "How does hepatic lipid accumulation lead to lipotoxicity in non-alcoholic fatty liver disease?," *Hepatol. Int.*, vol. 15, no. 1, pp. 21–35, Feb. 2021, doi: 10.1007/s12072-020-10121-2.
- [187] J. K. Reddy and M. S. Rao, "Lipid metabolism and liver inflammation. II. Fatty liver disease and fatty acid oxidation," *Am. J. Physiol. Gastrointest.*

Liver Physiol., vol. 290, no. 5, pp. G852-858, May 2006, doi:
10.1152/ajpgi.00521.2005.

- [188] D. W. Hein *et al.*, "Rodent models of the human acetylation polymorphism: Comparisons of recombinant acetyltransferases," *Mutat. Res. Mol. Mech. Mutagen.*, vol. 376, no. 1–2, pp. 101–106, May 1997, doi: 10.1016/S0027-5107(97)00031-6.
- [189] J. A. Loehle *et al.*, "N-acetyltransferase (Nat) 1 and 2 expression in Nat2 knockout mice," *J. Pharmacol. Exp. Ther.*, vol. 319, no. 2, pp. 724–728, Nov. 2006, doi: 10.1124/jpet.106.108662.
- [190] N. Laurieri *et al.*, "Differences between murine arylamine N-acetyltransferase type 1 and human arylamine N-acetyltransferase type 2 defined by substrate specificity and inhibitor binding," *BMC Pharmacol. Toxicol.*, vol. 15, p. 68, Nov. 2014, doi: 10.1186/2050-6511-15-68.

APPENDIX

TABLE OF CONTENTS

Figure A1. Increases in insulin receptor-target genes involved in gluconeogenesis following HCA and 3-MC treatment.....	177
Figure A2. Changes in gene expression and reactive oxygen species after HCA mixture treatment in cryopreserved human hepatocytes.....	178
Figure A3. Changes in expression of genes involved in gluconeogenesis and lipid droplet formation in cryopreserved human hepatocytes following HCA treatment in combination with high glucose.....	179
Figure A4. Changes in levels of proteins in the insulin signaling cascade following MeIQx treatment in HepG2 cells.....	180
Figure A5. Gene ontology (GO) biological processes significantly enriched among genes upregulated or downregulated by MeIQx and PhIP treatment in cryopreserved human hepatocytes.....	181
Figure A6. Gene Ontology (GO) biological processes, molecular functions, and cellular components significantly enriched among genes upregulated in MeIQx-treated cryopreserved human hepatocytes.....	182

Figure A7. Gene Ontology (GO) biological processes, molecular functions, and cellular components significantly enriched among genes upregulated in PhIP-treated cryopreserved human hepatocytes.....183

Figure A8. Gene Ontology (GO) biological processes, molecular functions, and cellular components significantly enriched among genes downregulated in MeIQx-treated cryopreserved human hepatocytes.....184

Figure A9. Gene Ontology (GO) biological processes, molecular functions, and cellular components significantly enriched among genes downregulated in PhIP-treated cryopreserved human hepatocytes.....185

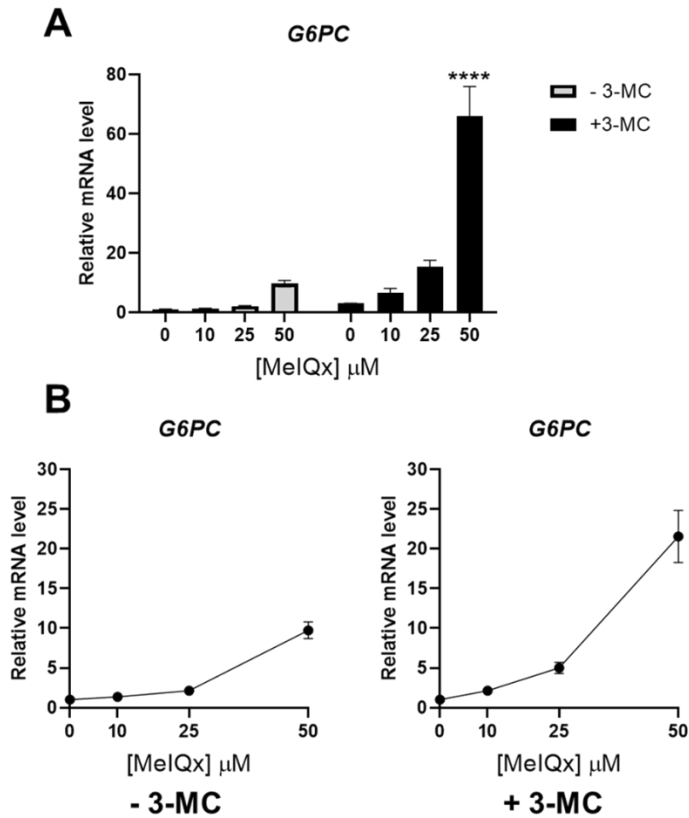


Figure A1. Increases in insulin receptor-target genes involved in gluconeogenesis following HCA and 3-MC treatment. HepG2 cells were cultured with varying concentrations of MelQx and 1 μM 3-MC for 3 days. The relative mRNA level of *G6PC* was measured by RT-qPCR using 18S ribosomal RNA as an internal control. The mRNA levels were expressed as changes relative to that in the vehicle-control. Bars or data points represent mean ± SEM. ****, $p < 0.0001$.

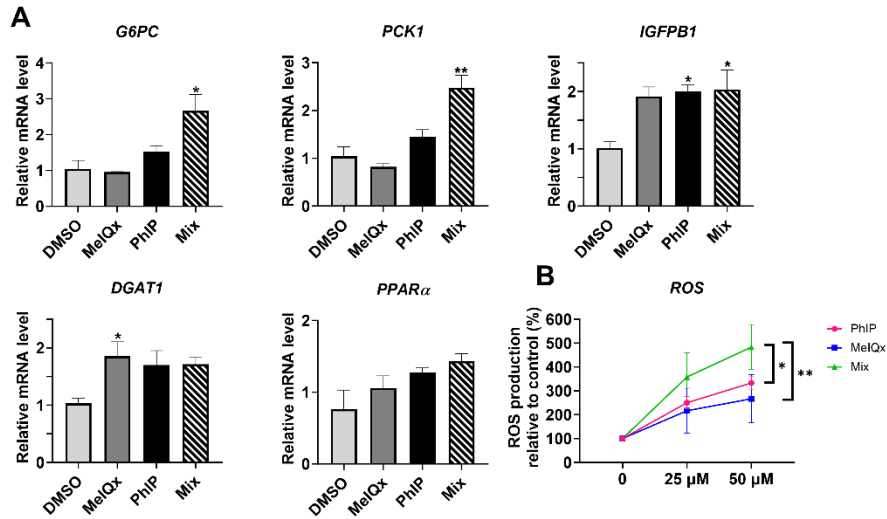


Figure A2. Changes in gene expression and reactive oxygen species after HCA mixture treatment in cryopreserved human hepatocytes. Panel A, Cryopreserved human hepatocytes were treated with 50 μ M total concentration of the indicated HCA (MelQx, PhIP, or mixture of MelQx and PhIP) for 24 hours. The mRNA levels were measured via qRT-PCR, and are expressed relative to the vehicle-control. Statistical significance was determined by one-way ANOVA followed by Dunnett's Multiple Comparisons Test. Bars represent mean \pm SEM. Panel B, Cryopreserved human hepatocytes were pre-treated with 20 μ M CM-H2DCFDA for 45 minutes, then treated with the indicated concentration of MelQx, PhIP, or a combination of both MelQx and PhIP for 24 hours. Fluorescence intensity was measured at Ex/Em = 485/528 nm using a microplate reader. The relative ROS generation is expressed as a percentage relative to the control. Statistical significance was determined by two-way ANOVA followed by Tukey's Multiple Comparisons Test. Data points represent mean \pm SEM. *, $p < 0.05$; **, $p < 0.01$.

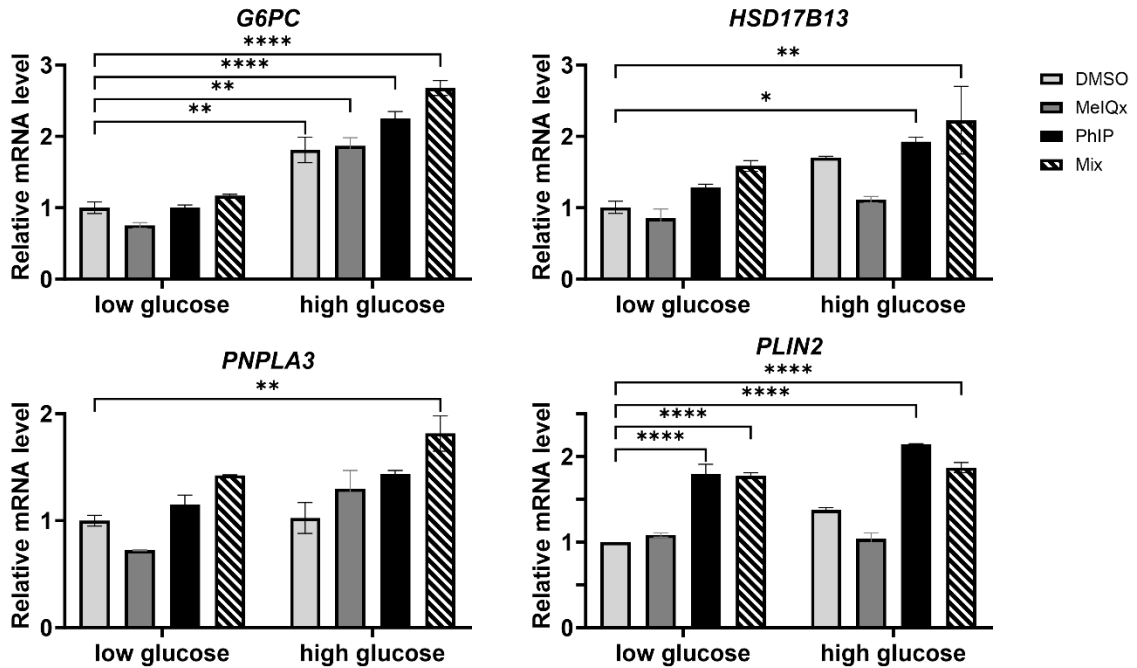


Figure A3. Changes in expression of genes involved in gluconeogenesis and lipid droplet formation in cryopreserved human hepatocytes following HCA treatment in combination with high glucose. Hepatocytes were treated with a 50 μ M total concentration of the indicated HCA (MeIQx, PhIP, or mixture of MeIQx and PhIP) for 24 hours in media containing low (5.5 mM) or high (25 mM) glucose. The mRNA levels were measured using qRT-PCR and are expressed relative to the vehicle-control. Statistical significance was determined by two-way ANOVA followed by Dunnett's Multiple Comparisons Test. Bars represent mean \pm SEM. *, $p < 0.05$; **, $p < 0.01$; ****, $p < 0.0001$.

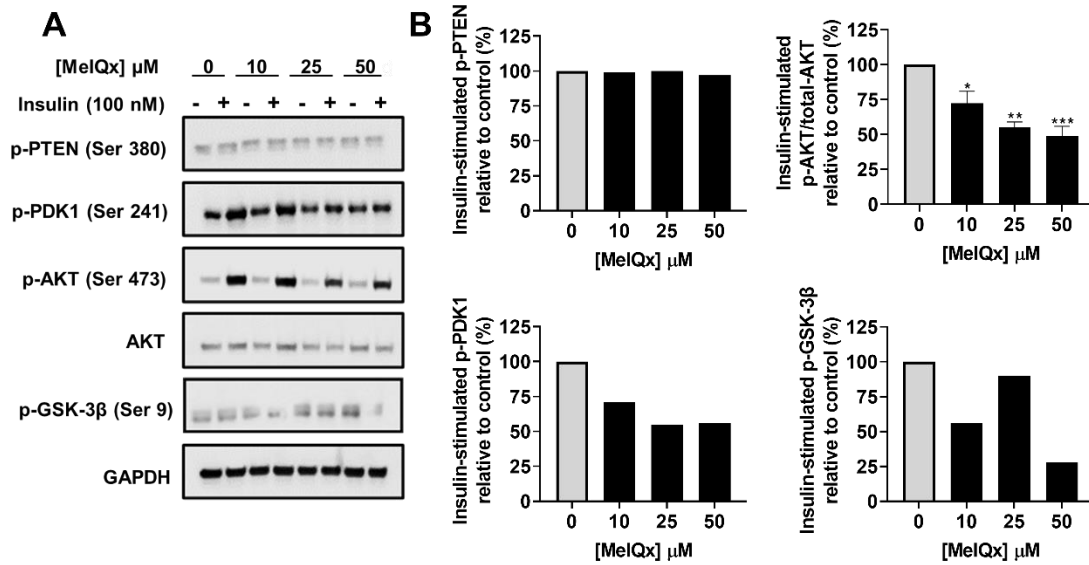


Figure A4. Changes in levels of proteins in the insulin signaling cascade following MelQx treatment in HepG2 cells. HepG2 cells were treated with the indicated concentration of MelQx for 2 days, followed by a serum-starvation overnight. Prior to harvest, cells were treated with 100 nM insulin for 10 minutes. The relative levels of the indicated proteins were measured using Western blot. The insulin-stimulated p-AKT/AKT ratio was expressed as a percentage of the vehicle-treated control cells (bars represent mean \pm SEM), and the remaining proteins were expressed as insulin stimulated protein/GAPDH ratio. Bars represent mean.

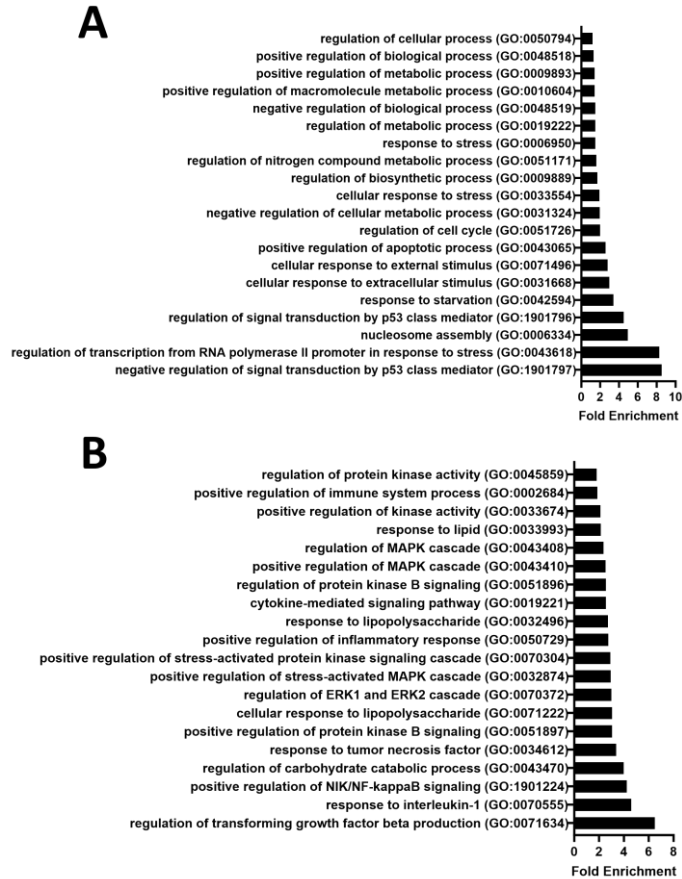


Figure A5. Gene ontology (GO) biological processes significantly enriched among genes upregulated or downregulated by MelQx and PhIP treatment in cryopreserved human hepatocytes. Panel A shows fold enrichment for selected GO biological processes (GO terms and their IDs) that are significantly enriched among the *upregulated* genes by both MelQx and PhIP. Panel B shows fold enrichment for selected GO biological processes (GO terms and their IDs) that are significantly enriched among the *downregulated* genes by both MelQx and PhIP.

MelQx

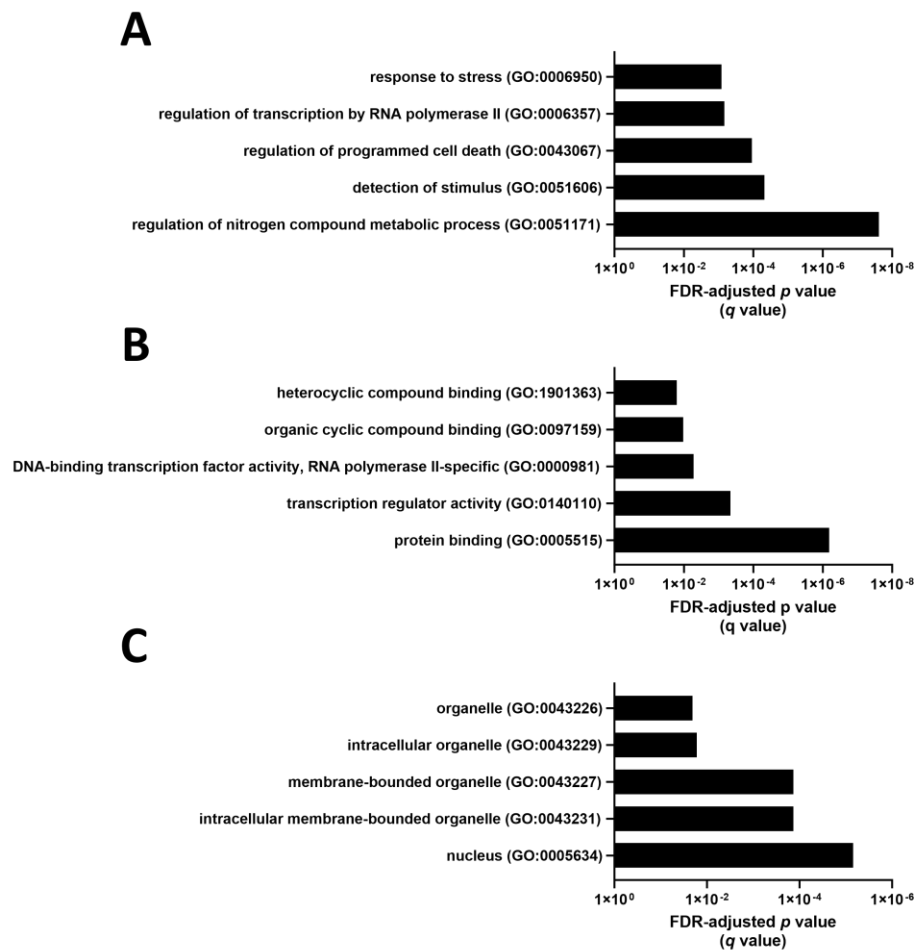


Figure A6. Gene Ontology (GO) biological processes, molecular functions, and cellular components significantly enriched among

genes upregulated in MelQx-treated cryopreserved human hepatocytes.

Panels A, B, and C show false discovery rate (FDR)-adjusted p values (i.e., q values) for selected GO biological processes, molecular function, and cellular component terms enriched among the *upregulated* genes, respectively.

PhIP

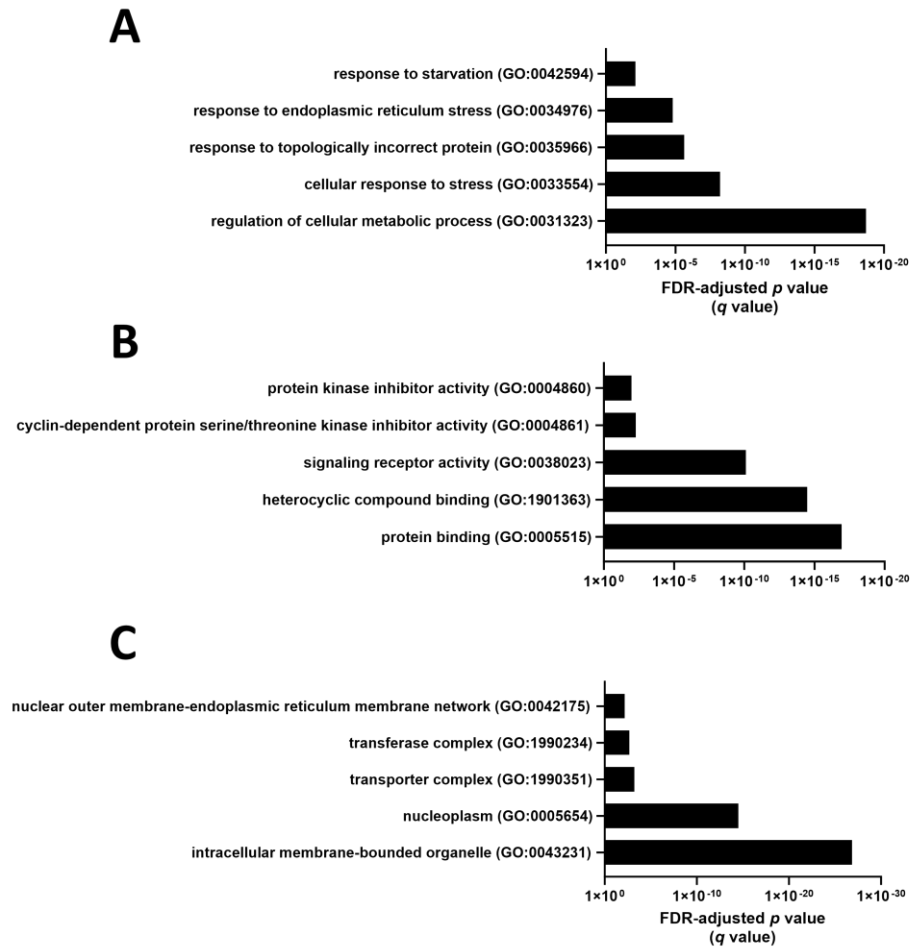


Figure A7. Gene Ontology (GO) biological processes, molecular functions, and cellular components significantly enriched among genes *upregulated* in *PhIP*-treated cryopreserved human hepatocytes.

Panels A, B, and C show false discovery rate (FDR)-adjusted p values (i.e., q values) for selected GO biological processes, molecular function, and cellular component terms enriched among the *upregulated* genes, respectively.

MeIQx

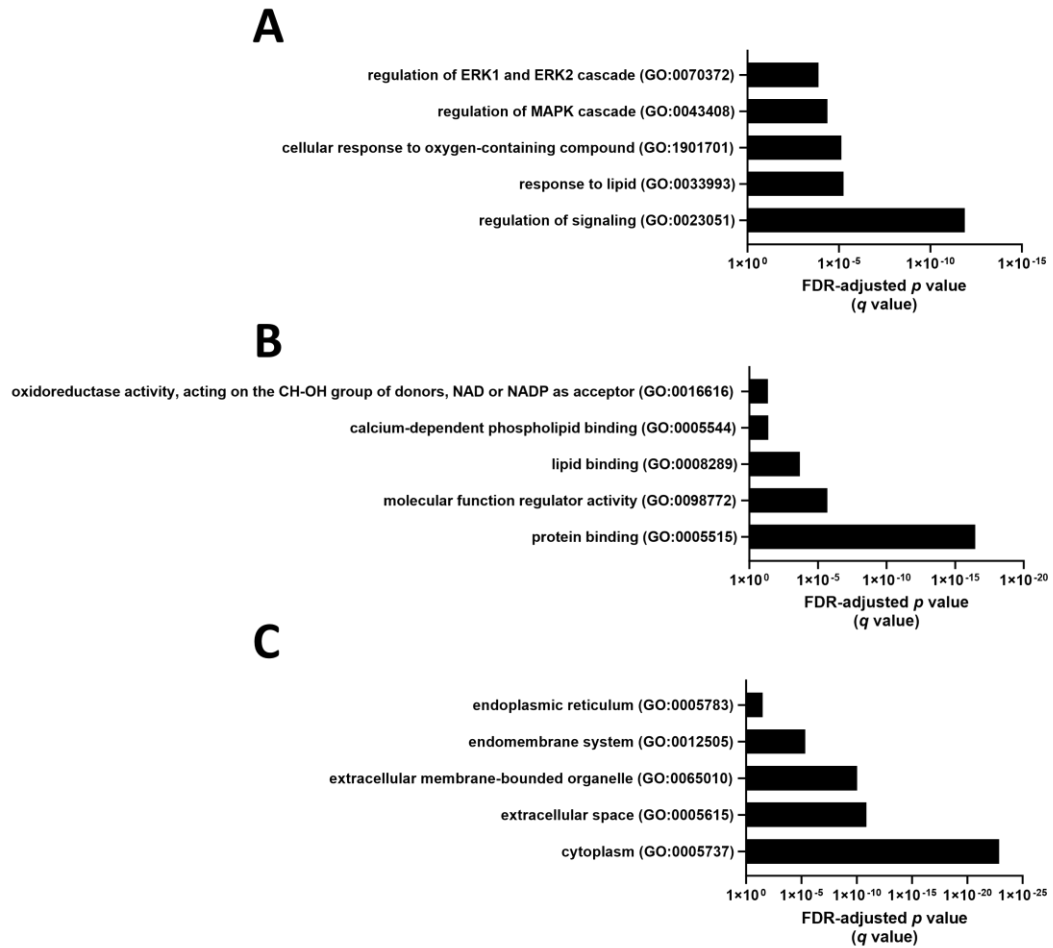


Figure A8. Gene Ontology (GO) biological processes, molecular functions, and cellular components significantly enriched among

genes *downregulated* in *MeIQx-treated* cryopreserved human hepatocytes.

Panels A, B, and C show false discovery rate (FDR)-adjusted p values (i.e., q values) for selected GO biological processes, molecular function, and cellular component terms enriched among the *downregulated* genes, respectively.

PhIP

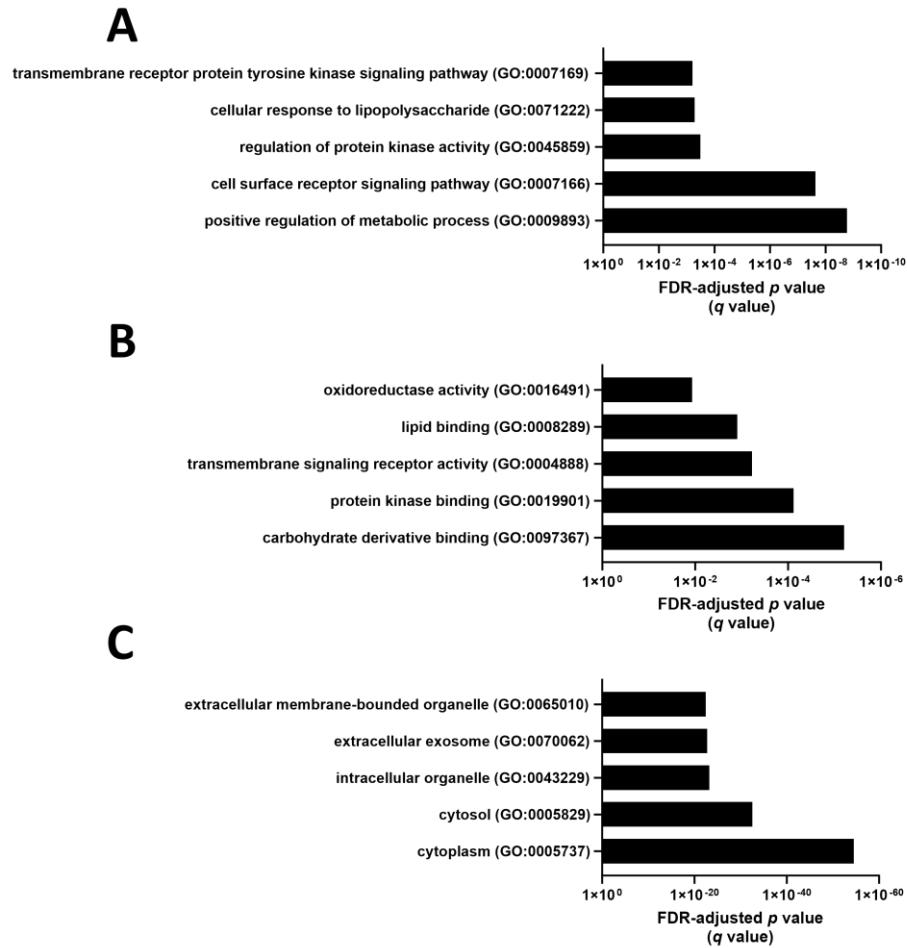


Figure A9. Gene Ontology (GO) biological processes, molecular functions, and cellular components significantly enriched among genes *downregulated* in *PhIP-treated* cryopreserved human hepatocytes. Panels A, B, and C show false discovery rate (FDR)-adjusted p values (i.e., q values) for selected GO biological processes, molecular function, and cellular component terms enriched among the *downregulated* genes, respectively.

CURRICULUM VITAE

Kennedy M. Walls

University of Louisville School of Medicine

Department of Pharmacology & Toxicology

505 South Hancock Street (CTRB 352)

Louisville, KY 40202

Email: kmwall06@louisville.edu

Phone: (859)319-4039

EDUCATION

BS	University of Louisville, Chemistry Focus in Biochemistry	May 2019
MS	University of Louisville, Pharmacology and Toxicology	May 2021
PhD	University of Louisville, Pharmacology and Toxicology	Dec 2023

HONORS, AWARDS, CERTIFICATIONS

NIEHS T32 Predoctoral Fellow Training Grant	2021-2023
Awarded by the University of Louisville NIEHS T32 Training Program in Environmental Health Sciences; training grant	
Ohio Valley Society of Toxicology PhD platform talk	2022
Awarded by the Ohio Valley Society of Toxicology for best PhD platform presentation at the annual fall meeting; monetary award	
Graduate Student Council Travel Award	2022
Awarded by the University of Louisville Graduate Student Council to attend the Society of Toxicology Annual Meeting; monetary award	
Ohio Valley Society of Toxicology PhD platform talk	2021
Awarded by the Ohio Valley Society of Toxicology for best PhD platform presentation at the annual summer trainee meeting; monetary award	

IPIBS Fellowship (full tuition and stipend)

2019 - 2021

Awarded by the University of Louisville upon admittance as a graduate student to the Department of Pharmacology and Toxicology

Rachel Davis Memorial Scholarship Recipient

Awarded by the Rachel Davis Memorial Scholarship Endowment Chair for displaying exceptional stewardship in environmental extracurriculars; monetary award 2019

University of Louisville Cancer Education Program Trainee

Participant in the 10-week summer Cancer Education Program, a competitive program funded by the National Institute of Health; aims to train the next generation of cancer researchers 2018

University of Louisville Undergraduate Research Grant

2018

Awarded by the University of Louisville to sponsor undergraduate research and poster presentation

Pharmacy Technician Certification

2017

Awarded by the National Healthcare Association upon passing the Exam of the Certified Pharmacy Technicians (ExCPT)

Speed School Academic Affairs Scholarship

2016

Awarded by the J.B. Speed School of Engineering Academic Affairs Committee for displaying academic excellence; monetary award to assist in paying for study abroad

P.E.O. STAR Scholarship Recipient

2015

Awarded by the national P.E.O chapter for exhibiting excellence in leadership, academics, extracurricular activities, community service and potential for future success; monetary award for higher education

Kentucky Governor's Scholar

2014

Participant in the Kentucky Governor's Scholars Program, a highly competitive summer program which provides opportunity for academic and personal growth

RESEARCH EXPERIENCE

University of Louisville, Department of Pharmacology and Toxicology 2019 – present

Graduate fellow, Hein Lab

- Determining effects of *N-Acetyltransferase 2 (NAT2)* genetic polymorphism on insulin sensitivity
- Evaluating impacts of heterocyclic amines (HCAs) on insulin resistance and glucose and lipid homeostasis
- Investigating the role of NAT2-mediated metabolism of HCAs in pathogenesis of insulin resistance and metabolic dysregulation

University of Louisville, Department of Microbiology and Immunology 2019
Research Scientist, Sokoloski Lab

- Selecting for viral revertants by serial passaging the existing SINV nsP1 mutants until genetic reversion was observed via a change in viral kinetics or an oblique alteration of virus phenotype
- Identifying the genetic basis of the reversion event(s) using next-generation sequencing technologies to map the amino acid changes with respect to time
- Biochemically and biologically assessing the revertants by using site-directed mutagenesis to recapitulate the observed amino acid changes in a clean genetic background to evaluate the impact of the reversion events on viral RNA synthesis and viral capping kinetics in tissue culture models of infection

Cancer Education Program, Department of Pharmacology and Toxicology 2018
Research Scientist, Siskind Lab

- Determining the effects on renal function of using erlotinib as an injury-ameliorating agent following the completion of the clinically relevant CDDP repeated dosing model

University of Louisville, Department of Pharmacology and Toxicology 2018
Research Scientist, Siskind Lab

- Utilizing a clinically relevant mouse model of cisplatin-induced kidney injury
- Determining the effects on renal function of using erlotinib, an EGFR inhibitor, in combination with cisplatin

PRESENTATIONS

Research!Louisville, Louisville, KY
October 2023

“Heterocyclic amines disrupt hepatic lipid homeostasis”

Brown Cancer Center Research Retreat, Louisville, KY

September 2023

“Heterocyclic amines disrupt hepatic lipid homeostasis”

Superfund Research Program annual meeting, Raleigh, NC

December 2022

“Hepatic metabolism of heterocyclic amines contributes to induction of glucose production and gluconeogenic gene expression in hepatocytes”

OVSOT annual fall meeting, Louisville, KY

November 2022

“Hepatic metabolism of heterocyclic amines contributes to induction of glucose production and gluconeogenic gene expression in hepatocytes”

Research!Louisville, Louisville, KY

September 2022

“Hepatic metabolism of heterocyclic amines contributes to induction of glucose production and gluconeogenic gene expression in hepatocytes”

OVSOT Summer Student Meeting, virtual

July 2022

“Transcriptional Regulation of Human Arylamine N-Acetyltransferase 2 Gene by Glucose and Insulin in Liver Cancer Cell Lines”

Society of Toxicology Annual Meeting, San Diego, CA

March 2022

“Heterocyclic amines induce changes in glucose production and insulin signaling in human hepatocytes”

OVSOT annual fall meeting, virtual

November 2021

“Heterocyclic amines induce changes in glucose production and insulin signaling in human hepatocytes”

Research!Louisville, Louisville, KY

October 2021

“Heterocyclic Amines Induce Changes in Glucose Production and Insulin Signaling in Human Hepatocytes”

OVSOT Summer Student Meeting, virtual

July 2021

“Changes in insulin signaling, gluconeogenic gene expression, and glucose production in cryopreserved human hepatocytes following exposure to heterocyclic amines”

American Society of Pharmacology and Experimental Therapeutics

April 2021

“Changes in Insulin Signaling and Gluconeogenic Gene Expression in Human Hepatocytes Following Exposure to Heterocyclic Amines”

Graduate Student Regional Research Conference, virtual

February 2021

“Changes in Insulin Signaling and Gluconeogenic Gene Expression in Human Hepatocytes Following Heterocyclic Amine Treatment”

Ohio Valley Society of Toxicology Annual Meeting, virtual

November 2020

“Depletion of arylamine *N*-acetyltransferase 2 results in dysregulation of gluconeogenic and lipogenic genes in HepG2 hepatocellular carcinoma cell line”

UofL Pharmacology and Toxicology Dept. Seminar, virtual

April 2020

“Heterocyclic Amines and Arylamine *N*-Acetyltransferase 2 Polymorphism in Insulin Resistance”

ACC Meeting of the Minds, Louisville, KY

March 2019

“Repeated administration of cisplatin increases EGFR/EGFR activation and renal fibrosis in *Kras4bG12D* lung adenocarcinoma-bearing mice, but kidney injury is further exacerbated with erlotinib/cisplatin combination treatment”

Posters at the Capitol, Frankfort, KY

February 2019

“Repeated administration of cisplatin increases EGFR/EGFR activation and renal fibrosis in *Kras4bG12D* lung adenocarcinoma-bearing mice, but kidney injury is further exacerbated with erlotinib/cisplatin combination treatment”

Research!Louisville Poster Presentation, Louisville, KY

October 2018

“Repeated administration of cisplatin increases EGFR/EGFR activation and renal fibrosis in Kras4bG12D lung adenocarcinoma-bearing mice, but kidney injury is further exacerbated with erlotinib/cisplatin combination treatment”

Cancer Education Program Poster Presentation, Louisville, KY

August 2018

“Repeated administration of cisplatin increases EGFR/EGFR activation and renal fibrosis in Kras4bG12D lung adenocarcinoma-bearing mice, but kidney injury is further exacerbated with erlotinib/cisplatin combination treatment”

University of Louisville Undergraduate Research Symposium

April 2018

“Repeated administration of cisplatin increases EGFR/EGFR activation and renal fibrosis in Kras4bG12D lung adenocarcinoma-bearing mice, but kidney injury is further exacerbated with erlotinib/cisplatin combination treatment”

PEER REVIEWED PUBLICATIONS

Walls KM, Hong KU, Hein DW. Induction of Glucose Production by Heterocyclic Amines is Dependent on N-acetyltransferase 2 Genetic Polymorphism in Cryopreserved Human Hepatocytes. *Toxicol Lett.* 2023 Jul 7:S0378-4274(23)00216-3. doi: 10.1016/j.toxlet.2023.07.002. Epub ahead of print. PMID: 37423373.

Walls KM, Hong KU, Hein DW. Heterocyclic amines reduce insulin-induced AKT phosphorylation and induce gluconeogenic gene expression in human hepatocytes. *Arch Toxicol.* 2023 Apr 2. doi: 10.1007/s00204-023-03488-2. Epub ahead of print. PMID: 37005939.

Hong KU, **Walls KM**, Hein DW. Non-coding and intergenic genetic variants of human arylamine N-acetyltransferase 2 (NAT2) gene are associated with differential plasma lipid and cholesterol levels and cardiometabolic disorders. *Front Pharmacol.* 2023 Apr 3;14:1091976. doi: 10.3389/fphar.2023.1091976. PMID: 37077812; PMCID: PMC10106703.

Hong KU, Tagnedji AH, Doll MA, **Walls KM**, Hein DW. Upregulation of cytidine deaminase in NAT1 knockout breast cancer cells. J Cancer Res Clin Oncol. 2022 Nov 3. doi: 10.1007/s00432-022-04436-w. Epub ahead of print. PMID: 36329350.

Hong KU, Salazar-González RA, **Walls KM**, Hein DW. Transcriptional Regulation of Human Arylamine N-Acetyltransferase 2 Gene by Glucose and Insulin in Liver Cancer Cell Lines. Toxicol Sci. 2022 Nov 23;190(2):158-172. doi: 10.1093/toxsci/kfac103. PMID: 36156098; PMCID: PMC9702998.

Wise JTF, Salazar-González RA, **Walls KM**, Doll MA, Habil MR, Hein DW. Hexavalent chromium increases the metabolism and genotoxicity of aromatic amine carcinogens 4-aminobiphenyl and β -naphthylamine in immortalized human lung epithelial cells. Toxicol Appl Pharmacol. 2022 Aug 15;449:116095. doi: 10.1016/j.taap.2022.116095. Epub 2022 Jun 2. PMID: 35662664; PMCID: PMC9382885.

Hong KU, Doll MA, Lykoudi A, Salazar-González RA, Habil MR, **Walls KM**, Bakr AF, Ghare SS, Barve SS, Arteel GE, Hein DW. Acetylator Genotype-Dependent Dyslipidemia in Rats Congenic for N-Acetyltransferase 2. Toxicol Rep. 2020 Sep 28;7:1319-1330. doi: 10.1016/j.toxrep.2020.09.011. PMID: 33083237; PMCID: PMC7553889.

WORK EXPERIENCE

PhD candidate trainee	2019-present
Walmart Pharmacy Certified Pharmacy Technician	2016-2019

PROFESSIONAL TRAINING

Society of Toxicology Annual Meeting
San Diego, CA, 2022
Attended and presented orally; participated in networking and professional development seminars

Toxicological Excellence for Risk Assessment (TERA) Bootcamp

Cincinnati, OH, 2021

Completed an accelerated, intensive hands-on training in hazard characterization and dose-response assessment

ACC Meeting of the Minds Annual Conference

Louisville, KY 2019

Attended and presented research poster; participated in networking and professional development seminars

Society of Women Engineers Annual Conference

Nashville, TN 2015

Attended and participated in networking and professional development seminars

PROFESSIONAL AFFILIATIONS

American Society of Pharmacology and Experimental Therapeutics, 2020-present

Society of Toxicology, 2020-present

Society of Undergraduate Chemistry Students, 2016-2019

Society of Women Engineers, 2015-2019

PROFESSIONAL SERVICE

University of Louisville Graduate Peer Mentor Host 2020-present
Provide mentorship to incoming students in the Pharmacology and Toxicology graduate program

University of Louisville Undergraduate Peer Mentor Host 2015-2019
Provide campus tours to prospective chemistry students at the University of Louisville

VESA Student Helper 2018-2019

Assist in distributing material to University of Louisville students about the Volunteer Eco Students Abroad program
Present orally about VESA experience to prospective students

GREEN Program On-Campus Ambassador 2017-2018

Lead a recruitment campaign on the University of Louisville campus for the GREEN study abroad program
Create and distribute marketing materials to provide information to students
Present orally at club meetings and relevant classrooms about the program

SERVICE ABROAD

Volunteer Eco Students Abroad

Volunteer, South Africa, May 2018

Volunteer focus in conservation, education, and construction

Built a watering hole at St. Lucia Crocodile Center, cleaned pens of savannah cats at The Emdoneni Cheetah Project

Taught mathematics/English at local school in the Zulu Village, prepared lunches at local orphanage

Built the foundation of a home gifted to a local family of 9 deemed in dire need of assistance

Elephant Haven

Volunteer, Thailand, July-August 2017

Offered time and compassion to feed and bathe elephants in a sanctuary setting during the rehabilitation process

EDUCATIONAL TRAVEL

Reykjavik University Iceland School of Energy

2016

Studied geothermal energy, hydroelectric energy, energy economics
Toured clean energy facilities

REFERENCES

David W. Hein

Professor and Chairman of the Department of Pharmacology and Toxicology
Kosair Charities CTR – Room 303
University of Louisville Health Sciences Center

505 South Hancock Street
Louisville, KY 40202
Telephone: 502-852-6252
Email: david.hein@louisville.edu

Kyung U. Hong

Associate Professor of Pharmacology
323 Center for Sciences & Pharmacy
1215 Wilbraham Road
Springfield, MA 01119
Telephone: 413-796-2474
Email: kyung.hong@wne.edu